# INFORMATION TO USERS

This manuscript has been reproduced from the microfilm master. UMI films the text directly from the original or copy submitted. Thus, some thesis and dissertation copies are in typewriter face, while others may be from any type of computer printer.

**The quality of this reproduction is dependent upon the quality of the copy submitted.** Broken or indistinct print, colored or poor quality illustrations and photographs, print bleedthrough, substandard margins, and improper alignment can adversely affect reproduction.

In the unlikely event that the author did not send UMI a complete manuscript and there are missing pages, these will be noted. Also, if unauthorized copyright material had to be removed, a note will indicate the deletion.

Oversize materials (e.g., maps, drawings, charts) are reproduced by sectioning the original, beginning at the upper left-hand corner and continuing from left to right in equal sections with small overlaps. Each original is also photographed in one exposure and is included in reduced form at the back of the book.

Photographs included in the original manuscript have been reproduced xerographically in this copy. Higher quality 6" x 9" black and white photographic prints are available for any photographs or illustrations appearing in this copy for an additional charge. Contact UMI directly to order.

# HYDROXYL RADICAL SCAVENGERS AND ANTIOXIDANTS IN RADIATION PROTECTION

K. J. Lenton

A thesis submitted to the

Faculty of Graduate Studies and Research

in partial fulfilment of the requirements

for the degree of

Doctor of Philosophy

Department of Physics,

Carleton University,

Ottawa-Carleton Institute for Physics,

Ottawa, Ontario,

Canada

28th April, 1998

Canada

The undersigned hereby recommend to

the Faculty of Graduate Studies and Research

acceptance of the thesis

# HYDROXYL RADICAL SCAVENGERS AND ANTIOXIDANTS IN

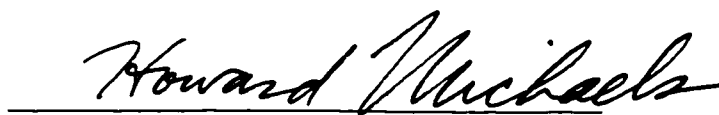# RADIATION PROTECTION

submitted by

K.J. Lenton, B.Sc., M.Sc.

in partial fulfilment of the requirements

for the degree of Doctor of Philosophy

_____
Thesis Supervisor

_____
Chair, Department of Physics

_____
External Examiner

Carleton University

**Abstract**

Antioxidants and free radical scavengers, by combatting oxygen radical-mediated oxidative stress, may protect against ionising radiation. A total antioxidant assay has been developed using a highly fluorescent molecule, ß-phycoerythrin (BPE), as the target for radiation generated free radicals. Serial dilutions of a solution of a test compound are made across a 96-well microwell plate and a standard BPE solution added to each well. Competition plots for combinations of BPE and scavenging compounds can then be generated by monitoring changes in fluorescence of the BPE solution in each well, before and after a radiation dose, as a function of compound concentration. As in other antioxidant assays one unit is defined as the quantity of antioxidant required to reduce by half the action of oxygen derived free radicals, in this case monitored by the fluorescence decay of a 340 ng mL$^{-1}$ solution of ß-phycoerythrin. The fluorescence decreases linearly with dose allowing radioprotective capacities to be determined after a single standard test dose. Using this technique, relative rate constants can be calculated for the reactions between hydroxyl radical scavengers and hydroxyl radicals. For antioxidants and hydrogen donors, there is a correlation between radioprotective capacity and oxidation potential. The assay then becomes a true measure of total radioprotective effect which can rank the compounds. Antioxidants are more than thirty times more effective than pure hydroxyl radical scavengers such as sugars, which is due to their competition with oxygen for the target radical intermediates. The antioxidant compounds could be ranked based on their chemical structure. Indoles, such as melatonin are the most effective (nine times more effective than ascorbic acid), followed by phenols and thiol compounds. The assay can also be applied to complex biological samples. Cell lysates and human blood plasma were measured to determine if variations in their radioprotective capacity could explain observed differences in cellular radiosensitivity. These samples proved to be

highly reductive, more reductive than ascorbate on a weight per weight basis. For total

blood plasma radioprotective effect an inverse trend was observed with donor age, which

is largely due to high molecular weight protein contributions that are inefficient in their

interaction with target radicals. However, only additions of a low molecular weight

antioxidant (melatonin) were able to modify radioprotection *in vitro*.

## Acknowledgements

# Table of Contents

# List of Tables

## List of Figures

x

xiii

xiv

# List of Appendices

# Chapter 1: INTRODUCTION

The aim of this thesis is to investigate mechanisms of chemical protection against ionising radiation damage and to develop a quantitative method with a molecular basis to measure this chemical radioprotection in model biological systems. This could rank protective compounds and biological samples in order of effectiveness. Such a method, using a fluorescent protein, $\beta$-phycoerythrin (BPE), as a target for radiation-generated free radicals, has been developed. This large (240 kDa) protein is highly fluorescent and is derived from sea algae, in which it assists with photosynthetic processes [1]. Oxidation of the chromophore decreases the specific fluorescence. The change in fluorescence during irradiation is a quantitative measure of the oxidative stress induced.

Chemical radioprotection deals with the modification of radiation chemical processes which, in turn, modifies their biological outcome.

Figure 1 shows how this is possible with a timeline of possible events ($10^{-12}$ to $10^{12}$ s ) after ionising radiation energy is deposited in a biological system. The scheme can be divided roughly into three sections. From $10^{-12}$ to $10^{-3}$ s , the chemical effects of the energy deposition occur. These include initial free radical formation and oxidation reactions initiated by oxygen-derived free radicals. Hydrogen donating compounds present in mammalian cells can inhibit these reactions. From $10^{0}$-$10^{5}$ s, the induced damage has immediate implications for the organism. The damage must be adequately repaired if the organism's constituent cells are going to survive. Long term genetic consequences of remaining damage occur at $10^{8}$-$10^{12}$ s. Reduction of the chemical reactions at $10^{-9}$ s would result in reductions of the biological implications at $>10^{2}$ s .

| TIME (s) | |
|---|---|
| $10^{-12}$ | Initial Energy Deposition - Free Radical Formation |
| $10^{-10}$ | Diffusion Controlled Reactions- Hydroxyl Radical Attack |
| $10^{-8}$ | Oxygen Fixation |
| $10^{-6}$ | Superoxide and Tertiary Reactions |
| $10^{-4}$ | |
| $10^{-2}$ | DNA Conformational Changes |
| $10^{0}$ | |
| $10^{2}$ | Changes Observed in RNA Transcription |
| $10^{4}$ | DNA Repaired/ Misrepaired Apoptosis/ Cell Death Observed |
| $10^{6}$ | |
| $10^{8}$ | Cancer Formation from Accumulated Damage |
| $10^{10}$ | Germline Mutation Expression |
| $10^{12}$ | Species Evolution |

Figure 1: The timeline of events ($10^{-12}$ -$10^{12}$ s) after ionising radiation damage to a human organism.

## 1.1 Thesis Overview

Ionising radiation damages cellular components by oxidative processes caused by oxygen-derived free radicals. Compounds can protect against radiation damage by hydroxyl radical scavenging and hydrogen donation (theory described in Chapters 2 and 3 respectively). Using a fluorescent protein as a target for radiation-generated free radicals (methodology described in Chapter 4) properties of radical scavengers and hydrogen donors can be examined practically (Chapters 5 and 6 respectively)[1]. The assay is also a measure of total radioprotective capacity (Chapter 7).

Cells have effective antioxidant mechanisms to protect against oxidative stress. Variations in antioxidant levels might be responsible for differences in radiosensitivity. Measurements made on human cell lysates (Chapter 8) were designed to test this hypothesis. Measurements of the radioprotective effect of human blood plasma (Chapter 9)[2] may clarify whether antioxidant variations are responsible for differences in radiosensitivity *in vivo*.

Antioxidants added to cells in tissue culture protect these cells against radiation damage (Chapter 10) and this strategy may be useful in practical situations.

---

[1] Data submitted as papers to Free Radical Research Communications and Redox Report.
[2] Data in this Chapter is submitted to Free Radical Biology and Medicine.

## 1.2 Oxygen Derived Free Radicals.

Free radicals are reactive species that frequently occur as intermediates in chemical reactions. Their main signature is an unpaired electron in the valence shell. Figure 2 shows the electronic structure of an oxygen atom. There are two unpaired electrons in the 2p orbital, as described by Hund's rule. Molecular oxygen has a more complex electronic structure due to the bonding and antibonding orbitals shown in Figure 2 (ii). The main characteristic of oxygen molecules is the two unpaired electrons in the antibonding $\pi*2p$ orbital, which results in molecular oxygen behaving as a biradical. These are available for reaction and help explain the relative reactivity of the oxygen molecule. Reduction of an oxygen molecule, by addition of an electron, results in the superoxide radical anion ($O_2^{\bullet-}$) shown in Figure 2 (iii), which has just one unpaired electron. A reaction scheme for the reduction of oxygen to water is further shown in Figure 3. The first reduction step is the addition of an electron to oxygen in solution forming a superoxide radical anion. The resultant electron structure in the $\pi*2p$ orbital is indicated by the arrows. The presence of an unpaired electron, which is available for reaction, qualifies this species as a radical. The superoxide radical anion can be further reduced by addition of a second electron and two protons to form hydrogen peroxide. This chemical form is more stable, and performs an oxidant role by accepting a further electron. This redox process dissociates the peroxide into an hydroxyl anion ($OH^-$)and a neutral hydroxyl radical ($^{\bullet}OH$). The hydroxyl anion is generally not very reactive nor produced in large enough quantities to affect pH under normal circumstances, whereas the hydroxyl free radical is very reactive.

Reduction of the hydroxyl radical, by accepting one more electron and a proton, completes the 4-step reduction of oxygen to water (see Reaction R1.1):

$$O_2 + 4e \xrightarrow{\ 4H^+\ } 2H_2O$$  (R1.1)

**Figure 2 diagram:**

(i) Atomic oxygen ground state:

| Orbital | Occupation |
|---|---|
| 2p | ↑↓ ↑ ↑ |
| 2s | ↑↓ |
| 1s | ↑↓ |

(ii) Oxygen molecule molecular orbitals:

| Orbital | Occupation |
|---|---|
| σ*2p | |
| π*2p | ↑  ↑ |
| π 2p | ↑↓ ↑↓ |
| σ 2p | ↑↓ |
| σ*2s | ↑↓ |
| σ 2s | ↑↓ |
| σ*1s | ↑↓ |
| σ 1s | ↑↓ |

(iii) Superoxide radical anion molecular orbitals:

| Orbital | Occupation |
|---|---|
| σ*2p | |
| π*2p | ↑↓ ↑ |
| π 2p | ↑↓ ↑↓ |
| σ 2p | ↑↓ |
| σ*2s | ↑↓ |
| σ 2s | ↑↓ |
| σ*1s | ↑↓ |
| σ 1s | ↑↓ |
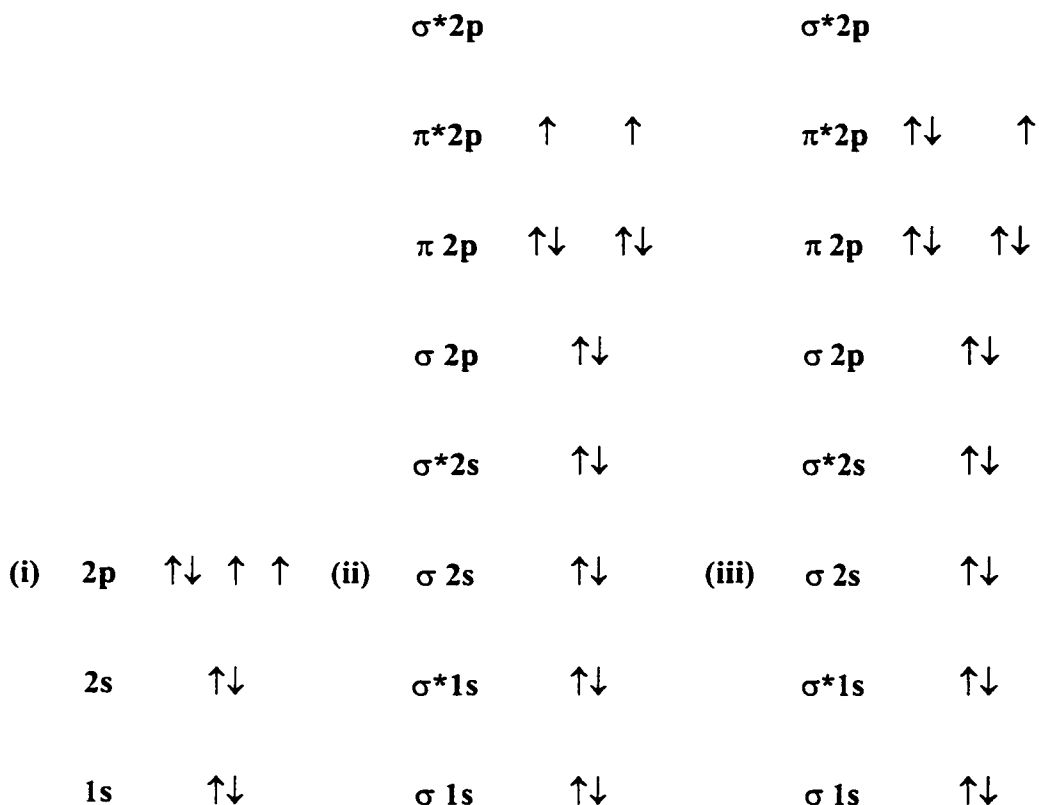
Figure 2: An energy state diagram of the electron structure of atomic oxygen in the ground state (i) and the occupation of the molecular orbitals for the oxygen molecule (ii) and the superoxide radical anion (iii). Antibonding orbitals are indicated by '*'.

(i) Attachment of an electron to oxygen and formation of a superoxide radical anion.

$$_\uparrow OO_\uparrow + e^- \longrightarrow _\uparrow OO_{\uparrow\downarrow}^-$$
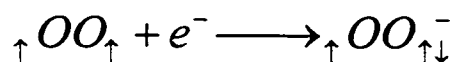
(ii) Reduction of the superoxide radical anion by an electron and two protons to form hydrogen peroxide.

$$_\uparrow OO_{\uparrow\downarrow}^- + e^- + 2H^+ \longrightarrow H_{\uparrow\downarrow} OO_{\uparrow\downarrow} H$$
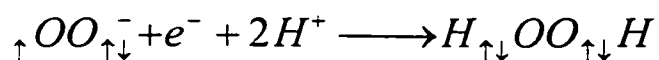
(iii) Reduction of hydrogen peroxide by an electron to form an hydroxyl ion and an hydroxyl free radical.

$$H_{\uparrow\downarrow} OO_{\uparrow\downarrow} H + e^- \longrightarrow _{\uparrow\downarrow} OH^- + _\uparrow OH$$
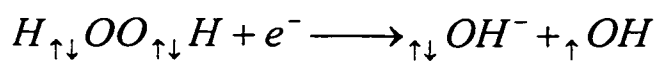
(iv) Reduction of the hydroxyl radical by an electron and a proton to form water ($H_2O$).

$$_\uparrow OH + e^- + H^+ \longrightarrow HOH$$
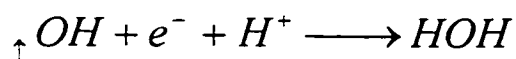
Figure 3: A reaction scheme showing the four-step reduction of oxygen to water via the oxidant intermediates hydrogen peroxide and hydroxyl radicals.

Reduction of oxygen, therefore, results in reactive oxygen species including oxygen-derived free radicals. These free radicals contain an unpaired electron, which increases their reactivity. Just as oxygen derived free radicals are produced during the reduction of oxygen, they can also be produced during the oxidation of water.

## 1.3 Deposition of low LET Ionising Radiation and Water Radiolysis.

An ionising radiation photon can deposit energy in a cellular environment by Compton scattering or secondary ionisation processes [2]. These events produce high energy primary electrons. Electrostatic interactions at the molecular level lead to the transfer of energy from the primary electron to many secondary electrons, which have lower energies. This produces a large number of ionisational events in the water matrix along the electron track. The water dissociates [ 3]:

$$H_2O \longrightarrow H \cdot + \cdot OH \ . \tag{R1.2}$$

The primary products of water radiolysis are hydroxyl radicals ($\cdot$OH) and hydrogen atom radicals (H$\cdot$).

Further energy degradation produces a number of very low energy electrons (<100 eV) [ 4], which negative charge polarizes adjacent water molecules (H$^-$OH$^-$) to form 'hydrated electrons' $e^-_{aq}$.

At these low energies, electrons have reaction cross-sections of ~$10^{-18}$ cm$^2$ [ 5] with water, oxygen and organic molecules. The electrons react at resonant energies, exciting

Time

$H_2O \xrightarrow{\text{Radiation energy}} H_2O^+ \quad + \quad e^- \qquad 10^{-16}s$

$H_2O$

$H_3O^- \quad + \quad OH \qquad\qquad\qquad\qquad 10^{-14}s$

$4.8e^-(aq) \qquad 10^{-12}s$

Spur expansion and reaction

$10^{-7}s$

$2.6e^-+0.6H^++2.7OH+0.45H_2$
$+0.7H_2O_2+2.6H_3O^-$
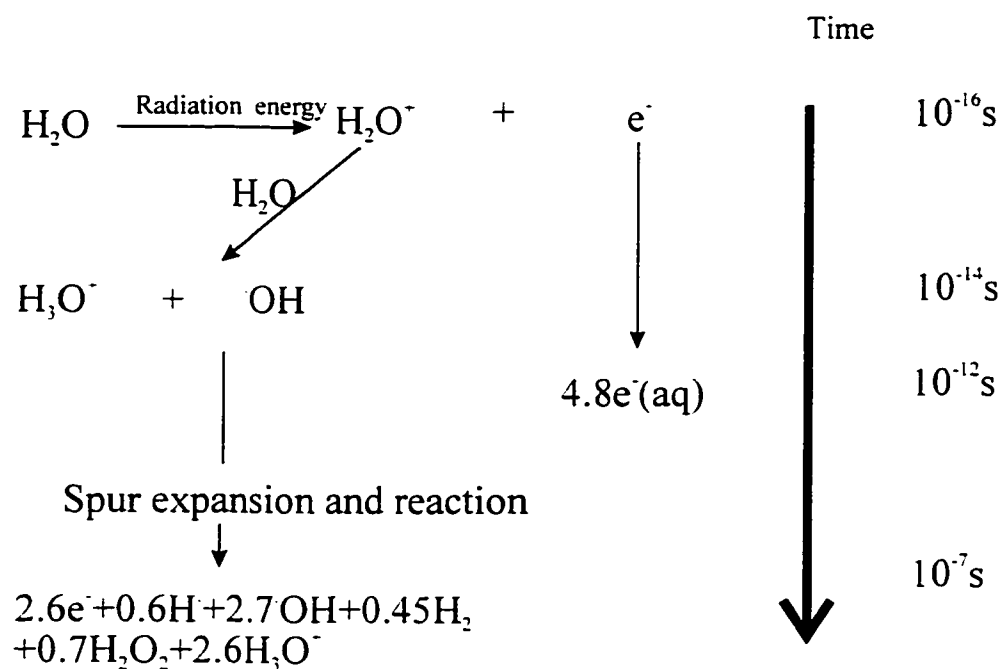
Figure 4: A scheme for the radiolysis of water. G-values (see page 9) are shown for species in neutral water at $10^{-16}$ to $10^{-7}$ s after irradiation. The final G values are: 2.6 for hydrated electrons, 0.6 for hydrogen radicals, 2.7 for hydroxyl radicals, 0.45 for hydrogen molecules, 0.7 for water and 2.6 for the hydoxolium ion. The electron yield at $10^{-12}$s (4.8) is that produced, theoretically, before spur expansion and reaction. Most of the final electrons react with oxygen to produce superoxide. Taken from ref.[ 6].

molecules into metastable states ($H_2O^*$). A metastable water molecule cleaves into a neutral hydrogen atom and an hydroxyl radical (see Reaction 1.3):

e.g.

$$H_2O^+ + e^- \longrightarrow H_2O^* \longrightarrow H \cdot + \cdot OH .$$
(R1.3)
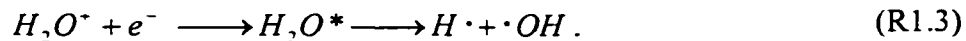
Oxygen present in the medium can also react with hydrogen atoms or 'hydrated electrons':

$$O_2 + e_{aq}^- \longrightarrow O_2^{\cdot -} ,$$
(R1.4)

$$O_2 + H \cdot \longrightarrow O_2^{\cdot -} + H^+ ,$$
(R1.4a)

forming a 'superoxide anion' ($O_2^{\cdot -}$) [ 7]. These are quite fast reactions $k \sim 10^{10} \ L \ mol^{-1} s^{-1}$ and therefore in the presence of oxygen, almost all of the available hydrated electrons and hydrogen atoms will be scavenged by oxygen. Since in aerated solutions the oxygen concentration is $2.5 \times 10^{-4}$ mol $L^{-1}$, other solutes (s) with similar hydrated electron reactivities $k_s[s]$ ($s^{-1}$), must be at much lower concentrations to make this assumption. For example, a protein with an average amino acid molecular weight of 300 and a fast reaction with hydrated electrons must be at concentrations much lower than 75 $\mu g \ mL^{-1}$. The resultant superoxide anions are much less reactive than hydroxyl radicals [ 8].

The 'G' value is often used as a measure of the quantity of chemical species produced or destroyed. It is defined as the number of resultant molecules formed or destroyed per 100 eV deposited. Figure 4 shows a simplified plot of 'G' values for the different species produced: the hydroxyl radical ($\cdot OH$), the hydrated electron ( which is the main precursor of superoxide production), the hydrogen atom ($H \cdot$) and hydrogen

peroxide ($H_2O_2$). Figure 4 shows that the hydroxyl radical is the predominant oxidising species produced. It is also the most reactive species and can react with neighbouring molecules.

This type of reaction where the radiation damage is expressed chemically, is termed 'indirect' radiation action. 'Direct' radiation action is ionising damage induced by charged particle tracks within large biomolecules themselves, and accounts for < 30% of DNA damage in cells [ 9], although this is highly variable depending on the experimental system [ 10].

## 1.4 Hydroxyl Radical Reactions.

Depending on the initial concentration of radicals generated, the first reactions that hydroxyl radicals in aqueous solution can undergo are recombinational events:

$$HO \cdot + \cdot OH \xrightarrow{2k_5} H_2O_2,$$ \hfill (R1.5)

forming quantities of hydrogen peroxide (see Figure 4). The rate constant for this reaction, $k_5$, is of the order of $10^{10}$ L $mol^{-1}$ $s^{-1}$ indicating a diffusion limited reaction. Hydroxyl radicals may also react with organic molecules present in the medium. The radicals can react with saturated and unsaturated organic molecules by different pathways. In saturated compounds, they 'abstract' a hydrogen atom from the surface of the target molecule ($T^{-H}$) with a rate constant $k_6$ :

$$T^{-H} + \cdot OH \xrightarrow{k_6} T \cdot + H_2O,$$ \hfill (R1.6)

leading to the creation of a 'target radical' ($T \cdot$ or $T^*$) and water.

In compounds containing unsaturated carbon bonds (i.e. double bonds) the reaction

scheme is slightly different. The hydroxyl radical reacts with, and saturates, a carbon double bond on the target molecule (T):

$$T + \cdot OH \xrightarrow{k_{\cdot}} T^{\bullet}_{-OH} \, .$$

<div align="right">(R1.7)</div>

This results in an hydroxyl group attached to one end of the previous double bond and an unpaired electron radical on the other end, referred to as an OH-adduct radical.

The rate constants for Reactions R1.6 and R1.7, $k_{\iota}$, $k_{\tau}$ are of the order $10^9$-$10^{10}$ L mol$^{-1}$ s$^{-1}$ and are also diffusion limited. They depend greatly on the size and conformation of the target e.g. whether a monomer or a single- or double-stranded polynucleotide.

The resultant target radicals ( $T^{\bullet}_{-OH}, T^{\bullet}$ ) can then react with other compounds and radicals in the medium. The most commonly available reactive molecule in the normal tissue environment is oxygen. Oxygen reacts with the target radical to form a peroxyl radical:

$$T^{\bullet} + O_2 \xrightarrow{k_{\iota}} T^{-OO\bullet}$$

<div align="right">(R1.8)</div>

or for double bonds:

$$T^{\bullet}_{-OH} + O_2 \xrightarrow{k_{\iota}} T^{-OO\bullet}_{-OH} \, .$$

<div align="right">(R1.8a)</div>

The damage is then said to be 'fixed' and this peroxyl radical site may be capped by a hydrogen atom, completing the reaction and forming a hydroperoxide moiety. The rate constant for this oxygen fixation, $k_9$, is of the order $10^7$-$10^9$ L mol$^{-1}$ s$^{-1}$ and therefore these reactions are much slower than the primary reactions ($k=10^9$-$10^{11}$ L mol$^{-1}$ s$^{-1}$; Reactions R1.5-1.7).

Target radicals can also react with other organic radicals (R$^{\bullet}$) or molecules (R) in recombination reactions:

$$T^{\bullet} + {}^{\bullet}R \xrightarrow{k_9} T - R \qquad \text{(R1.9)}$$

$$T^{\bullet} + R \xrightarrow{k_9} T - R^{\bullet}, \qquad \text{(R1.9a)}$$

producing cross-linked molecules or tertiary radicals. These reactions tend to be even slower than oxygen fixation and therefore only become significant in anoxic environments. Tertiary and subsequent reactions involving radical transfer to other target molecules can also occur [ 11][ 12].

Each of these oxidative reactions (Reactions R1.5-1.9) is classed as 'oxidative stress', a term which includes other radical reactions e.g. those induced by bleomycin (a chemo-therapeutic agent), hydrogen peroxide oxidation and some environmental carcinogen action [ 13]-[ 19].

Target restitution can occur by hydrogen donation or 'chemical repair' reactions of target radicals with reducing agents (RH) or antioxidants:

$$T^{\bullet} + RH \longrightarrow T^{-H} + R^{\bullet} \qquad \text{(R1.10)}$$

Although target radical formation following ${}^{\bullet}OH$ attack (Reaction R1.6) is the same in the presence (oxia) or absence (hypoxia) of oxygen, the subsequent fate of this reactive intermediate is strongly influenced by its secondary reaction with oxygen and other redox components.

$$T^{-H} + {}^{\bullet}OH \xrightarrow{oxia-H_2O} T^{\bullet} + O_2 \xrightarrow{fixation} TOO^{\bullet} + RH \longrightarrow TOOH + R^{\bullet} \qquad \text{(R1.11)}$$

$$T^{-H} + {}^{\bullet}OH \xrightarrow{hypoxia} T^{\bullet} + RH \xrightarrow{restitution} T^{-H} + R^{\bullet} \qquad \text{(R1.12)}$$
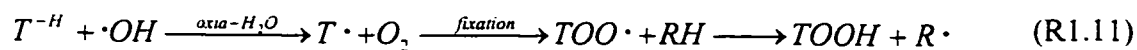
These competing reactions are believed to provide the basis for the universally observed

radiobiological oxygen effect [ 9]. The enhanced chemical damage arising from 'fixation'

by oxygen of potential target radical damage is mitigated against in the absence of

oxygen by a competing back reaction between target radical and reducing agents that

'chemically repair' the target damage and reconstitute the target.

On the basis of Reaction R1.11, the presence of even low levels of the ubiquitous

oxygen favours the oxidative fixation of target radicals resulting in maximal damage

equal to the yield of radiolytic $^{\bullet}OH$ radicals. Each hydroxyl radical produces an

equivalent amount of damage via oxygen mediated target peroxidation. In the absence of

oxygen, mediated damage is expressed due to the partial restitution of the target (R1.12).

This is the kinetic basis of the oxygen effect where molecular and cellular systems exhibit

a ~3-fold change in radiosensitivity in the presence versus the absence of oxygen. In

addition to oxygen, other oxidants render biological systems more radiosensitive,

whereas radical scavengers, antioxidants and other reducing agents confer

radioresistance.

Free radical-mediated damage, generated chemically, biochemically,

photochemically or radiation chemically, may be sensitised by trace metals such as $Fe^{3+}$

and $Cu^{2+}$ in the oxidised state, which act as oxygen-mimics, but this is generally restricted

to anoxic systems. In cellular systems, where oxygen tension may be quite

heterogeneous, trace metals may influence radiosensitivity particularly when scoring end-

points or damage to sites that may be metabolically inclined to hypoxia. Important

reactions in this regard [ 20] are the Fenton reaction [ 21]:

$$Fe^{++} + H_2O_2 \longrightarrow Fe^{+++} + {}^{\bullet}OH + OH^-, \qquad\qquad \text{R1.13}$$
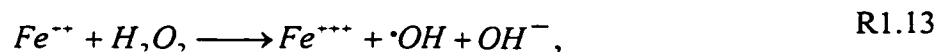
the reaction of $\cdot OH$ with $Fe^{--}$ which is the basis of the Fricke dosimeter,

$$Fe^{--} + \cdot OH \longrightarrow Fe^{---} + OH^{-} \qquad \text{R1.14}$$
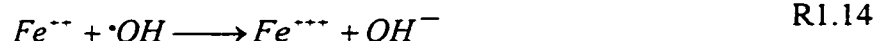
and the Haber-Weiss reaction which is a combination of the Fenton reaction and the reaction of iron with superoxide

$$Fe^{---} + O_2^{\cdot -} \longrightarrow Fe^{--} + O_2 \qquad \text{R1.15}$$

to produce:

$$O_2^{\cdot -} + H_2O_2 \xrightarrow{Fe} O_2 + \cdot OH + OH^{-} \qquad \text{R1.16}$$
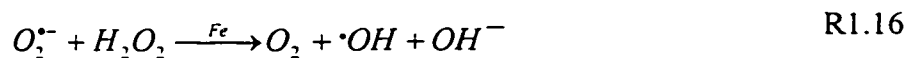
In these circumstances, chelating agents can be added *in vitro* to inactivate such trace metals.

Although reactions involving hydroxyl radicals are not strongly dependent on pH, the reactions of hydrated electrons and superoxide radicals may be. Furthermore, certain compounds such as glutathione, cysteamine and ascorbic acid are ionised at neutral pH. For this reason, all reaction conditions should be strongly buffered and the pH kept constant.

## 1.5 The Target Molecules in Radiation Biology.

Although all molecules can be damaged by oxygen-derived free radicals and are therefore target molecules, there are certain biological molecules that, if damaged, can have long term effects on cellular material and concomitant biological effects. Of these target molecules, the most important is thought to be DNA [ 22][ 23]. Figure 5 shows a section of a typical DNA strand and demonstrates the double-helix construction with a deoxyribose-phosphate 'backbone'. This backbone links the purine and pyrimidine complementary bases paired by hydrogen bonding. This molecule contains coding for the production of all the proteins necessary for cellular function and therefore is the genetic program for life. Damage to this molecule can result in the disruption of normal cell function leading to biological consequences such as apoptosis [ 24], necrosis [ 25] and genetic events, which have possible mutagenic implications [ 26]. The section of DNA shown in Figure 5, for example, has two single strand breaks (SSBs)
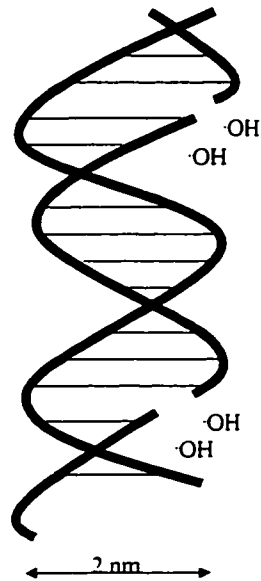
Figure 5: A schematic outline of the structure of DNA. The phosphate back-bone is

shown as a dark helix. One strand has been broken in two places by hydroxyl radical

(˙OH) damage, possibly resulting in a deletion of genetic information .

Cell membrane contains
vitamin E to prevent lipid
peroxidation

Cell nucleus contains water
soluble antioxidants. It also
concentrates some antioxidants
e.g. melatonin

TARGET: LIPIDS

TARGET: DNA
Chromosomes in
metaphase

Mitochondria
contain Mn-
superoxide dismutase

Nuclear membrane

Peroxisomes contain Cu, Zn-
superoxide dismutase and
catalase antioxidant enzymes.

Cytoplasm contains water
soluble antioxidants:
vitamin C, glutathione,
phenols etc.

Figure 6: A generalised diagram of a eukaryotic cell (not to scale) showing the target

molecules (DNA and membrane lipids) and the location of common antioxidants and

protective compounds. The cell is shown in metaphase, at which time the DNA is clearly

visible as distinct chromosomes.

induced by hydroxyl radicals on the same strand. The section between the breaks may have enough energy to break the hydrogen bonds and detach from the main molecule.

This lesion would then have to be repaired if this section of DNA were to be used for protein synthesis. In this process restriction enzymes nick the strand on either side of the damage, removing the damaged material. Other enzymes (DNA ligases) prime the site so that DNA polymerases can attach to the strand and synthesise a section containing the correct base sequence using the complementary DNA strand as a template. Errors could occur at each of these stages resulting in dysfunctional or afunctional proteins, which alter normal cellular processes. Extensive DNA damage could be too great for the repair processes, leading to cell lethality.

Cells that survive, but contain mutated, deleted or translocated genetic information can also be detrimental for the organism. They can eventually kill the organism by initiating neoplastic events [ 27]. They can also affect the organism's progeny, by passing on altered genes. One beneficial aspect is that these genetic mutations also provide the necessary variance that powers evolution.

Other target molecules include lipid membranes (see Figure 6). The membrane represents the cell's connection with its immediate environment and responds to external changes by 'sending' signal molecules to the nucleus, a process termed 'signal transduction' [ 28]. The membrane is made up of a lipid bilayer. Lipids consist of a hydrophilic headgroup and a hydrophobic tail. The tail section often contains a high fraction of unsaturated bonds, which are vulnerable to oxidation by free radicals. The resultant lipid radical can then be oxidised by oxygen to a peroxyl radical (Reaction R1.8). Because of the close proximity to other lipid molecules this peroxyl radical

abstracts hydrogen from a neighbour stabilising the damage and resulting in a fresh radical. This 'chain propagation' can quickly oxidise a large number of lipids [ 29]. Extensive lipid damage may also lead to cell death. However, lipid soluble antioxidant compounds such as vitamin E protect against this damage [ 30]. Membrane proteins, particularly hypothesised 'sentinel' proteins, may act as reporter molecules during oxidative stresses.

Reductions in the amount of radiation damage to these target molecules by chemical radioprotection would also reduce many of the later consequences. This has some important practical applications. For radiation therapy, for example, it would be advantageous to preferentially protect normal tissues, allowing a larger dose to be given to the tumor volume. In emergency nuclear response, radioprotection of essential workers would reduce acute radiation effects.

In this study the fluorescent $\beta$-phycoerythrin (BPE) protein has been used as a target molecule in model aqueous solutions. Although DNA would be the target molecule of choice, it is difficult to use for quantitating oxidative damage. Damage to the BPE protein is easy to monitor by changes in the intense solution fluorescence. The size of the protein (~240 kDa) means that it has a well defined hydration layer [ 31] , which DNA and other large target macromolecules also possess. It is simpler (a protein vs. nucleic acid) and smaller (kDa vs. GDa for DNA) minimising some practical problems (solubility and viscosity). A reasonable assumption is that the chromophore is knocked out by a single-hit process which makes it more sensitive than, e.g. DNA double strand breaks. For examining mechanisms of radioprotection the BPE target molecule should be a suitable substitute for other biological target molecules.

# Chapter 2: MECHANISMS OF RADIOPROTECTION

Compounds can protect target molecules against radiation damage at the primary site (Reaction R1.6) by 'hydroxyl radical scavenging' and at the secondary reaction site (Reaction R1.8) by 'chemical repair'.

## 2.1 Hydroxyl Radical Scavenging

Hydroxyl radical scavengers ($Scav_{-H}$) , added to a target molecule (BPE) solution, will also react with hydroxyl radicals produced during irradiation:

$$Scav_{-H} + \cdot OH \xrightarrow{\quad k_{10} \quad} Scav \cdot + H_2O, \qquad (R2.1)$$
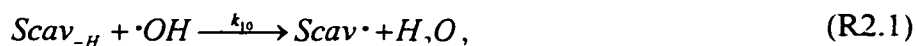
and in this way protect by competing with the target molecule for hydroxyl radicals:

$$BPE + \cdot OH \xrightarrow{\quad k_6 \quad} BPE^\bullet + H_2O, \qquad (R1.6)$$

The value of $k_6$ is not known for reactions of hydroxyl radicals with $\beta$-phycoerythrin. However, using the Smoluchowski equation [ 32] ($k_{diff}=4\pi N(D_A+D_B)(r_A+r_B)\times 10^3$ L mol$^{-1}$ s$^{-1}$), which relates the diffusion coefficient $D_i$ and the reaction radius r to the diffusion limited rate constant for reactions between species A and B, a value can be estimated for $k_6$. Values for $D_{OH}=2.2\times 10^{-9}$ m$^2$ s$^{-1}$ and $r_{OH}=0.22$ nm can be assumed [6]. Because the protein target is very large it is assumed to have a very small diffusion coefficient relative to $D_{OH}$ and its diffusion coefficient is therefore ignored. A value of $r_{target}$ of $5$-$10\times 10^{-10}$ m for a BPE subunit is not unreasonable. These values give an estimated $k_{diff}$ for such a protein on the order of $10^{10}$ L mol $^{-1}$s$^{-1}$ .

Subsequent reactions of $Scav^\bullet$ and $BPE^\bullet$ present at very low concentrations will

20

not interfere with the primary competing reactions and are not considered here. Assuming second order kinetics, which is reasonable for a diffusion limited reaction, it is then possible to write an equation for the rate of change of the hydroxyl radical concentration [·OH] with respect to time , $\dfrac{d[\cdot OH]}{dt}$ , based on a combination of reaction rates $k_5$, $k_6$ and $k_{10}$. The recombination component and the components that react with the target molecule and the scavenger molecule are subtracted from the rate of change with respect to time of the concentration of hydroxyl radicals created in the absence of other reactants, $(d[\cdot OH]/dt)_0$:

$$\frac{d[\cdot OH]}{dt} = (\frac{d[\cdot OH]}{dt})_G - 2k_5[\cdot OH]^2 - k_{6(or\ 7)}[BPE][\cdot OH] - k_{10}[Scav_{-H}][\cdot OH]. \qquad \text{(E2.1)}$$

In the steady state condition $\qquad \dfrac{d[\cdot OH]}{dt} = 0$ .

If a particular concentration of scavenger that competes with BPE for ·OH and reduces this reaction to the 50% level is chosen i.e. the concentration of radicals available to react with the target molecule is reduced by half: $[\cdot OH]_{50\%}$, then Equation E2.1 can be rewritten:

$$\frac{d[\cdot OH]_{50\%}}{dt} = (\frac{d[\cdot OH]}{dt})_0 - 2k_5[\cdot OH]_{50\%}{}^2 - k_6[BPE][\cdot OH]_{50\%} - k_{10}[Scav_{-H}]_{50\%}[\cdot OH]_{50\%} = 0$$

$$\text{(E2.2)}$$

If another experiment is performed, under identical conditions, with a second scavenger concentration also providing 50% reduction $[Scav_{-H}']_{50\%}$, Equation E2.1 becomes:

$$\frac{d[\cdot OH]_{50\%}}{dt} = (\frac{d[\cdot OH]}{dt})_0 - k_5[\cdot OH]_{50\%}^{2} - k_6[BPE][\cdot OH]_{50\%} - k_{10}'[Scav_{-H}']_{50\%}[\cdot OH]_{50\%} = 0$$

.....(E2.3) .

Solving Equations E2.2 and E2.3 simultaneously, assuming [˙OH]$_{50\%}$ is equal in both

instances, yields:

$$k_{10}'[Scav_{-H}']_{50\%} = k_{10}[Scav_{-H}]_{50\%} \quad \text{or} \quad \frac{[Scav_{-H}']_{50\%}}{[Scav_{-H}]_{50\%}} = \frac{k_{10}}{k_{10}'} . \qquad \text{(E2.4)}$$

Therefore, the ratio of the concentrations of scavengers to provide 50% reduction

under a particular condition is inversely related to the ratio of their rate constants with

hydroxyl radicals. This means that if the 50% reduction concentrations are found

experimentally and one of the rate constants is known, then the other can be calculated.

Note that Equation E2.4 is independent of the target molecule concentration [BPE] and

the hydroxyl radical concentration [˙OH] (i.e. it is independent of dose and dose-rate).

Chapter 5 describes measurements made with hydroxyl radical scavengers using

changes in BPE solution fluorescence to determine the 50% reduction concentrations.

## 2.2 Chemical Repair Kinetics

Under normal aeration, oxygen, present in solution, will 'fix' the target radicals (BPE˙) to

form a peroxyl radical:

$$BPE\cdot + O_2 \xrightarrow{\phantom{x}k_{11}\phantom{x}} BPE^{OO\bullet}.$$ (R2.2)

However, the secondary radical (BPE˙) can be chemically repaired to its original state by hydrogen from a donor molecule ($AO_{-H}$ : where the subscript 'H' represents a donatable hydrogen) with rate constant $k_{12}$:

$$BPE\cdot + AO_{-H} \xrightarrow{\phantom{x}k_{12}\phantom{x}} BPE_{-H} + AO\cdot$$ (R2.3)
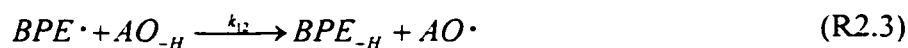
If a saturated site is involved, the ˙OH-adduct $BPE^{\bullet}_{-OH}$, is also reconstituted by hydrogen donation, followed by a rapid dehydration step [ 33]:

$$BPE^{\bullet}_{-OH} + AO_{-H} \xrightarrow{\phantom{x}k_{13}\phantom{x}} BPE^{-H}_{-OH} + AO\cdot \longrightarrow BPE + H_2O + AO\cdot$$ (R2.4)

Therefore, repair by hydrogen donation competes with oxygen fixation.

Antioxidants such as vitamin E, vitamin C and bioflavonoids are effective hydroxyl radical scavengers. But they can radioprotect at much lower concentrations by competing with oxygen in this slower secondary reaction.

The rate of change of the target radical concentration [BPE˙] as a function of additions of antioxidant concentrations [AO] in an oxygenated environment can be described by second order kinetics. Analogous to hydroxyl radical scavenging kinetics, if a concentration of scavenger that competes with $O_2$ for BPE˙ and restitutes the BPE˙ to the 50% level* is chosen, then $\dfrac{d[BPE\cdot]_{50\%}}{dt}$ can be written as:

$$\frac{d[BPE\cdot]_{50\%}}{dt} = (\frac{d[BPE\cdot]}{dt})_0 - k_{11}[BPE\cdot]_{50\%}[O_2] - k_{12(or13)}[BPE\cdot]_{50\%}[AO]_{50\%} = 0 \dots\dots(E2.5).$$

---

* Note that 50% level is used here as meaning the ½ maximal restitution level.

$(d[BPE^-]/dt)_0$ is the initial rate of change with respect to time of the concentration of

target radicals generated by hydroxyl radical attack, in the absence of other reactants.

For a second antioxidant AO', with reaction rate constant $k_{12}'$, a similar equation can be

written:

$$\frac{d[BPE^\bullet]_{50\%}}{dt} = (\frac{d[BPE^\bullet]}{dt})_0 - k_{11}[BPE^\bullet]_{50\%}[O_2] - k_{12}'[BPE^\bullet]_{50\%}[AO']_{50\%} = 0 \quad (E2.6).$$

If conditions for the two antioxidant compounds are identical then solving

simultaneously, assuming that $[BPE^\bullet]_{50\%}$ is equal in both instances yields:

$$\frac{[AO]_{50\%}}{[AO']_{50\%}} = \frac{k_{12}'}{k_{12}} \qquad (E2.7)$$

This implies that the ratio of the 50% restitution concentrations $[AO]_{50\%}$ for two

antioxidants measured under the same conditions is inversely related to the ratio of the

reaction rate constants for their hydrogen donation to the target radical. This is simplistic

because tertiary and subsequent reactions may occur in the overall mechanism which

complicate the analysis. However, the ratio of reference and test compound

concentrations producing a 50% restitution (Equation E2.7), seems to be a convenient

indicator of the relative radioprotective effectiveness of antioxidants. This quantity

should also be a measure of hydrogen donating ability, or oxidation potential, if these

compounds are protecting by hydrogen donation (Chapter 6 describes measurements

made on antioxidants). If this approach is a true measure of antioxidant capacity, the BPE

assay should also be useful to measure the total radioprotective (antioxidant) capacity of

any biological sample.

## 2.3 Methods For Determining Radioprotective Effect.

The properties of hydroxyl radical scavenging and hydrogen donation can be determined by other techniques. The rate constant for the reaction between hydroxyl radicals and radical scavengers is a measure of the scavenging effectiveness of a compound. The best method for measuring this parameter is **pulse radiolysis** [6][ 34][ 35]. This involves direct measurement of the change in absorbance of a target molecule solution immediately after a short input pulse of ionising radiation, usually electrons, on a nanosecond time scale. This approach provides absolute rate constant measurements[ 36]. However the technique is limited in that it requires very specialised apparatus and can only be applied to compounds that have a strong absorbance band. Other methods have used a competition approach, summed up by Equation E2.4, using targets such as thiocyanate or ferrous ions [ 37][ 38]. After irradiation in steady state conditions, the absorbance changes provide good data on rate constant values. But the absorbance of these ions is in the UV , where many other molecules also absorb. Also, these small charged ions may be susceptible to electrostatic interactions and do not develop a hydration layer in the same manner as large biological molecules. Although enzymatic activity has also been used as an indicator of oxidative damage, extreme doses are required (1.5 kGy) and the endpoints are not easily measured [39-41]. The use of the fluorescent protein, β-phycoerythrin, as a target molecule in a competition assay minimises many of these possible problems. The measured parameter is fluorescence, rather than absorbance, and the large molecule should react with hydroxyl radicals in a similar manner to biological molecules *in vivo* (see section 1.5).

A measure of the hydrogen (or electron) donating ability of compounds is more

difficult to define. This parameter is usually measured as a redox potential by polarography, which measures the current flowing through a compound solution as a function of applied voltage. The oxidation potential, the voltage at which the current is half maximum ($E_{1,2}$), is used as a measure of hydrogen donating ability. This parameter is difficult to measure for most compounds due to the difficulty in interpreting the multi-step processes. Although there is circumstantial evidence, a conclusive link between the oxidation potential and radioprotective ability has not been reported.

There are several assays that use non-radiation-derived free radicals as the oxidative stress to measure antioxidant and therefore hydrogen donating ability. These include azo-initiators in aqueous systems or *tert*-butyl radicals in lipid systems. Cao *et al.* [ 42] have reported an oxygen-radical absorbance capacity assay for antioxidants based on peroxyl radicals, produced by the azo-initiator 2-2'-azobis(2-amidinopropane) dihydrochloride, oxidising BPE molecules. This method oxidises the sample completely over a 1 hour time scale; but these conditions are not physiologically relevant. This particular assay has successfully been applied to human blood serum and plasma by Ghiselli *et al.* [ 43]. It was shown that the protein fraction of blood serum provides the majority of protective action. Other radical generators are often based on hydrogen peroxide dissociation either by additions of ferrous ions or acetone. Some of these assays show a loose trend with oxidation potential [44-45]. The nature of the experiments often leads to imprecise results, perhaps due to the complex reaction kinetics of the radical generator. A clean radical generator (ionising radiation) and an accurate and quick measuring system would provide better data. These requirements would be met by using β-phycoerythrin as a target molecule.

## 2.4 Chemical Radioprotection *in vivo* and *in vitro*

In 1942 W. Dale from the University of Manchester showed that additions of compounds could protect the activity of enzymes from the effects of ionising radiation [46]. The field of chemical radioprotection was born.

Just a few years later, a loose theory of the protective action led to tests of the protective effect in bacteriophages by Latarjet and Ephrati [ 47]. They identified sufhydryl and amine containing compounds that were particularly effective. During the next few years experiments with mice were published [ 48]. The role of oxygen was recognised as being crucial. Results from mice injected with cyanide (which makes them hypoxic because of haemoglobin binding -although this was not the original point of the experiment) showed that this treatment was extremely effective against radiation toxicity: seventy percent survived a 7 Gy dose, compared with total lethality in the controls [49].

The effects of modifiers on the yield of hydroxyl radicals on the radiosensitivity of mammalian cells have been investigated extensively [ 50]. However, measurements of hydrogen donating compounds *in vivo* have largely been restricted to thiols and indoles. However there were several problems with these compounds, the most significant being their inherent toxicity. This is typified by the 'Walter Reed' compounds such as WR2721. These thiol compounds show a strong radioprotective effect, but are very toxic [ 20]. Most thiols are also vaso-active and interrupt redox reactions involving normal intra-cellular thiols. Often animals survive the radiation dose (in $LD_{50}$ experiments) only to die some time later of the treatment.

In this light, it would be more practical to identify and investigate other

compounds that radioprotect, particularly the large array of plant-derived antioxidants that are present in the natural world and other intra-organism biotics that produce a reductive environment.

Many compounds, again particularly thiols, have been shown to radioprotect cells *in vitro*. Although the quantity of research into the various compounds is immense, the myriad of cellular systems and protocols often means that the data cannot be meaningfully compared. Also the data are sometimes incomplete, with 50% restitution levels undetermined. This is understandable given the difficulty and complexity of doing such experiments.

Two groups of researchers have made important progress in overcoming some of these problems *in vitro*. Roots and Okada [ 51] measured the protective effect of eight different compounds using radiation-induced DNA single strand breaks as the end-point. Sasaki and Matsubara [ 52] measured eight free radical scavengers and antioxidants using protection of irradiated human lymphocytes against chromosome aberration formation as the end-point. The two groups obtained similar qualitative results for the different compounds. Quantitatively the results were very different, highlighting the fact that the end-point and cellular system are important parameters.

# Chapter 3: INTRA-CELLULAR PROTECTIVE SYSTEMS

The 'Oxygen Paradox' is that aerobic organisms cannot exist without oxygen [ 53], and yet oxygen is a highly reactive and therefore potentially dangerous molecule [ 54]. Although complete reduction of oxygen to water, by electron-transport, is a relatively safe process, it involves intermediate reactive oxygen species such as the hydroxyl radical, superoxide anion and hydrogen peroxide (see Figure 3). These agents are thought to be responsible for oxygen toxicity, because they constantly escape from the metabolically active centres and attack sensitive targets in the cell. For this reason, cells possess highly effective antioxidant defense mechanisms, which mitigate the majority of the possible damage.

These defense systems can be classed in two main divisions: hydrogen donating compounds, represented by the vitamin E-vitamin C- glutathione **antioxidant cascade**, and the **enzyme antioxidants**, superoxide dismutase, catalase and glutathione peroxidase. These substances, which protect target molecules against metabolic oxidative stresses, should also protect them against radiation damage by similar mechanisms.

## 3.1 Hydrogen Donation: The Antioxidant Cascade

A major antioxidant pathway has been determined in mammalian cells. It is based on radical transfer from membranes to energy centres in the cell, allowing for the maintenance of a reductive environment throughout the cell cytoplasm [ 55]. Oxidation of a membrane lipid by an oxygen derived free radical results in a lipid radical and after oxidation with oxygen, a peroxyl radical. This radical can easily be propagated

through the membrane. The main defense that cells employ against this is the antioxidant α-tocopherol (vitamin E), which also has an important stabilising influence on membrane fluidity. This lipid soluble molecule has a phenolic headgroup, which can effectively scavenge lipid radicals, forming a quinone radical on the headgroup. The quinone radical is quite stable. However, the oxidised vitamin is rendered useless in defense against lipid peroxidation.

Rather than discard the molecule, it is reduced *in situ* so that it can continue to perform its role. This is achieved by the transfer of the radical from the vitamin E to ascorbic acid (vitamin C) present in the cytoplasm, by hydrogen donation from the ascorbic acid to the quinone radical [ 56]. The oxidised ascorbate radical can, in turn, be reconstituted by hydrogen donation from glutathione [ 57]. This thiol compound is present at high (~5 mmol $L^{-1}$) concentrations inside cells and represents a large fraction of the intracellular antioxidants. The glutathione radical is then reduced by NADPH, the molecular mechanism for energy transfer around the cell. Each component of the cascade can also act independently. In this way, cells expend energy to maintain a reductive environment throughout the cytoplasm, which mitigates oxidative stresses.

## 3.2 Antioxidant Enzymes

The antioxidant enzymes, superoxide dismutase and catalase are also thought to interact to reduce oxidation stress. Superoxide dismutases (SOD) are metallo-proteins that dismute the superoxide anion to hydrogen peroxide.

$$2O_2^{\bullet-} + 2H^{\bullet} \xrightarrow{\quad SOD \quad} H_2O_2 + O_2 \qquad (R3.1)$$
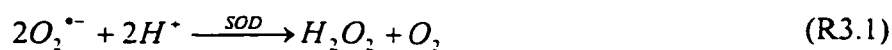
Cu, Zn superoxide dismutase is found in the cytoplasm of mammalian cells and, in

particular, within peroxisome enzyme crystals. Mn superoxide dismutase is found in mitochondria and in prokaryotic cells. Another, undetermined superoxide dismutase has been postulated in blood serum [ 58].

The product of the reaction, hydrogen peroxide, is also a powerful oxidant and needs to be protected against. This is achieved by catalase, another metallo-enzyme found in peroxisome crystals, that catalyses the conversion of hydrogen peroxide to water and oxygen:

$$2H_2O_2 \xrightarrow{\ \ catalase\ \ } 2H_2O + O_2 \ . \tag{R3.2}$$
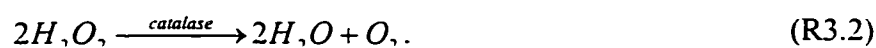
Thus, with the aid of antioxidant enzymes the superoxide radical has been reduced to more benign non-radical forms. Down's syndrome patients over-express Cu, Zn superoxide dismutase by 50%. The resultant imbalance in superoxide detoxification [59-60] may occur due to hydrogen peroxide build up. This may be responsible for observed differences in radiosensitivity. Catalase is also able to remove hydrogen peroxide formed by ionising radiation.

Selenium-containing glutathione peroxidase is the most important antioxidant enzyme, in that it removes peroxide from oxidised molecules (ROOH). It is therefore a secondary line of defense. It utilises hydrogen donated by glutathione (GSH) to produce the restored molecule (RH) and oxidised glutathione (GSSG):

$$ROOH + 4GSH \xrightarrow{\ \ glut.perox.\ \ } RH + 2H_2O + 2GSSG \ . \tag{R3.3}$$
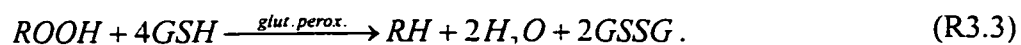
This mechanism is effective in removing damage from proteins that have become oxidised by metabolic processes. It is unclear, however, how effective this enzyme is in protecting against extensive radiation insult. These enzymes have been implicated in the adaptive response. Small doses of radiation induce changes, to varying degrees, in their

activity levels [ 61][ 62], which can be maintained for several cell divisions post-irradiation.

Cells also contain high concentrations of thiolated proteins. The surface sulfhydryl groups are able to effectively donate hydrogen. The proportional effect of these proteins is also unclear.

## 3.3 Other Dietary Antioxidants

The antioxidants vitamin C and vitamin E are essential human dietary nutrients and are often taken in large quantities. A quantity of dietary antioxidants in the form of bioflavonoids and phenols ( up to a gram per day) are also consumed. This often makes these compounds the largest antioxidant component of the diet. It is conceivable that these may also contribute to the cellular defense system. The exact action and biochemistry of these compounds is not well understood. However, phenol and bioflavonoid antioxidants have been shown to modify free radical effects [ 63][ 64].

All these effects come together in biological systems to produce a reductive environment that protects against oxidative stress.

## 3.4 Influence on Inherent Radiosensitivity.

Antioxidant compounds and enzymes, which protect against oxygen-derived metabolic radicals, should also protect against radiation generated radicals. By this logic, cells that naturally have high levels of protective compounds would be better protected against radiation insult. Investigators have tried to correlate radiosensitivity with measured antioxidant levels in cell lysate, particularly the antioxidant enzyme activity. Jaworska *et al.* [ 65] examined superoxide dismutase and catalase activities in two different, but related, murine leukaemia cell lines: L5178Y_R (radioresistant) and L5178Y_S (radiosensitive). They report that the radioresistant line has twice as much superoxide dismutase activity, consistent with the hypothesis that this enzyme was reducing radiation damage. The approach of taking two distinct, but very similar cell lines is important because there are different mechanisms that could radioprotect. These could be: DNA repair, cell cycle arrest or DNA conformation. By using very similar cell lines, these other parameters may be taken as equivalent. This is an assumption that can only be tested with a larger number of data points. Measurement of just two cell lines is inadequate.

Marklund *et al.* [ 66] took the reverse approach, by measuring antioxidant enzyme levels in a larger number (seven; six of which were neoplastic) of widely different human cell lines. They measured Cu, Zn and Mn superoxide dismutase, catalase and glutathione peroxidase activities. The only correlation that they found was between the quasi-threshold dose of the survival curve and glutathione peroxidase levels. It is unclear what this means.

No author has reported measurements made of cell lysate antioxidant capacity for a number of cells of similar type. A suitable model is that of the lymphoblastoid cell line. These immortalised cell lines are human lymphocyte-derived and therefore have similar properties, but also exhibit a wide variance in individual radiosensitivity. Measurements of total radioprotective capacity using the BPE assay made on eight lymphoblastoid cell lines are reported in Chapter 8. Measurements of superoxide dismutase activity are also reported for a number of cell lines.

Human diets vary greatly in the quantity of antioxidants that are consumed. There are also genetic components contributing to variations in cellular antioxidant levels. These parameters could be responsible for some of the variations observed in human radiosensitivity. The use of blood plasma is an effective way of getting a representative sample of a human. Although measurements of blood plasma antioxidant content are found in the literature, no investigators report measuring the total radioprotective effect of plasma. Measurements of total radioprotective capacity made on a number of human blood plasma samples are reported in Chapter 9. The results offer insight into whether variances in human radiosensitivity can be attributed to changes in total antioxidant levels. The indole compound melatonin, which was the best water-soluble antioxidant measured in this study, was able to protect cells *in vitro* from radiation damage (Chapter 10).

# Chapter 4: MATERIALS AND METHODS

This chapter describes the development of the idea of using β-phycoerythrin fluorescence as a measure of radiation induced oxidative stress towards a practical assay. The assay should be a simple, rigorous, quantitative and reproducible technique that is relevant to radiation chemistry. Possible complexities that needed to be examined were the linearity of solution fluorescence with dose (see Appendix I for dose calculations) and quenching effects due to changes in BPE concentration and sample volume. Unfortunately, different batches of BPE solutions showed wide variations in fluorescence intensity. However, this had no bearing on the results using competition kinetics with a fixed end-point, which are shown to be independent of BPE concentration.

## 4.1 Irradiation Of β-phycoerythrin Solutions

Figure 7 shows the effect of irradiating 1 mL volumes of a 24 μg mL$^{-1}$ aqueous aerated solution of BPE, in polystyrene cuvettes, with different concentrations of an antioxidant enzyme, bovine catalase, to different radiation doses. The fluorescence after irradiation is expressed as a percentage of the original fluorescence, as measured by a JASCO FX-777 spectrofluorimeter, using excitation and emission filter wavelengths of 445 and 475 nm respectively. Solutions containing high concentrations of antioxidant show a much slower rate of decrease of fluorescence after irradiation than less concentrated solutions. The response at high concentrations of antioxidant (500 μg mL$^{-1}$) is linear. The slope of the 500 μg mL$^{-1}$ line does not change up to 1500 Gy, where significant damage to catalase begins to occur. This is consistent with the inactivation and

loss of activity indicative of extensive protein damage for catalase and other enzymes of

similar molecular weight, at this dose level, in accordance with target theory.
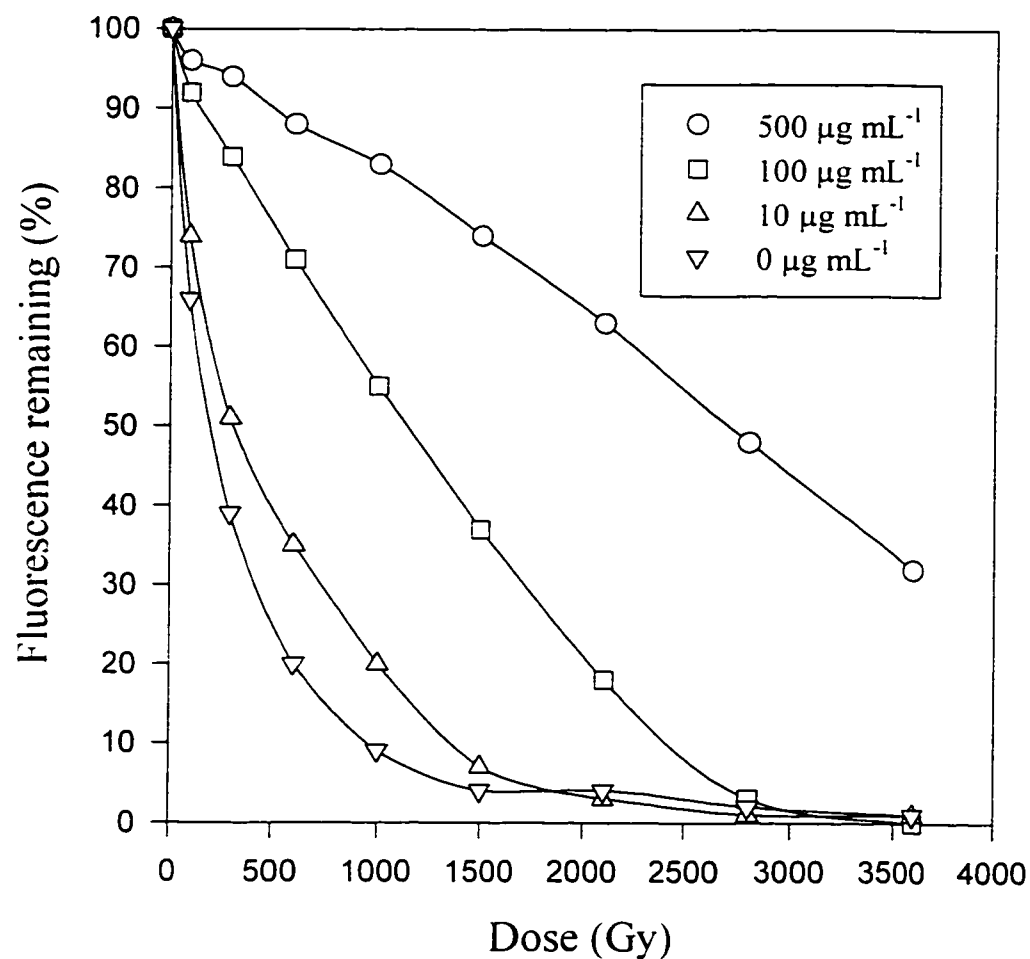
Figure 7: A molecular inactivation curve showing the loss of fluorescence (excitation

wavelength 445 nm; emission wavelength 475 nm) of an aerated BPE solution

(24 μg mL$^{-1}$) as a function of dose, and the protective effect of different bovine catalase

concentrations (0-500 μg mL$^{-1}$). Error bars are smaller than the symbols.
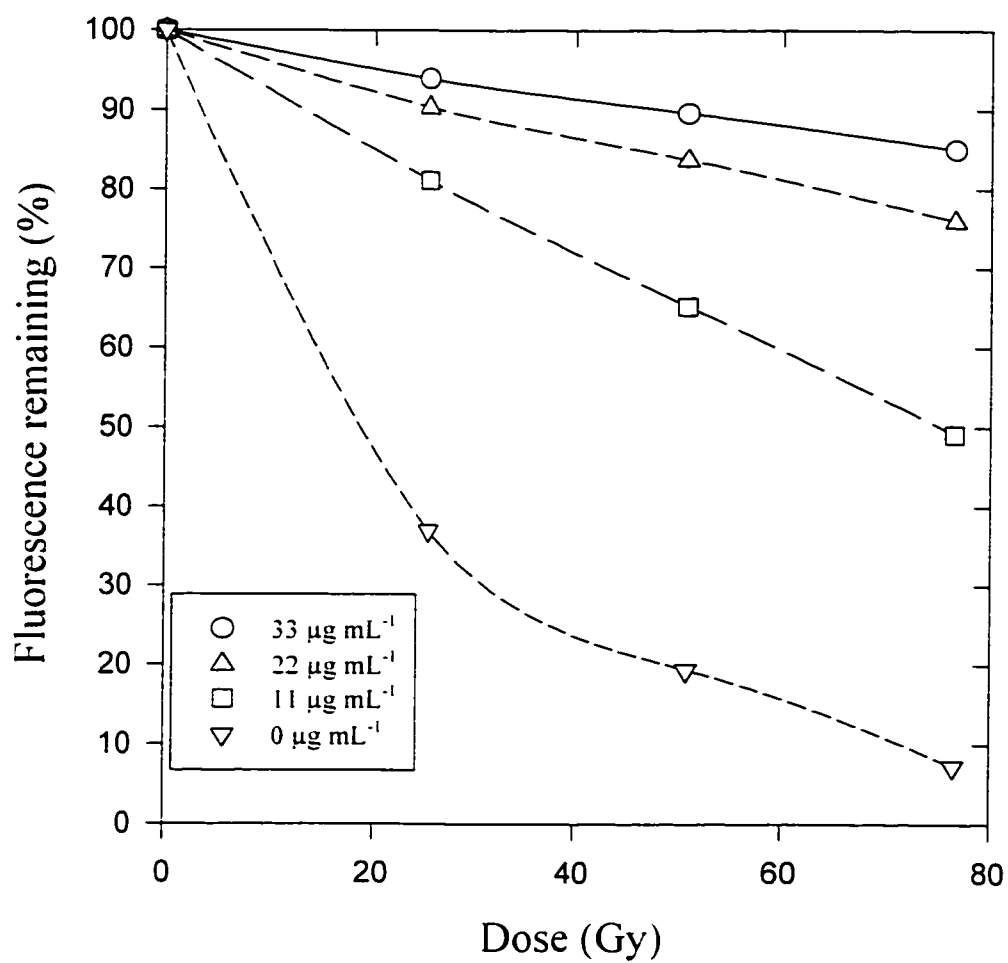
Figure 8: A dose-response curve showing the changes in fluorescence (excitation wavelength 445 nm; emission wavelength 475 nm) for BPE solutions (340 ng $mL^{-1}$) containing different concentrations of bovine Cu, Zn superoxide dismutase as a function of dose. Error bars are smaller than the symbols.
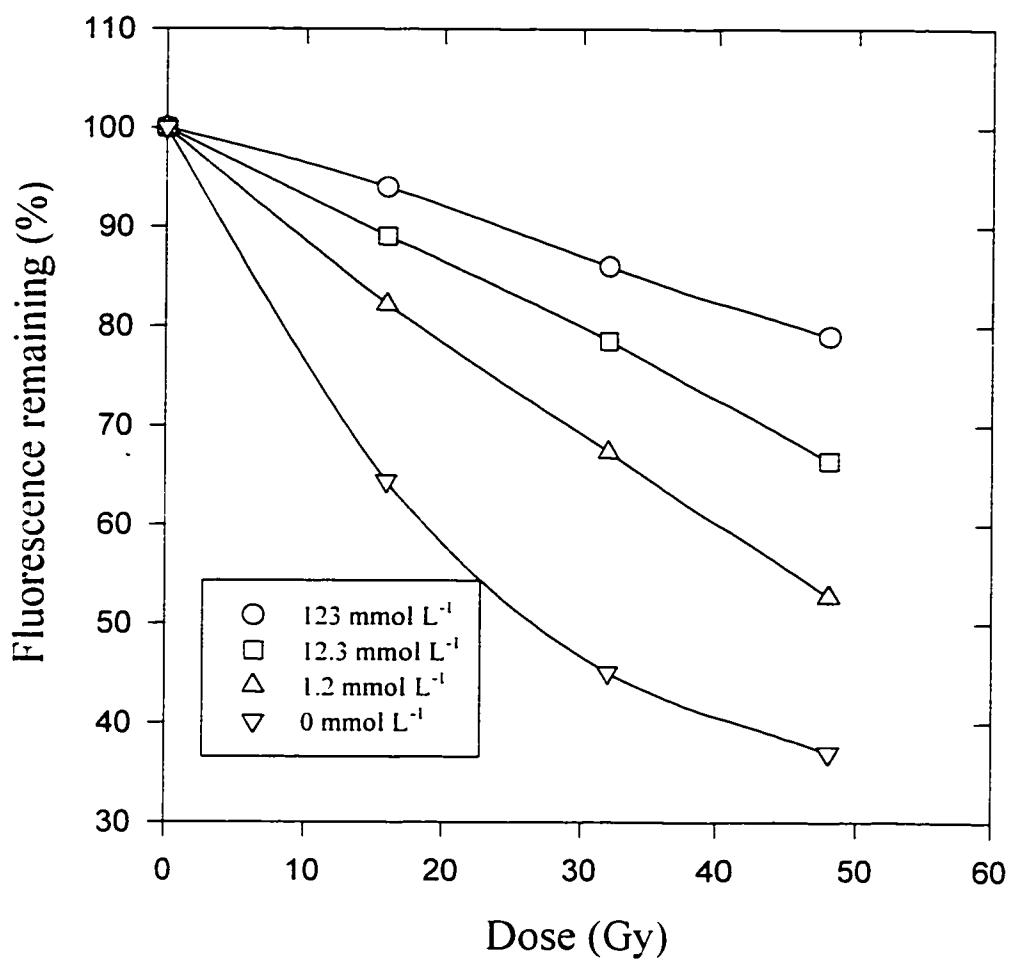
Figure 9: The reduction in fluorescence (excitation wavelength 445 nm; emission wavelength 475 nm) of an aerated BPE solution (340 ng mL$^{-1}$) as a function of dose for different sucrose concentrations (0-123 mmol L$^{-1}$). Error bars are smaller than the symbols.

Figure 10: The changes in fluorescence (excitation wavelength 445 nm; emission

wavelength 475 nm) of a BPE solution (340 ng mL$^{-1}$) after a fixed irradiation (23 Gy;

aerated) as a function of bovine catalase concentration. The 50% restitution concentration

( 1/2 maximal restitution) was found to be 18.5 μg mL$^{-1}$. The 50% restitution

concentration will be used as a standard measure of effectiveness.

The response decreases exponentially with dose for lower antioxidant concentrations. Figure 8 shows a similar curve for another antioxidant enzyme, superoxide dismutase, and Figure 9 confirms the response for a radical scavenger, sucrose. The consistency of the graphical forms suggests that this is a standard response. This would mean that the change in fluorescence after a single radiation dose given to a BPE solution containing a fixed concentration of radioprotector is a representative measure of the direct competition between BPE and added radioprotector for damage as reflected in the slopes of the dose-response curves (Figures 7-9) of the BPE solution fluorescence. Figure 10 shows the response of BPE solutions after a single 27 Gy radiation dose as a function of added bovine catalase concentration. High levels of radioprotector protect the solution resulting in minimal loss of fluorescence after irradiation, although there is always some direct radiation damage. Low levels do not protect as much, resulting in maximal changes in fluorescence. The sigmoid shape on this log-linear scale is an indication of competition for free radicals between catalase and BPE.

## 4.2 The Effect Of Different Radicals On The Protein

A dose of 27 Gy corresponds to an hydroxyl radical production of ~8 $\mu$mol $L^{-1}$, a superoxide production of ~7 $\mu$mol $L^{-1}$ and ~2 $\mu$mol $L^{-1}$ hydrogen peroxide using the G values in Figure 4. The large amount of bleaching with minimal protector (70% loss of fluorescence) after irradiation indicates that these oxidants are effectively damaging the fluorescent protein.

Brief experiments indicated that high concentrations of hydrogen peroxide

(mmol L$^{-1}$) and superoxide radicals generated by a xanthine-xanthine oxidase system also reduce the fluorescence of the BPE solution by 10% in 20 minutes. This is compared with the bleaching by radiation, which produces much lower radical concentrations and acts over much shorter times. This indicates that the most damaging radical produced by water radiolysis, the hydroxyl radical, is orders of magnitude more effective than the other oxidants $O_2^-$ and hydrogen peroxide, in reacting with and destroying the fluorescence of BPE.

## 4.3 The Use Of Microwell Plates

The use of cuvettes was unsuitable because of the large volume of solutions needed (1 mL per cuvette). Another problem was protein bleaching from ultra-violet light pollution. It was observed that BPE solutions were bleached by 20% after an hour under a normal fluorescent lamp. This required that the samples be kept in the dark for as long as possible. These problems were reduced by using 96-well microwell plates, and measuring the fluorescence of each well in a microwell plate fluorescence plate reader. The use of microwell plates allows measurements to be taken in bulk, with small volumes (<0.2 mL), uniform handling and constant excitation times. These properties improve the quality of the data. Microwell plate parameters and dimensions are shown in Figure 11. Although it cannot be ruled out that radiation products from the plastic can react with the BPE protein, this effect is assumed negligible.

## 4.4 Parameters Affecting Solution Response.

The two parameters that might affect solution response were the concentration of BPE and the effect of variations in the volume within each microwell.

The effect of concentration is shown in Figure 12. Different concentrations of

1 mL BPE solutions (pipetted to an accuracy of ~±2%) were irradiated in polystyrene

cuvettes, and the fluorescence measured in the JASCO FX-777 Spectrofluorimeter. It can

be seen that at these concentrations the response is independent of concentration at or

above 250 ng mL$^{-1}$. This indicates a Poissonian type exponential process where the rate of

change of fluorescence is proportional to the BPE concentration

(i.e. $\dfrac{d[BPE_{fluor}]}{dDose} \propto -\lambda \cdot [BPE_{fluor}]$). This might be expected because the probability of a

target surviving (i.e. receiving no hits) when the average number of hits is h is given by

$$P = \frac{h^{0}}{0!} e^{-h}.$$

Figure 13 shows the percent change of a 340 ng mL$^{-1}$ BPE solution after a dose of

radiation (23 Gy) as a function of microwell volume. Although there is variation in the

results (~5%) the regression line shows that there is no correlation between well volume

and response in this assay arrangement.

It was a concern that the much smaller volumes were more sensitive to

contaminants such as dust and stray light irradiation. Special care was needed to avoid

these complications. Plates were only used from freshly opened packets and prepared

solutions were shielded from direct lighting.

For the purposes of consistency a standardised protocol was adopted and a BPE

concentration (340 ng mL$^{-1}$) and a total microwell volume of 250 µL were used. These

values gave a good measurable level of fluorescence while avoiding, somewhat, the

problems of extraneous contaminants.
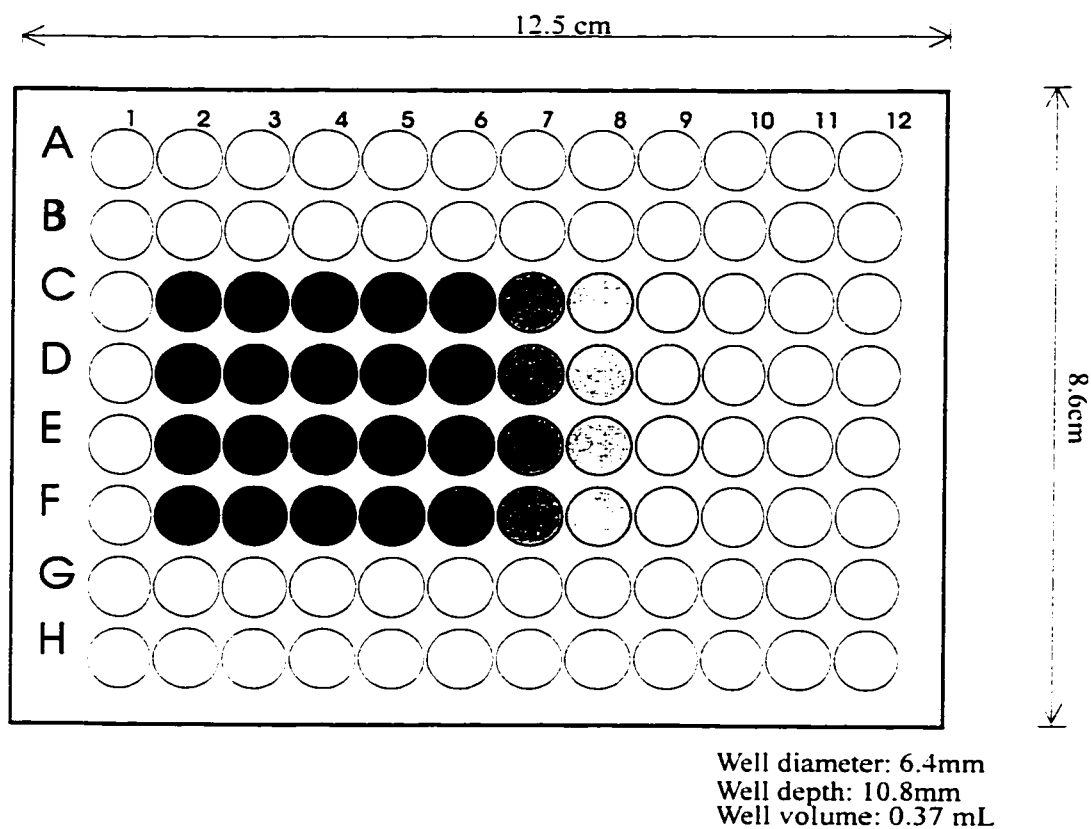
Figure 11: A diagram showing the layout of a 96-well microwell plate. The shading

represents concentration after a serial dilution across the plate.
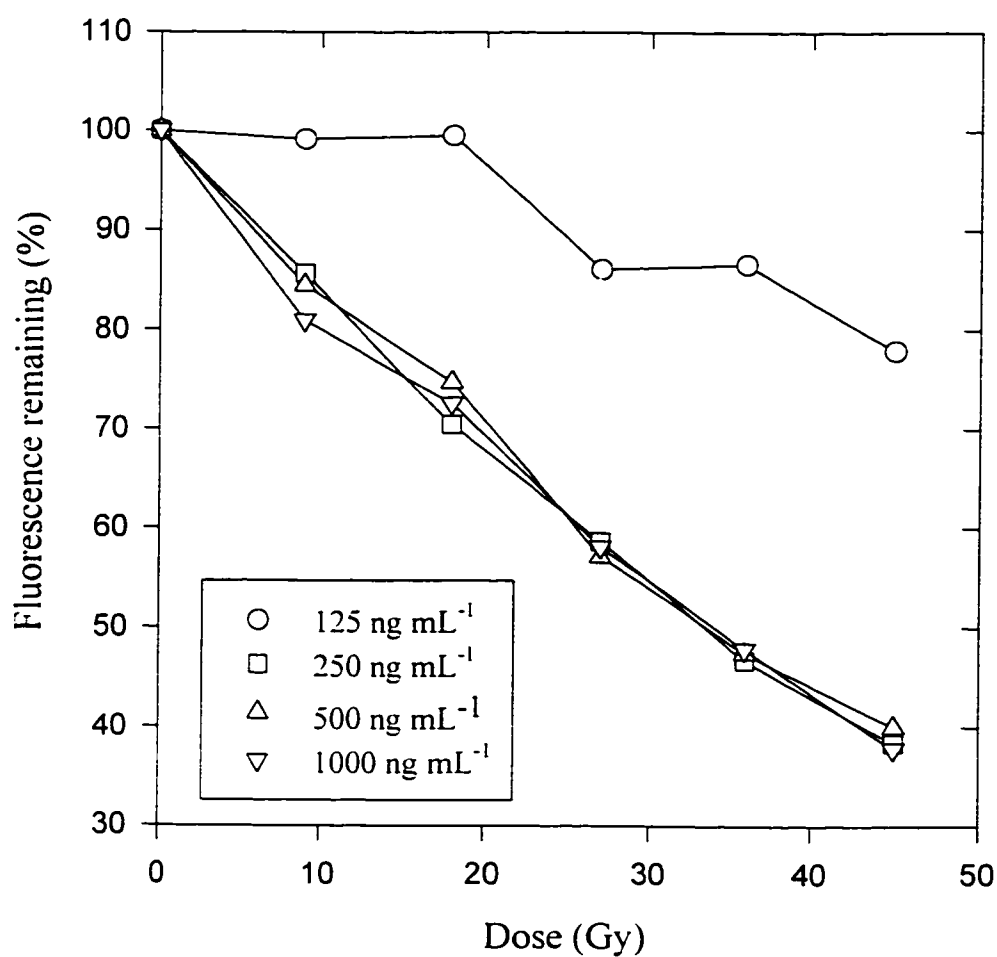
Figure 12: The change in fluorescence (excitation wavelength 445 nm; emission wavelength 475 nm) of different concentrations of BPE as a function of dose without added scavengers. The 125 ng mL$^{-1}$ concentration is near the limit of detection on this medium gain setting. Errors are not shown because of the resulting confusion but are under ±10%, except for the 125 ng mL$^{-1}$ set which approach 20%.
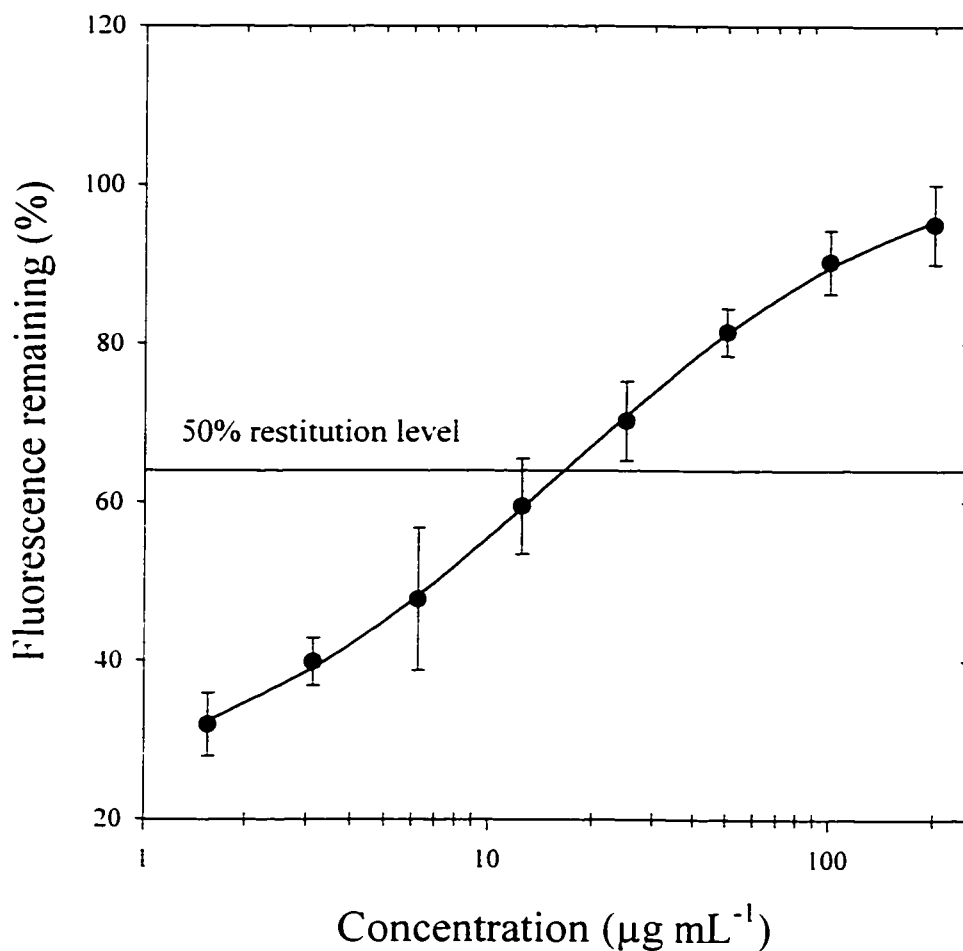
Figure 13: The change in % fluorescence (excitation wavelength 445 nm; emission wavelength 475 nm) of a BPE solution after irradiation as a function of sample volume.

## 4.5 Protocol for the BPE Assay

A 50 µL volume of phosphate buffered saline (PBS) pH 7.4 was placed in each well of a clear polystyrene Nunc 96-well plate with v- shaped bottoms. A further 50 µL of the test sample was then placed in each of the second column of wells (A2-H2 in Figure 11). Using a multiwell pipetter, serial dilutions were made across the plate (9 in total), with each column having half the sample concentration of the previous column. The wells edging the plate were not used as these received a radiation dose 95% that of the central wells. The final column utilised always contained a control with PBS alone. To each well, 200 µL of a stock β-phycoerythrin (BPE) 340 ng mL$^{-1}$ solution in PBS was added. The final concentration of BPE was 272 ng mL$^{-1}$. The fluorescence of each well was measured using an IDEXX Fluorescence Concentration Analyzer (FCA) set on a gain of 5, measuring at an excitation wavelength of 545 nm and emission wavelength of 575 nm. The plate was then placed in an AECL Gammacell 220 cobalt 60 irradiation unit for 30 s at a dose-rate of ~0.6 Gy s$^{-1}$ (see Appendix I). The plate was immediately remeasured in the FCA and the percentage fluorescence remaining calculated for each concentration. The 50% inhibition level was found by fitting the data with errors to a logist function.

The logist function, which describes a sigmoid curve is given by:

$$y = \frac{-(A-D)}{(1+(\frac{x}{C})^B)} + A \qquad \text{(E4.1)}$$

where  A= upper plateau level
D= lower plateau level
C= turning point of the curve (50% restitution level)
B= exponent (indicates gradient)

Fits were performed using the least squares analysis provided by the Sigmaplot

graphics program to provide the constants A, B, C and D with their standard

deviations. Repeat experiments were performed with independent solutions and with

two measurements per point for each experiment run. The 50% restitution

concentration at the point of inflection was chosen because it is the most practical and

reproducible indication of effectiveness. For compound screening this point maximises

differences in effectiveness and serves as a useful parameter for compounds with

different slopes at the point of inflection.

# Chapter 5: CHEMICAL RADIOPROTECTION

**The effectiveness of hydroxyl radical scavenging and hydrogen donation in chemoprotection can be quantitated by using changes in fluorescence of a target protein, β-phycoerythrin.**

This hypothesis can be tested by generating competition curves to calculate 50% restitution concentrations and then substituting these values into Equations E2.4 and E2.7 (see Chapter 2). A correlation with existing literature would be a proof of principle.

Data for hydroxyl radical scavengers is presented in this Chapter. Data for hydrogen-donors and antioxidants is presented in Chapter 6. These results also rank the relative radioprotective effect of these compounds and shed light on the mechanisms by which they protect.

## 5.1 Application of the BPE assay to Hydroxyl Radical Scavengers.

According to Equation E2.4 (Chapter 2) the product of the rate constant, $k$, for the reaction of a scavenger compound with hydroxyl free radicals and the concentration of scavenger [S] to reduce the reaction by 50% should be a constant. If a known value of the rate constant for a reference compound is used then relative rate constants can be

determined for other compounds by $k_{unknown} = k_{known} (\frac{[S_{known}]_{50\%}}{[S_{unknown}]_{50\%}})$ (Equation E2.4). This

approach was tested using the BPE assay.

The compound chosen as the reference standard was dimethyl sulphoxide (DMSO), the structure of which is shown in Figure 14. This is a proven hydroxyl radical scavenger [11]. It was compared for radioprotective effect with other solvents and some sugars.

## 5.2 Solvents as Scavengers in the BPE Assay

The solvents DMSO, ethanol and *tert*-butanol (t-butanol) were tested using the

BPE assay. The results of measurements obtained in the BPE assay are shown in

Figure 15 for DMSO and ethanol. High concentrations of scavenger protect against the

radiation induced loss of fluorescence, low concentrations provide minimal protection.

The forms of the response are the same for the two compounds and both plateau at a

similar fluorescence level (~81%). This could indicate that ethanol, whose structure is

also shown in Figure 14, is protecting by a similar process to DMSO even though they

are structurally different. That is to say, both are competing for free radicals. The results

of the 50% reduction concentrations for three independent repeats are shown in Table 1.

The ratio of the 50% concentrations is also shown together with the average and standard

error of the relative reaction rate constant calculated from these values. The results for

ethanol compare well with previously calculated values [6].
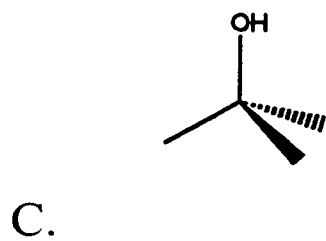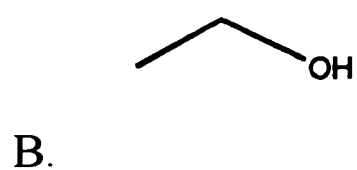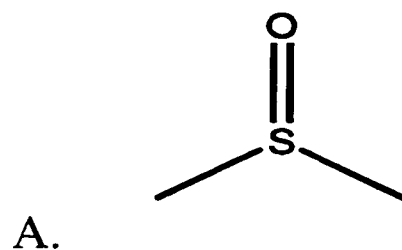
Figure 14: The chemical structures of A. DMSO, B. ethanol and C. *tert*-butanol.

*tert*-Butanol ( Figure 14) is an important solvent in chemical radioprotection. Hydrogen abstraction from one of the methyl groups results in a carbon centred radical which is shielded by the other methyl groups. This results in the reduction of interfering secondary radical reactions, such as the transfer of the radical to another target molecule [ 67]. It is not a particularly efficient radical scavenger with a reaction rate constant about 30% that of ethanol. A typical example of this solvent in the BPE assay is shown in Figure 16. Because of the low rate of reaction with hydroxyl radicals, high concentrations of radical scavenger are required (20% v/v) to compete. The effect of adding such high concentrations of a solvent to a protein can be seen in the distorted data which were repeatable. This was due to denaturation and perhaps micro-precipitation of the protein under these extreme conditions. The 50% restitution concentrations of the experiments are also shown in Table 1. The final result for the reaction rate constant for *tert*-butanol with hydroxyl free radicals is about half what one would expect based on the well established value [6].

This problem of protein-solvent interaction represents a limitation for the assay because there are other solvent radical scavengers e.g. acetone, that have a lower reaction rate. Higher concentrations of such compounds are required to compete in the assay. These problems could be overcome by adjusting the concentration of BPE so that lower concentrations of solvent could be used. The lower concentrations of BPE could be measured by increasing the gain of the photomultiplier tube and by increasing the solution volumes. These changes were difficult to achieve using the IDEXX FCA.

| | 50% Reduction Concentrations ( μmol L⁻¹) | | | [Ref.]$_{50\%}$/ [Test.]$_{50\%}$ | $k_{OH}$calculated (L mol⁻¹s⁻¹) | $k_{OH}$established (L mol⁻¹s⁻¹) |
|---|---|---|---|---|---|---|
| Ref.: DMSO | 96.0 | 334 | 94.5 | | | $6.6\times10^9$ |
| Test: Ethanol | 367.0 | 1420 | 357.6 | 0.25±0.01 | 1.67±0.09×10⁹ | $1.7\times10^9$ |
| Ref.: DMSO | 48.3 | 319.4 | | | | $6.6\times10^9$ |
| Test: t-Butanol | 1288 | 5418 | | 0.05±0.01 | 3.2±0.07×10⁸ | $6.0\times10^8$ |

Table 1: The results for a series of experiments with solvents ethanol, tert-butanol and DMSO using the BPE assay. 50% reduction concentrations are shown together with calculated and established reaction rates [6].

| | 50% Reduction Concentrations ( mmol L⁻¹) | | | [Ref.]$_{50\%}$/ [Test]$_{50\%}$ | $k_{OH}$calculated (L mol⁻¹s⁻¹) | $k_{OH}$established (L mol⁻¹s⁻¹) |
|---|---|---|---|---|---|---|
| Ref. :DMSO | 0.172 | 0.139 | 0.141 | | ------- | $6.6\times10^9$ |
| Test: Sucrose | 0.462 | 0.436 | 0.436 | 0.34±0.02 | 2.23±0.16×10⁹ | $2.3\times10^9$ |
| Ref.: Sucrose | 0.710 | 1.249 | 0.933 | | 2.23×10⁹ | $2.3\times10^9$ |
| Test: Glucose | 1.074 | 1.549 | 1.322 | 0.72±0.06 | 1.61±0.13×10⁹ | $1.5\times10^9$ |
| Ref.: Sucrose | 4.263 | 2.599 | 2.859 | | 2.23×10⁹ | $2.3\times10^9$ |
| Test: Sorbitol | 4.156 | 3.375 | 3.356 | 0.88±0.11 | 1.96±0.24×10⁹ | None established |

Table 2: The results for three experiments with the sugars sucrose, glucose and sorbitol using the BPE assay. The 50% reduction concentrations are shown together with calculated and established rate constants [6].
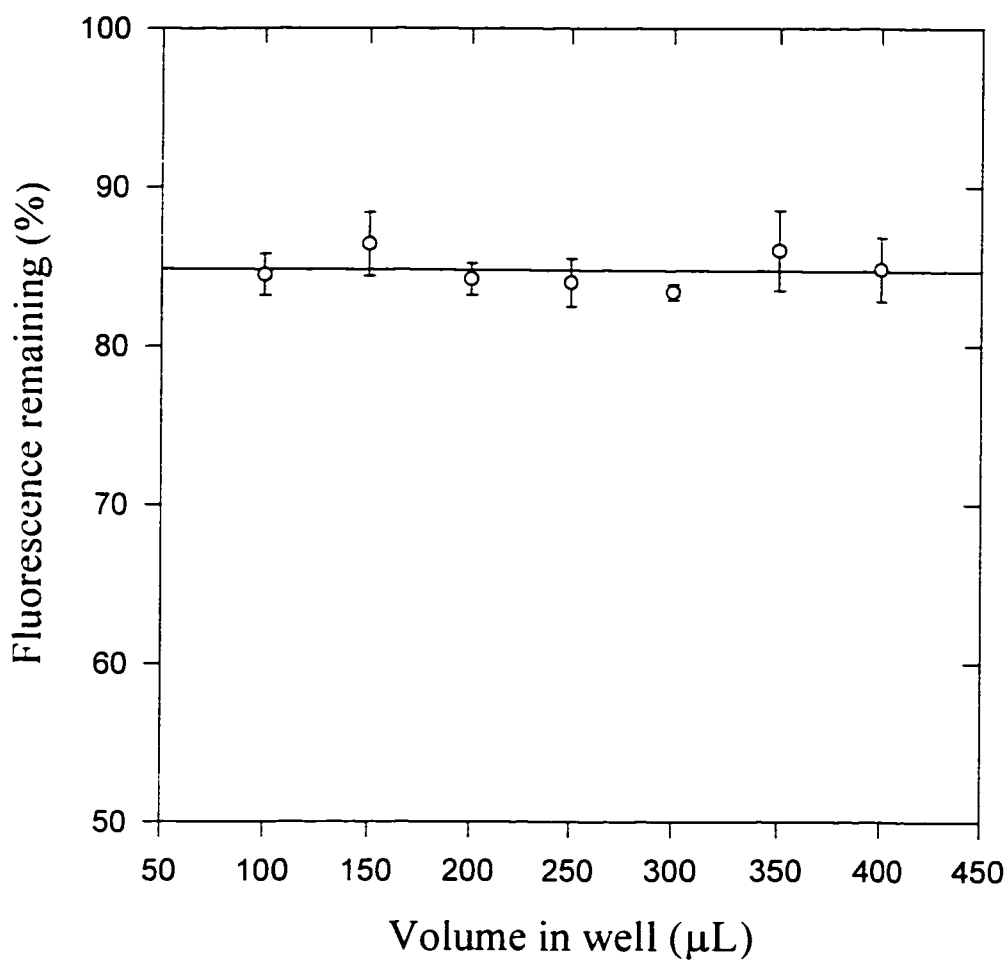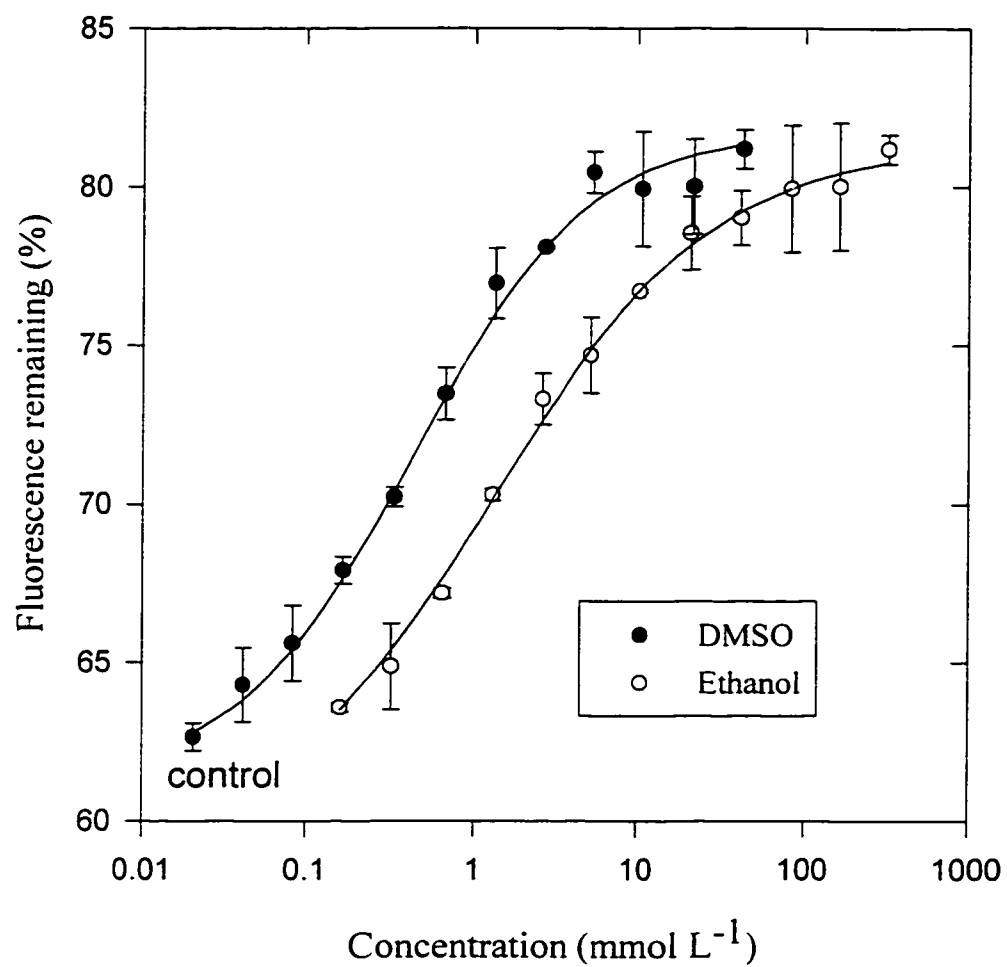
Figure 15: The change in fluorescence (excitation wavelength 545 nm; emission wavelength 575 nm) of a BPE solution after irradiation as a function of ethanol and DMSO concentration.
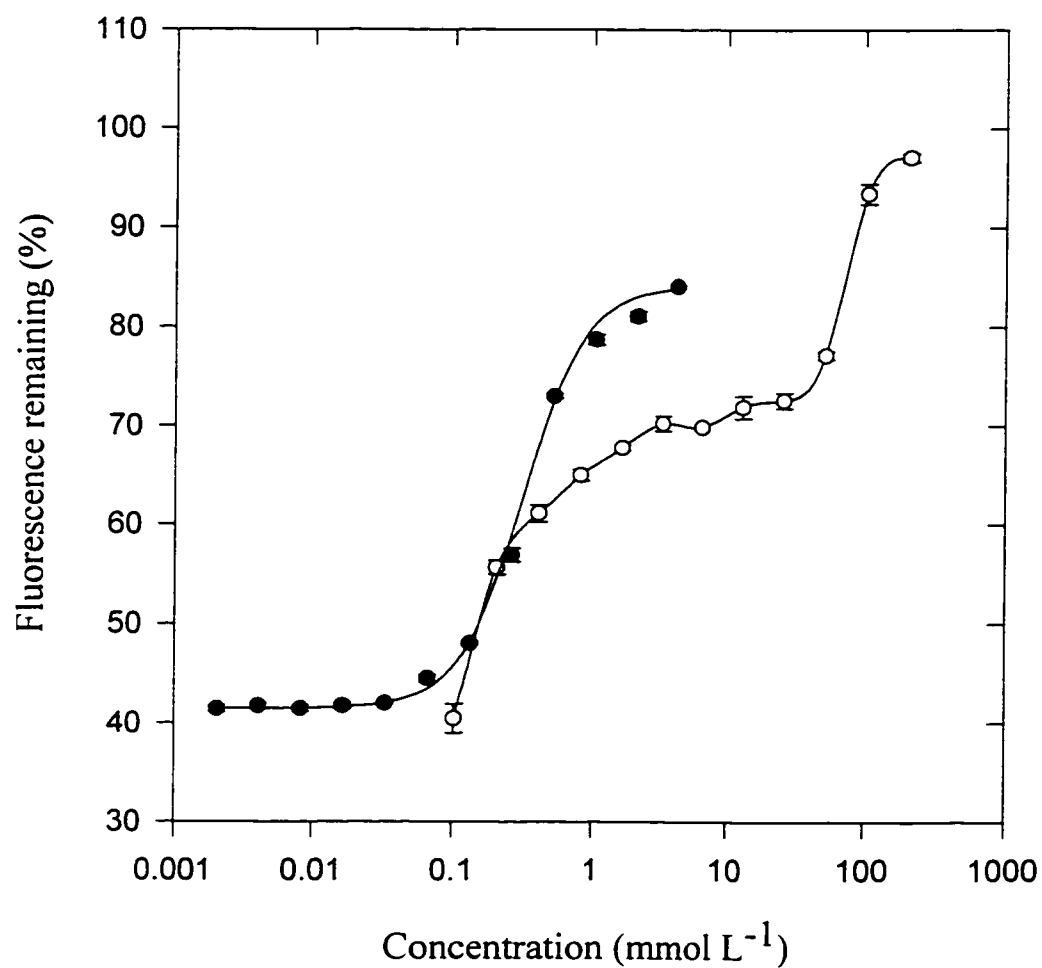
Figure 16: The reduction in fluorescence (excitation wavelength 545 nm; emission

wavelength 575 nm) of a BPE solution after irradiation as a function of *tert*-butanol and

reference (DMSO) concentration.

## 5.3 The Sugars: Sucrose and Glucose

Figure 17 shows the structures of the sugars sucrose, glucose and sorbitol. The results of one experiment with sucrose in the BPE assay are shown in Figure 18. DMSO was again used as the reference standard. The form is similar to that described previously. Table 2 shows the 50% reduction concentrations from three independent experiments. The reaction rate constants calculated from these values, also shown in Table 2, are very similar to the established values, within error margins.

Glucose is the basis for many complex carbohydrates such as cellulose and starch and therefore its scavenger properties are indicative of the radioprotective ability of these other more complex compounds. Figure 19 shows the results for glucose in the BPE assay and Table 2 shows the good reproducibility of triplicate results. The relative standard used was sucrose because the two sugars are more structurally related to each other than to DMSO. The rate constant value used for sucrose is the one obtained here ($2.23 \times 10^9$ L mol$^{-1}$s$^{-1}$) which is in good agreement with the literature value ($2.3 \times 10^9$ L mol$^{-1}$s$^{-1}$) [6].

Sorbitol's structure is shown in Figure 17 as an open sugar ring. It is commonly found in pharmaceutical products, particularly vitamin preparations and tablets, which means it is frequently found in products that are gamma sterilised.

The reaction rate constant between sorbitol and hydroxyl free radicals has not been measured previously. Figure 20 shows the results of one experiment with sorbitol in the BPE assay. Sucrose was again used as a relative standard. The form of the curves are similar indicating that sorbitol too is a free radical scavenger. The 50% reduction

A.

B.

C.
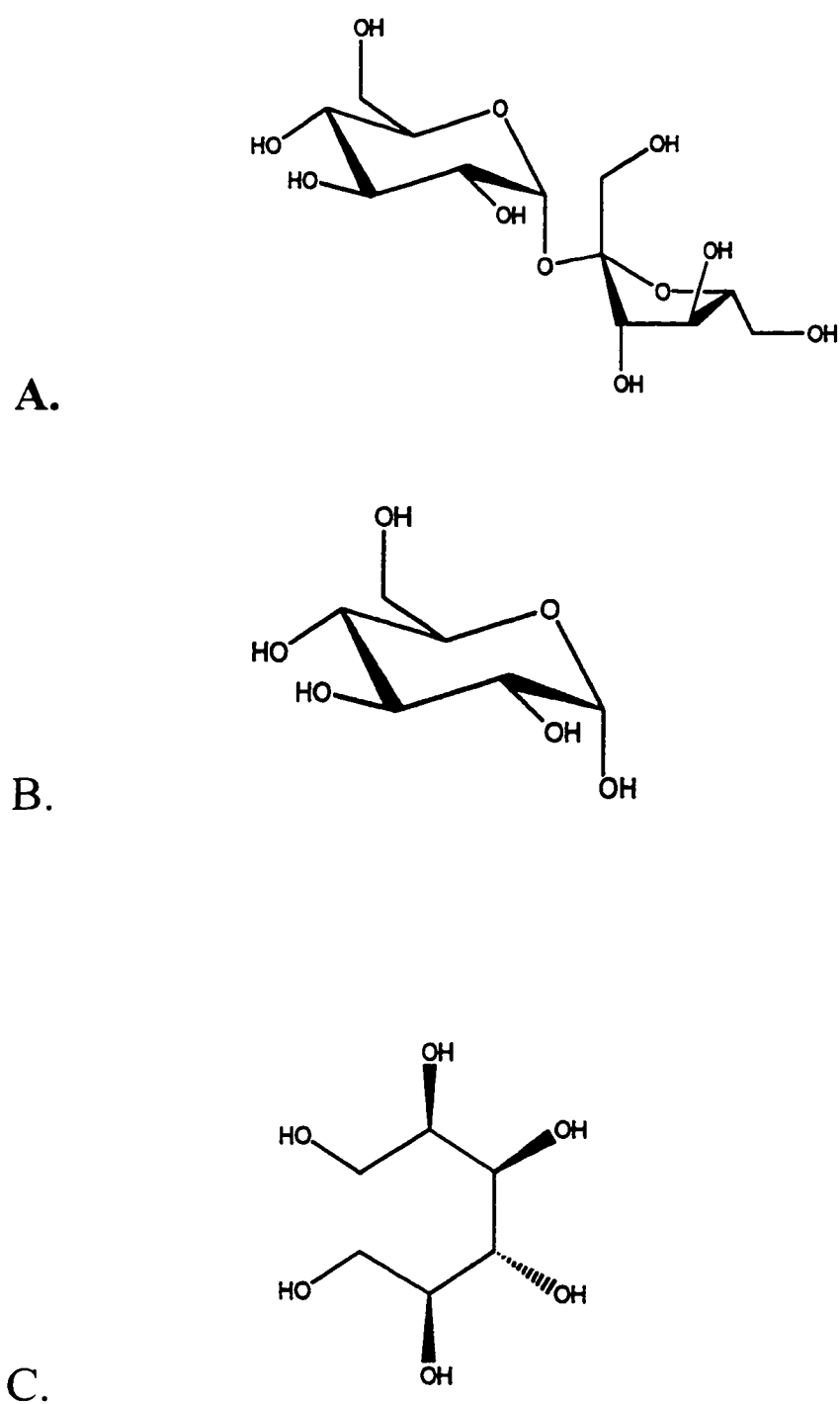
Figure 17: The chemical structures of A. sucrose, B. glucose and C. sorbitol, showing their three dimensional nature.
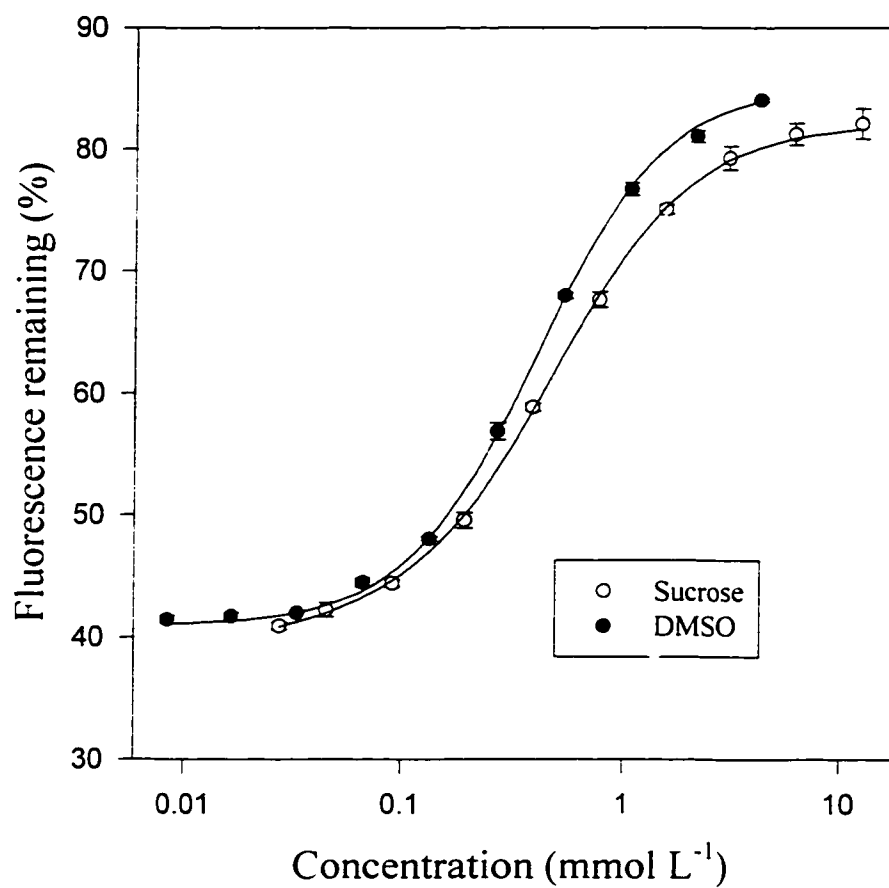
Figure 18: The change in fluorescence (excitation wavelength 545 nm; emission

wavelength 575 nm) of a BPE solution after irradiation as a function of sucrose and

reference (DMSO) concentration.
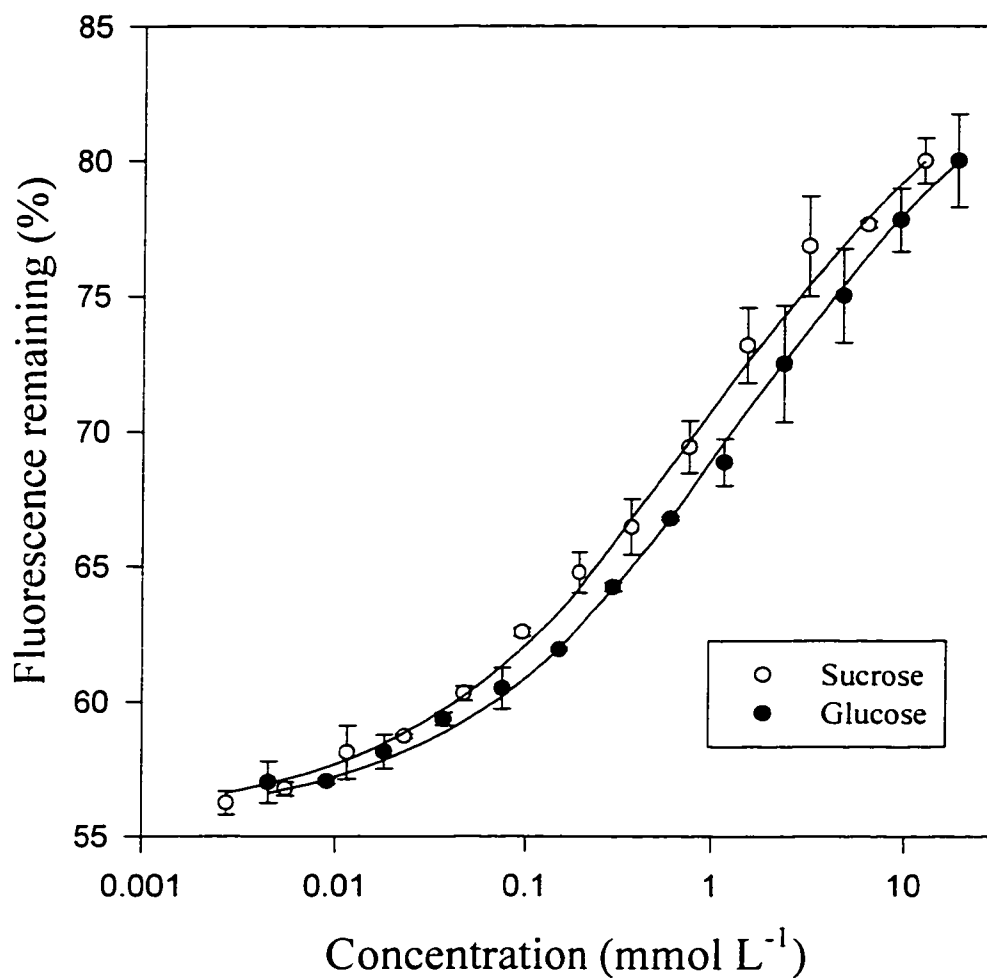
Figure 19: The change in fluorescence (excitation wavelength 545 nm; emission

wavelength 575 nm) of a BPE solution after irradiation as a function of glucose and

reference (sucrose) concentration.
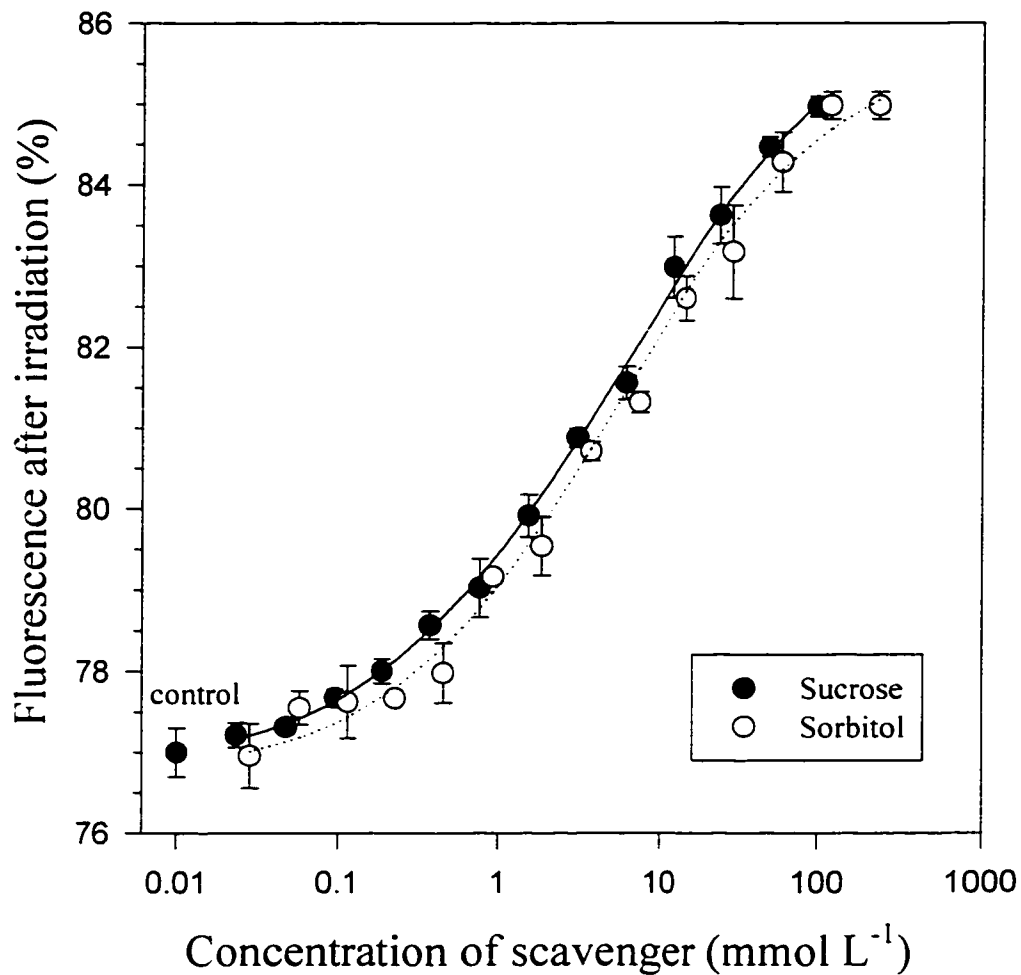
Figure 20: The change in fluorescence (excitation wavelength 545 nm; emission wavelength 575 nm) of a BPE solution after irradiation as a function of sorbitol and reference (sucrose) concentration.

concentrations of three experiments are shown in Table 2. The calculated reaction rate

constant, shown in Table 2 is similar to compounds with similar structures such as

glycerol ($k_{OH}$=1.9×10$^9$L mol$^{-1}$s$^{-1}$) [6].

## 5.4 Discussion

Figure 21 shows a summary of the results for measurements made on these pure

free radical scavengers. The calculated values are plotted against the established values

published in reference [6]. The regression line was calculated excluding the results for

*tert*-butanol and sorbitol. The slope of the regression is 0.996±0.9% ($r^2$=0.999). The

excellent agreement between the calculated and established values indicates that hydroxyl

radical scavenging is the principal mode of radioprotective action for these compounds. It

also indicates that carbon centred radicals produced by the primary radical reactions are

not interfering with, or contributing significantly to, the reduction in BPE fluorescence.

The BPE assay can therefore determine reaction rate constants between hydroxyl radical

scavengers and hydroxyl radicals within error margins.

Using this method the reaction rate constant for sorbitol, a hydroxyl radical

scavenger, which had not been previously measured, was calculated to be

1.96×10$^9$ L mol$^{-1}$s$^{-1}$. This is similar to what might be expected on the basis of compounds

with similar structures e.g. glycerol ($k$=1.9×10$^9$ L mol$^{-1}$s$^{-1}$).

An observation is that the results for these compounds are grouped in the region

of 0.5-5×10$^9$ Lmol$^{-1}$s$^{-1}$. DNA, whose deoxyribose sugar backbone is a site for hydroxyl

radical attack, is also in this range and has a reported reaction rate of $5.8 \times 10^8$ L mol$^{-1}$s$^{-1}$ [6]. DMSO is a somewhat better scavenger than these other molecules. The result for *tert*-butanol does not show a gross deviation from the regression line even with the known interference.

Figure 22 is a plot of the data presented here, against the concentration ($[P]_{1,2}$) required to provide half-maximal protection *in vitro*, as measured by other authors for DNA damage endpoints. The data for DMSO come from Littlefield *et al.*[ 68] for chromosomal aberrations. The rest of the data comes from Roots and Okada [51] for modulation of DNA single strand breaks (SSBs). On this log-log plot the slope is -1.1±0.1 ($r^2$=0.981), indicating an inverse correlation between the two data sets. This indicates that the BPE assay is an indicator of radioprotective effect for chromosomal damage, and therefore for enhanced radiation survival *in vitro* for free radical scavengers such as those described here.

Examination of the 50% reduction concentrations as a whole indicates significant variation between experiments (>30%). This was due to inter-batch BPE differences and day to day handling variations. However, the ratio of the 50% restitution concentrations is highly consistent between experiments. This highlights the necessity of measuring the test and reference compound samples under identical conditions. The 10-15% error in the rate constants probably arises from the weighing and dilution errors. The time between pre- and post-irradiation measurements was kept to below 5 minutes. Care was taken to minimise these errors at each stage.
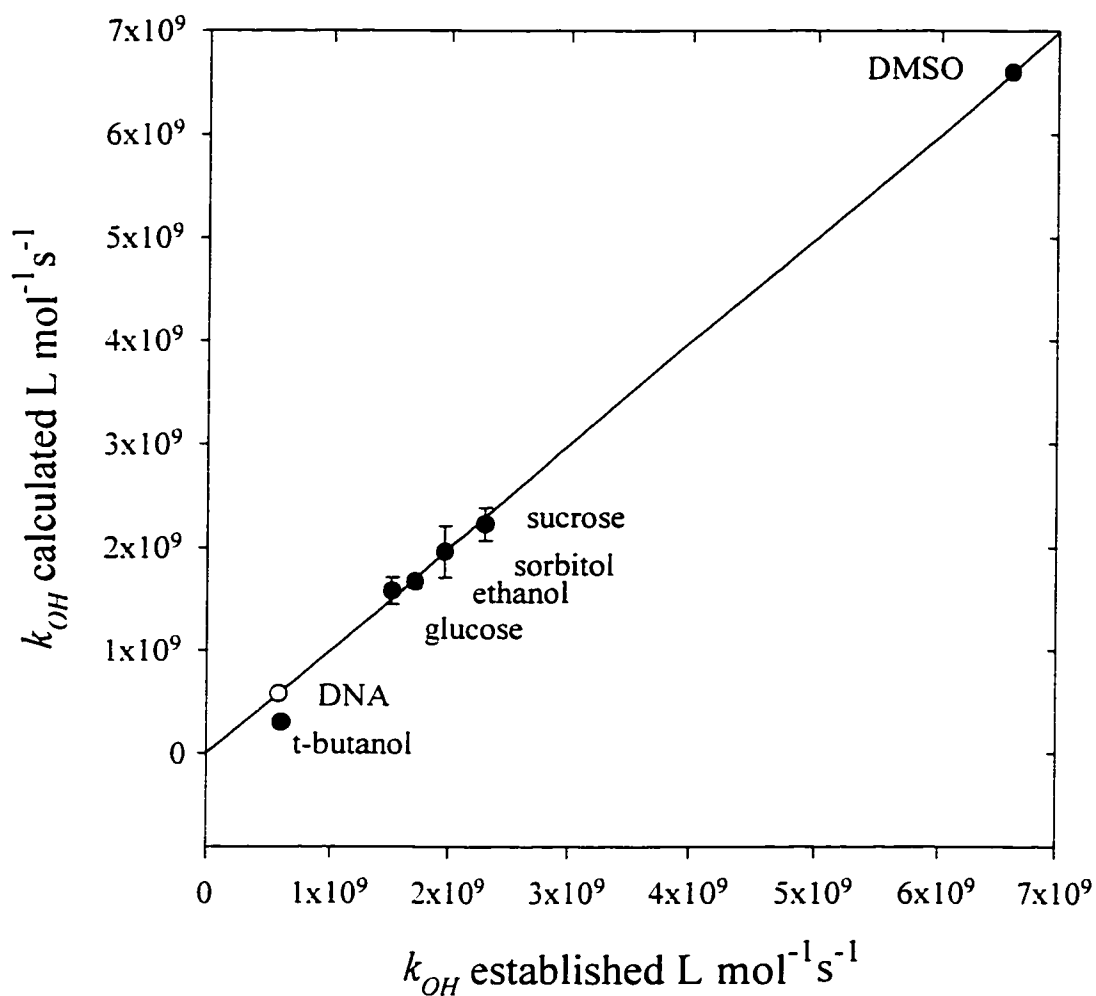
Figure 21: A comparison between measured and published rate constants for the reactions of free radical scavengers with hydroxyl free radicals. The value for sorbitol is on the graph but was not included in the calculation for the regression. The DNA point is for demonstration purposes only. The error bars for *tert*-butanol are smaller than the symbol on this scale.

1 ●

DMSO

sorbitol

ethanol

$k_{compound}/k_{DMSO}$

0.1

*tert*-butanol

0.1                    1

$[P]_{1/2}$ (mol L$^{-1}$)
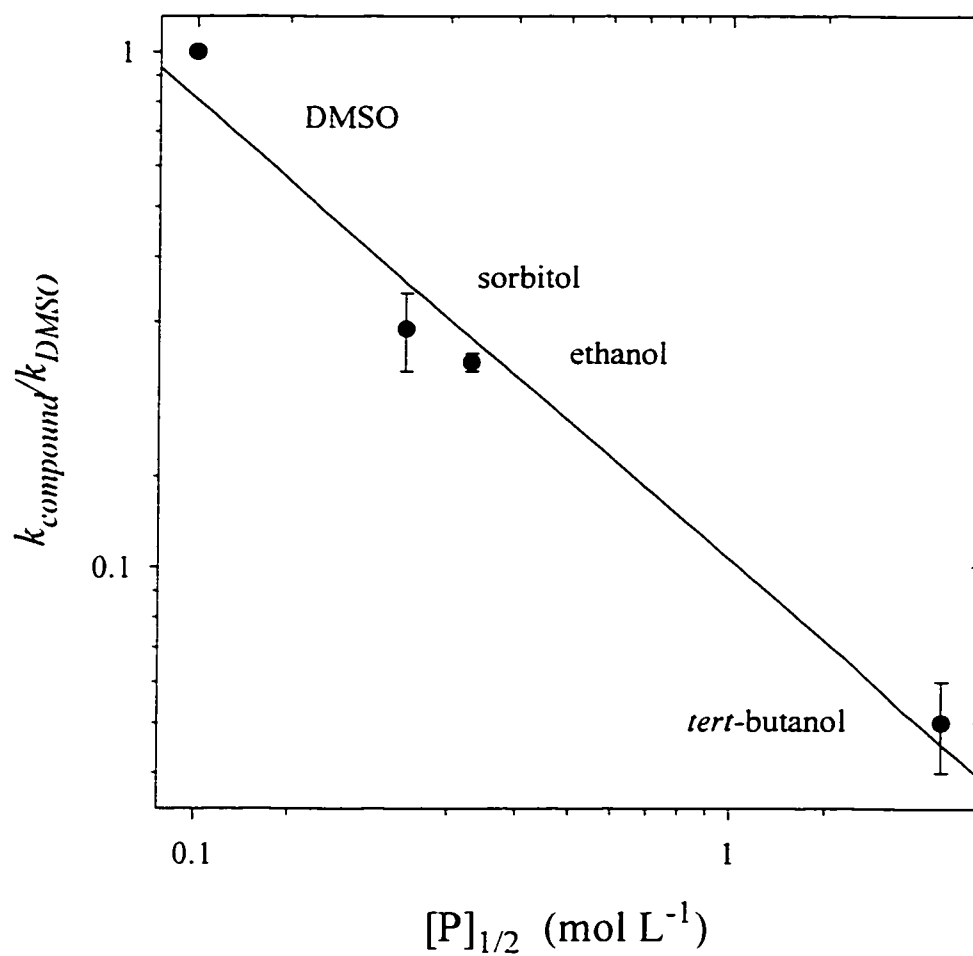
Figure 22: The measured ratio of hydroxyl radical reactivities for solvents (*tert*-butanol,

sorbitol and ethanol) relative to that of DMSO, as a function of their concentrations to

halve the number of radiation-induced single strand breaks in DNA ( $[P]_{1/2}$ ) as reported

by Roots and Okada [51]. Data for sorbitol were not included in the regression fit.

## 5.5 Ascorbic Acid

Ascorbic acid (Vitamin C) is one of the most commonly used and abused antioxidant vitamins. Because of its importance in terms of diet and its high solubility in water this compound was chosen as the first antioxidant to be measured in the BPE assay. The structure of vitamin C (shown in Figure 23) consists of a phenol ring with two hydroxyl groups. This compound was initially compared to the reference free radical scavenging compound (DMSO). The reaction rate constants for these compounds with hydroxyl free radicals are about equal ( $k_{vitC}$=6.0×10$^9$ L mol$^{-1}$s$^{-1}$ ; $k_{DMSO}$=6.6×10$^9$ L mol$^{-1}$s$^{-1}$). The 50% reduction concentrations are shown in Table 3 with one experiment being shown graphically in Figure 24. The results of the 50% reduction concentrations show clearly that the antioxidant is a much more effective radioprotector than DMSO in the BPE assay. DMSO is protecting primarily by free radical scavenging. Ascorbic acid must be protecting by a different mechanism. The shape of the curve is very similar to that of DMSO indicating a competition type process. The fact that both compounds saturate to the same level of protection indicates that this different process also acts indirectly. These observations are consistent with the known qualities of antioxidants competing with oxygen fixation by donating a hydrogen atom (or an electron). Calculation of reaction rates for antioxidants with hydroxyl radicals assuming hydroxyl radical scavenging mechanisms would result in reaction rates orders of magnitude higher than those allowed purely on the basis of diffusion restrictions. Therefore, the 50% level for vitamin C and other antioxidants is a measure of the restitution of the target rather than a measure of the reduction in the reduction in reaction.

Pulse radiolysis experiments confirm this fact. Redpath and Willson have examined the complex radiation chemistry of ascorbic acid in a pulse radiolysis system [ 69]. They examined the direct scavenging of the primary oxidative hydroxyl radicals, the scavenging of secondary free radicals (formed by reaction of primary species with non-target molecules) and the repair of the oxidative free radical lesion by electron transfer or hydrogen donation. This additional protection mechanism involves secondary reactions in competition with the oxygen fixation step (Reaction R1.11), and is described by Reaction R5.1:

$$BPE \cdot + vitC_{-H} \longrightarrow BPE_{-H} + vitC \cdot \qquad (R5.1)$$

For a similar reaction involving a malonate radical, the reaction rate constant between the malonate radical and ascorbate was found to be $k = 1.3 \pm 0.7 \times 10^7 \ L \ mol^{-1}s^{-1}$.
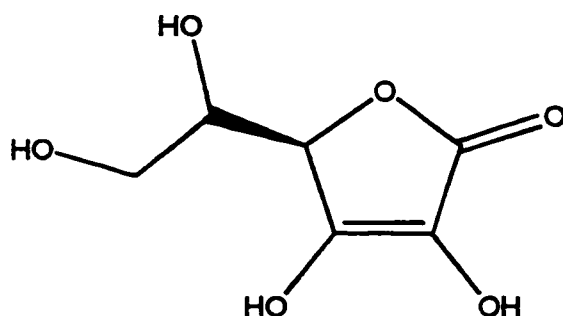
Figure 23: The chemical structure of ascorbic acid.

| | Test: Vitamin C<br>($\mu$mol L$^{-1}$) | Reference: DMSO<br>($\mu$mol L$^{-1}$) |
|---|---|---|
| Experiment 1 | 3.66 | 114.6 |
| 2 | 3.75 | 141.7 |
| 3 | 4.50 | 186.8 |
| [DMSO]$_{50\%}$/[ Vit.C]$_{50\%}$ | 36.8±4.2 | |

Table 3: The 50% reduction concentration of DMSO compared with the 50% restitution concentration of ascorbic acid for three experiments using the BPE assay.
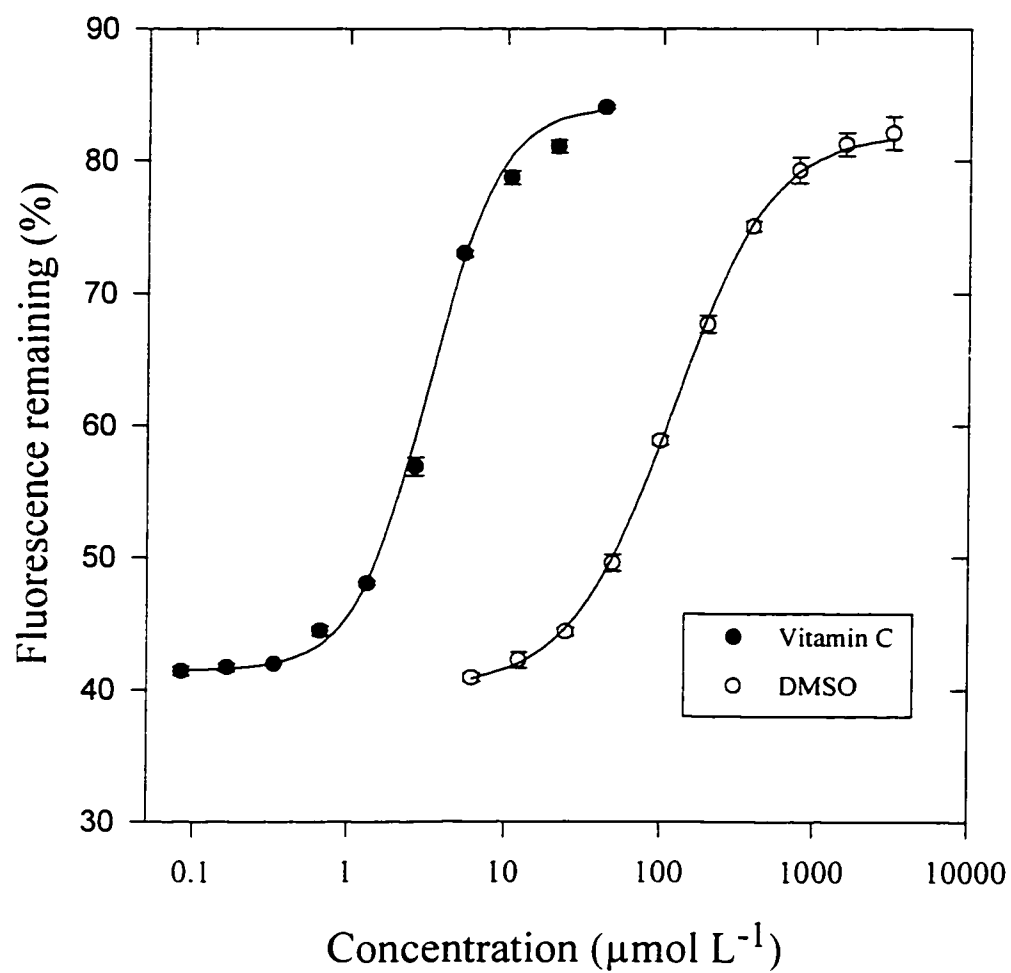
Figure 24: The change in fluorescence after irradiation of a BPE solution as a function of

vitamin C concentration. The reference compound is DMSO.

# Chapter 6: ANTIOXIDANTS IN THE BPE ASSAY

Three different classes of water soluble antioxidants have been examined using ascorbic acid as a reference compound.

**Thiols**, such as glutathione, cysteine and mercaptoethanol (see Figure 25) , have long been associated with radioprotection [27][ 70]. They contain effective hydrogen donating sulphhydryl groups and have a relatively low toxicity. However, they do not protect at levels that could be used practically as radioprotectants because of inherent systemic toxicities [49].

**Phenols** (see Figure 26), such as those derived from plant bioflavonoids and tannins, are also effective radioprotectors [ 71][ 72]. The delocalised carbon rings are electron donating and are readily oxidized by loss of a hydrogen from an hydroxyl side group. They are often constituents of plant flavonoids and tannins which account for a large fraction of dietary antioxidants.

**Indoles** (see Figure 27) have also been recognised as efficient antioxidants and have been the subject of renewed interest with the recent developments in melatonin research [ 73].

## 6.1 Materials And Methods

Trolox, a water soluble vitamin E analog, was supplied by the Aldrich Chemical Co., and all other compounds were obtained from the Sigma Chemical Co. Antioxidant compounds were dissolved in PBS to an initial concentration of 10 mg mL$^{-1}$. Each stock solution was diluted to 100 µg mL$^{-1}$ in PBS. Stock solutions were made freshly on a daily basis. Each sample was then measured by the BPE assay.

## 6.2 Results And Discussion

Figure 28 shows the change in fluorescence of a 340 ng mL$^{-1}$ BPE solution after irradiation as a function of added antioxidant (mercaptoethanol) concentration. Ascorbic acid (vit. C) was used as the reference compound and its response is also shown . High concentrations of antioxidant protect the BPE protein, although there is always some damage due to direct radiation effects. Low concentrations provide minimal protection. The 50% restitution levels are indicated. It is unclear why the slopes at the 50% restitution level are different for the two compounds. It was observed that most compounds had slopes similar to the mercaptoethanol slope rather than that found for ascorbic acid. This could be due to the two electron oxidation possible for ascorbic acid compared with a one electron oxidation for the other compounds [55].

These data represent duplicate measurements on the same sample. Experiments were repeated three times with each independent sample being measured in duplicate. The triplicate results for 50% restitution concentrations of this test compound and 15 others are shown in Table 4, together with the ratio $[vitC]_{50\%}$/$[test]_{50\%}$, as an indication of relative radioprotective effect, and standard deviation as a measure of the uncertainty involved in this assay. The compounds are listed in increasing order of effectiveness. Figure 29, which is a graphical form of Table 4, clearly shows that the compounds can be grouped into three main antioxidant classes.

Sulfhydryl compounds range from 1.27 to 2.85 times more effective than vitamin C.

Cysteine hydrochloride and acetyl cysteine are not statistically different from each other, although the acetyl group seems to confer a slight advantage. Homocysteine was
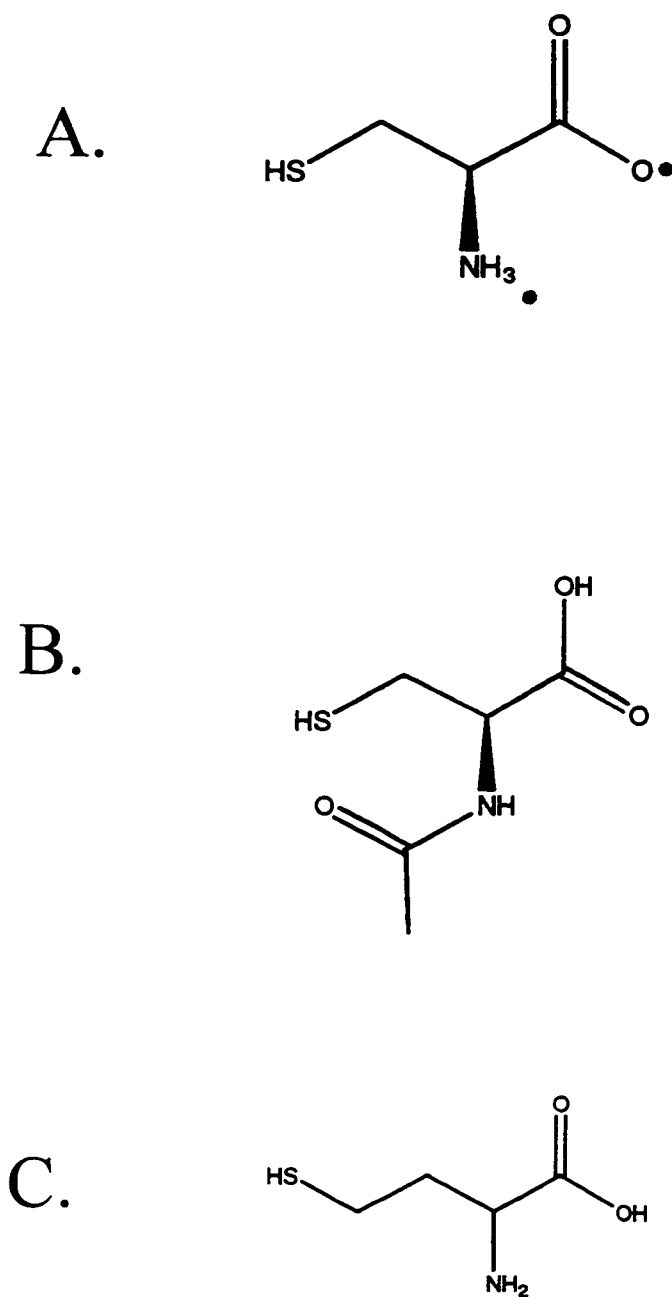
Figure 25: The chemical structures of A. L-cysteine; B. acetyl-cysteine and C.

homocysteine.
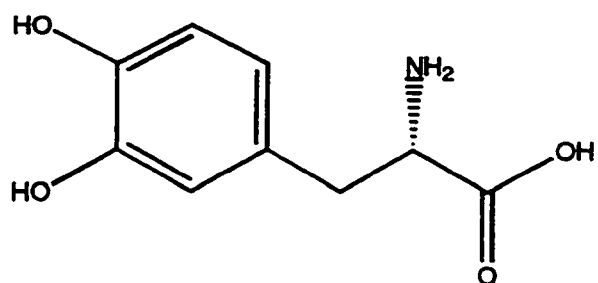
A.
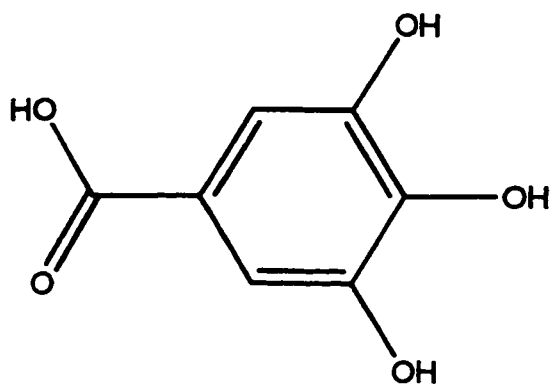
B.
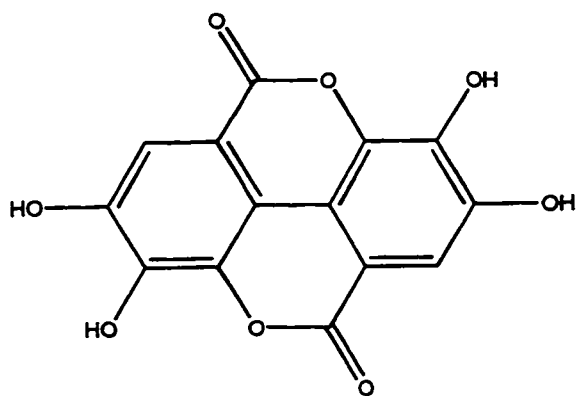
C.

Figure 26: The structures of A. L-dopa; B. gallic acid and C. ellagic acid.
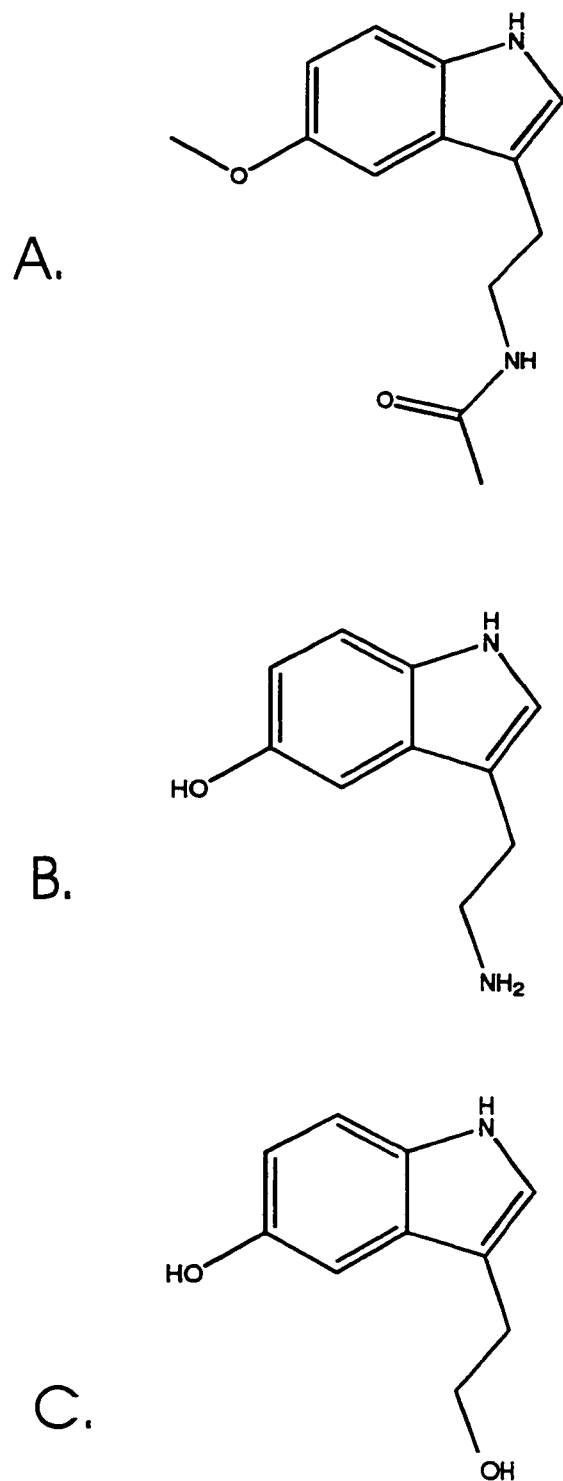
Figure 27: The chemical structures of A. melatonin; B. serotonin; C. 5-hydrox-indole-3-acetic acid.

significantly higher, however. This could be due to the increased separation between the sulfhydryl group and the electron-affinic acid group, thereby increasing its hydrogen donating properties. Mercaptoethanol and the other thiol compounds are also highly protective confirming that it is the sulfhydryl group which is the effective moiety in all these compounds.

The most effective phenol was catechol (7.17 times more effective than ascorbic acid) and the least, trolox ( a water soluble vitamin E analog) with $[vitC]_{50\%}/[trolox]_{50\%} = 3.2$, indicating that these compounds are more effective than sulfhydryls in terms of the radioprotective effect. The catechol data are consistent with other data for catechol-containing bioflavanoids, which are also the most effective antioxidants in their class [ 74] . Trolox however is found to be not as effective in these studies as it is in other assays, particularly those that use peroxyl radical generators [ 75].

Unfortunately phenol and pyrogallol, which contain one and three hydroxyl side groups respectively, showed interferences in this assay, and so their results cannot be reported here. Just one measurement was made for ellagic acid as this compound exhibited solubility problems. The value quoted here probably represents a lower limit on its actual value.

Indoles range from 6-9 times more effective than vitamin C. The structures of the three indoles measured here are shown in Figure 27. Each of the three compounds contains an indole double ring but with different side groups. The high level of effectiveness for each of these compounds shows that the indole group is the important radioprotecting moiety. This effectiveness can be slightly modified by side groups. As

was the case for cysteine and acetyl cysteine, acetylation of the serotonin terminal amino group to form melatonin slightly increases the radioprotective effect. Lack of an hydroxyl group on the 5-indole site does not seem to affect the protecting properties of the compounds, supporting the mechanism of hydrogen donation from the nitrogen within the indole ring. The similarity of the melatonin and serotonin data differs from that of Marshall *et al.* [ 76] who found that serotonin was much more effective in their assay. They examined a lipid system, however, in which differences in lipid solubility between the two compounds could account for the discrepancies between their observations and ours.

The ascorbic acid data as a whole show a large variation in response. This variation could have been due to inter-batch differences as well as some degradation of the BPE stock solutions upon storage (see Figure 32). This variance was an important reason for measuring the reference and test compounds simultaneously and under identical conditions, for each measurement. Samples were also kept in the dark to avoid background bleaching effects.

Data reported in Chapter 5 show that ascorbic acid protects 37 times better than expected in this assay, based on hydroxyl radical scavenging alone. The other antioxidants reported here are even more effective than ascorbic acid, which is consistent with a mechanism of action for these antioxidants protecting by chemical repair at the secondary reaction site (Equation E2.7; Chapter 2).

Figure 30 is a plot of the competition kinetic data presented here, against oxidation potentials ($E_{1.2}$) reported by Meites *et al.* [ 77] for thiols and some phenols. There is a correlation between the kinetic and thermodynamic parameters ( regression equation

given by: [vitC]/[test] = $0.83\text{-}2.45 \times E_{12}$ $r^2 = 0.996$ ; p<0.01). This indicates that the

method used here is an indicator of oxidation potential for these compounds, particularly

for phenols, and confirms that antioxidants which radioprotect are acting through

hydrogen donation reactions. It suggests a similar mechanism for oxidation potential and

radiation protection by hydrogen donation. These regression fit parameters allow

estimation of relative radioprotection for aqueous soluble compounds from their

oxidation potential data. However, it is not known whether the graph can be extrapolated

to other compounds, such as indoles, that lie outside the range, or to other structurally-

different compounds. Uric acid, for instance, was shown to be an excellent radioprotector

in the BPE assay even though its oxidation potential (+ 0.33V) would suggest that it is

only a weak antioxidant. This could be due to its low solubility leading to

microprecipitation in the immediate BPE protein environment.

Figure 31 shows a log-log plot of the data presented here for some compounds,

against concentrations to give 50% protection against chromosome damage in cells

irradiated *in vitro*. Data for cysteine, cysteamine and mercaptoethanol were derived from

Sasaki *et al.* [52]. Melatonin was found to inhibit chromosome damage to the 50% level

at 1 mmol $L^{-1}$ as estimated from the results of Vijayalaxmi *et al.* [ 79]. Both data sets are

for chromosome damage to human lymphocytes. The data are limited because of the

paucity of published results for experiments performed under comparable conditions.

However, there is a correlation between the two parameters. The slope was found to be:

-0.87 ± 0.15 ($r^2 = 0.996$). This is consistent with an inverse relationship between them and

suggests that these compounds are probably radioprotecting by anti-oxidation in the

cellular environment. This also suggests that melatonin is radioprotecting intracellularly

by its hydrogen donating ability in chemical repair rather than by purely hydroxyl radical scavenging as reported by Vijayalaxmi *et al.*[ 79].

As pointed out by both authors, the compounds used in their experiments also induce other protective mechanisms within cells. These cellular effects may account for the large amount of scatter observed when comparing them, particularly in the case of cysteamine.

The BPE assay has been demonstrated to be a simple, yet effective, tool for examining problems in antioxidant biochemistry and radiation chemistry. The results of Chapter 5 and Chapter 6 indicate that the use of the BPE protein as a target molecule is a valid approach. The data in both chapters are consistent with the molecular framework based on free radical kinetic mechanisms as outlined in Chapter 2.
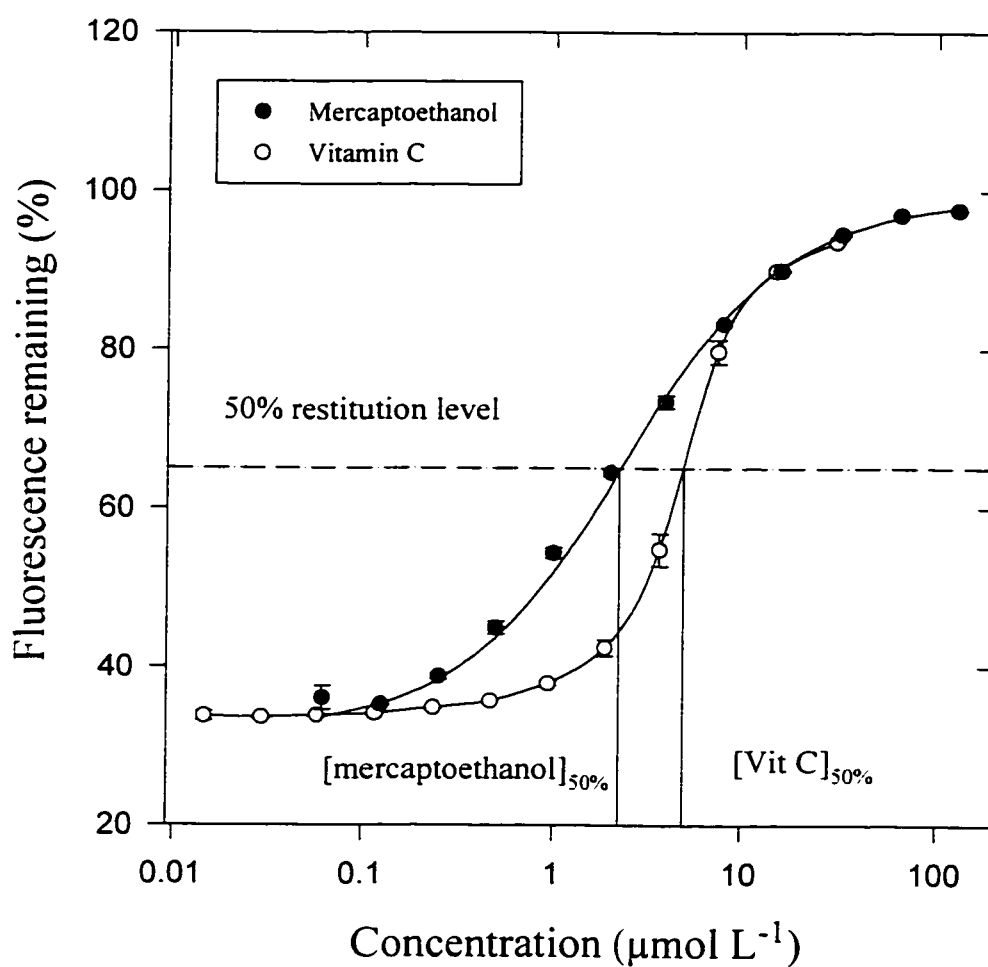
Figure 28: The percent change in fluorescence (excitation wavelength 545 nm; emission wavelength 575 nm) of a BPE solution after irradiation as a function of added antioxidant concentration (mercaptoethanol and ascorbic acid ). The antioxidant concentrations required to produce a 50% restitution in BPE fluorescence after irradiation, are also shown. Further examples are shown in Figures 33-37.
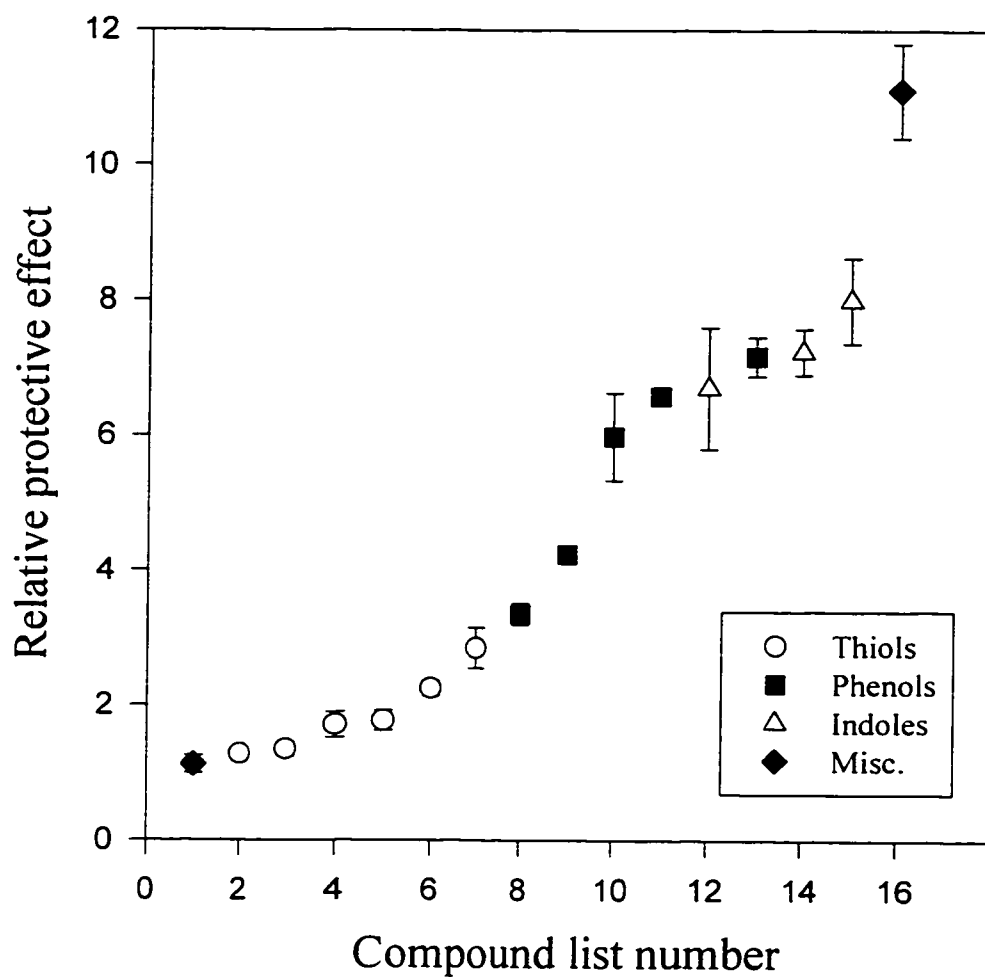
Figure 29: The relative radioprotective effects (compared to ascorbic acid) of thiols,

indoles, phenols and miscellaneous (Misc.) compounds in order of effectiveness.

| | Compound | 50% restitution concentrations ($\mu$mol L$^{-1}$) | | | [vitC]/[test] |
|---|---|---|---|---|---|
| 1.TEST | carnosine | 3.99 | 2.44 | 3.14 | 1.12 ± 0.13 |
| REF. | ascorbic acid | 3.77 | 3.09 | 3.64 | |
| 2. TEST | *cysteine.HCl* | 2.74 | 2.67 | 2.74 | *1.27 ± 0.07* |
| REF. | ascorbic acid | 3.42 | 3.22 | 3.76 | |
| 3. TEST | *acetyl cysteine* | 3.13 | 3.14 | 3.26 | *1.34 ± 0.10* |
| REF. | ascorbic acid | 3.82 | 4.62 | 4.41 | |
| 4. TEST | *homo cysteine* | 2.38 | 1.85 | 2.39 | *1.71 ± 0.19* |
| REF. | ascorbic acid | 3.76 | 3.69 | 3.74 | |
| 5. TEST | *cysteamine* | 1.07 | 0.91 | 0.88 | *1.77 ± 0.15* |
| REF. | ascorbic acid | 1.68 | 1.76 | 1.60 | |
| 6. TEST | *mercaptoethanol* | 2.10 | 1.97 | 1.95 | *2.25 ± 0.11* |
| REF. | ascorbic acid | 5.02 | 4.17 | 4.37 | |
| 7. TEST | *glutathione* | 1.20 | 1.18 | 1.56 | *2.85 ± 0.31* |
| REF. | ascorbic acid | 3.77 | 3.54 | 3.78 | |
| 8. TEST | **trolox**[a] | 1.18 | 0.83 | 1.17 | **3.35 ± 0.17** |
| REF. | ascorbic acid | 3.71 | 2.97 | 3.90 | |
| 9. TEST | **gallic acid** | 0.96 | 0.86 | 0.83 | **4.25 ± 0.10** |
| REF. | ascorbic acid | 3.99 | 3.78 | 3.49 | |
| 10. TEST | **l-dopa** | 0.59 | 0.57 | 0.64 | **6.51 ± 0.34** |
| REF. | ascorbic acid | 3.93 | 3.90 | 3.87 | |
| 11. TEST | **ellagic acid** | 0.56 | | | **6.58** |
| REF. | ascorbic acid | 3.69 | | | |
| 12. TEST | 5-hydroxyindole-3-acetic acid | 0.45 | 0.36 | 0.31 | 6.23 ± 1.03 |
| REF. | ascorbic acid | 2.24 | 2.25 | 2.32 | |
| 13. TEST | **catechol** | 0.51 | 0.55 | 0.61 | **7.17 ± 0.28** |
| REF. | ascorbic acid | 3.79 | 4.03 | 4.14 | |
| 14. TEST | serotonin | 0.52 | 0.56 | 0.48 | 7.30 ± 0.35 |
| REF. | ascorbic acid | 3.67 | 3.95 | 3.75 | |
| 15. TEST | melatonin[b] | 0.36 | 0.38 | 0.40 | 8.46 ± 0.37 |
| REF. | ascorbic acid | 3.23 | 3.15 | 3.25 | |
| 16. TEST | uric acid | 0.31 | 0.37 | 0.35 | 11.21 ± 0.61 |
| REF. | ascorbic acid | 3.74 | 3.92 | 3.85 | |

Table 4: The 50% restitution concentrations for a range of antioxidants using the BPE assay. Each test compound (TEST) was measured in triplicate, simultaneously with a reference (REF.) compound. The effective ratios [vitC]/[test] are also shown. They are listed in order of radioprotective effect. *Sulfhydryl* compounds are shown in italics, **phenols** in bold and indoles are underlined.

[a] dissolved initially in 1 mol $L^{-1}$ sodium bicarbonate; [b] dissolved initially in *tert*-butanol.

These solvents did not interfere with the measurements.
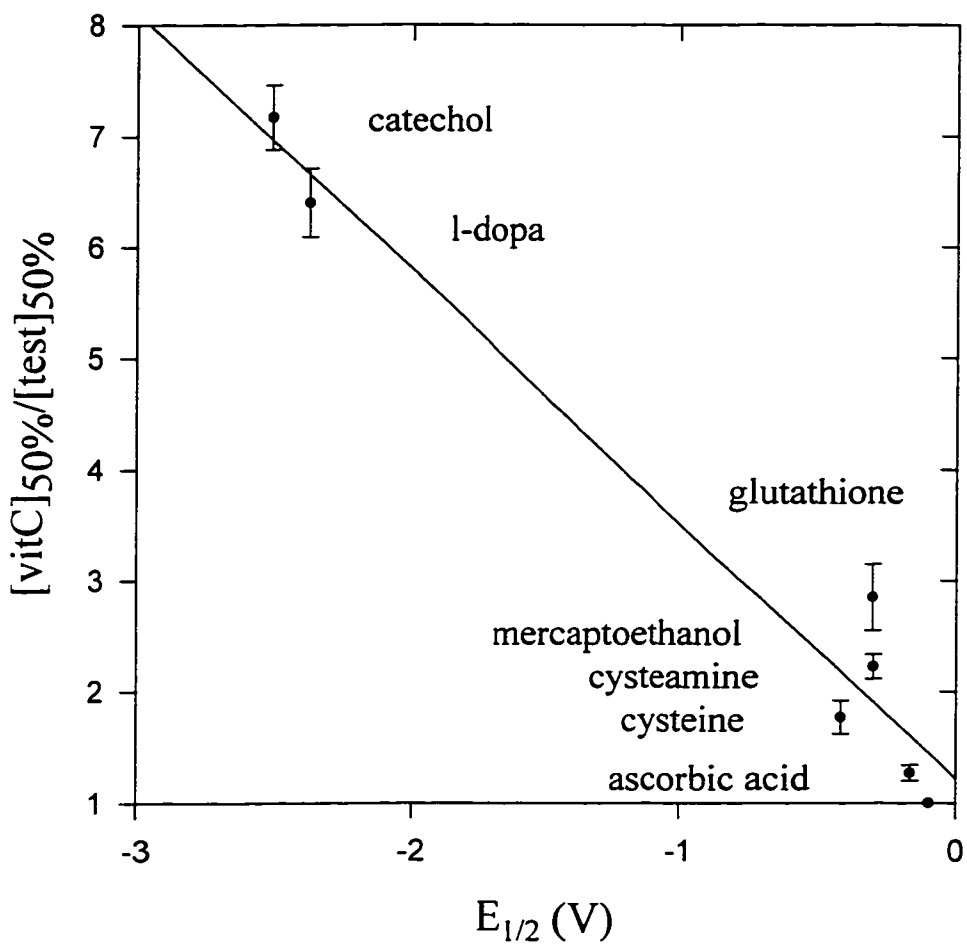
Figure 30: The correlation between the radioprotective effect of various antioxidants relative to vitamin C, and their previously-published oxidation potentials $[E_{1/2}(V)]$. Oxidation potentials for ascorbic acid and glutathione are corrected for pH.
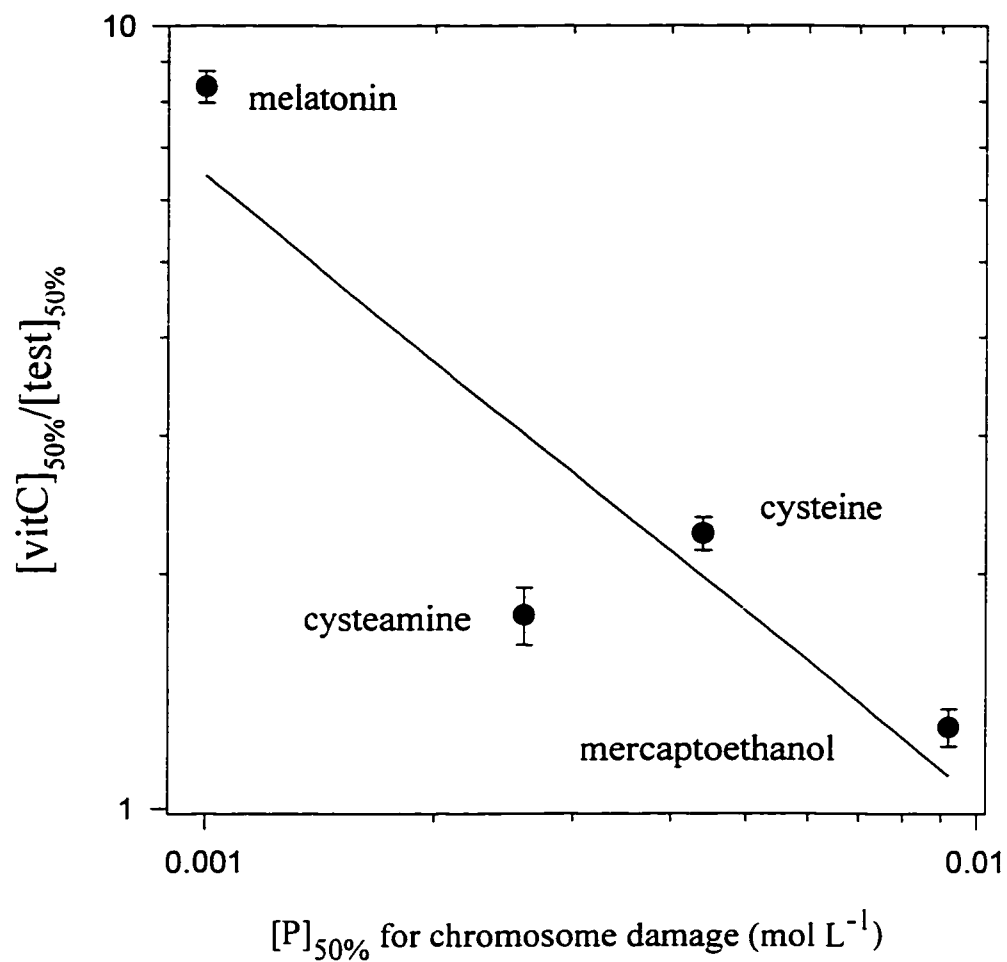
Figure 31: The protective effect of some antioxidants relative to vitamin C in the BPE

assay as a function of their concentrations to provide 50% inhibition of chromosome

damage in irradiated human lymphocytes $[P]_{50\%}$.
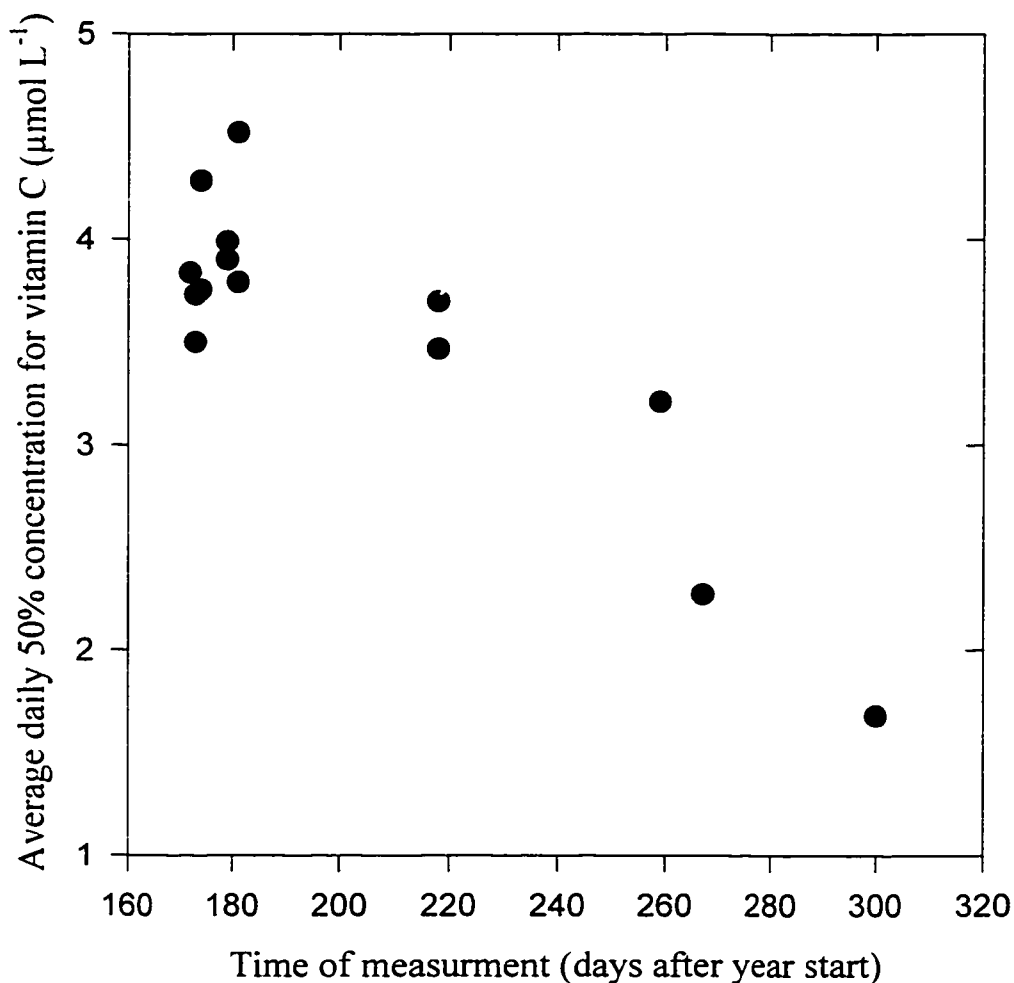
Figure 32: Degradation of a stock solution of BPE over a 4 month period, as determined

by vitamin C 50% concentrations in the BPE assay. There is a significant decrease in the

average levels of vitamin C 50% restitution concentrations during this time period. This

is consistent with storage changes in the protein solution characteristics. However the

ratio $[test]_{50\%}$ /$[VitC]_{50\%}$ remained highly consistent.
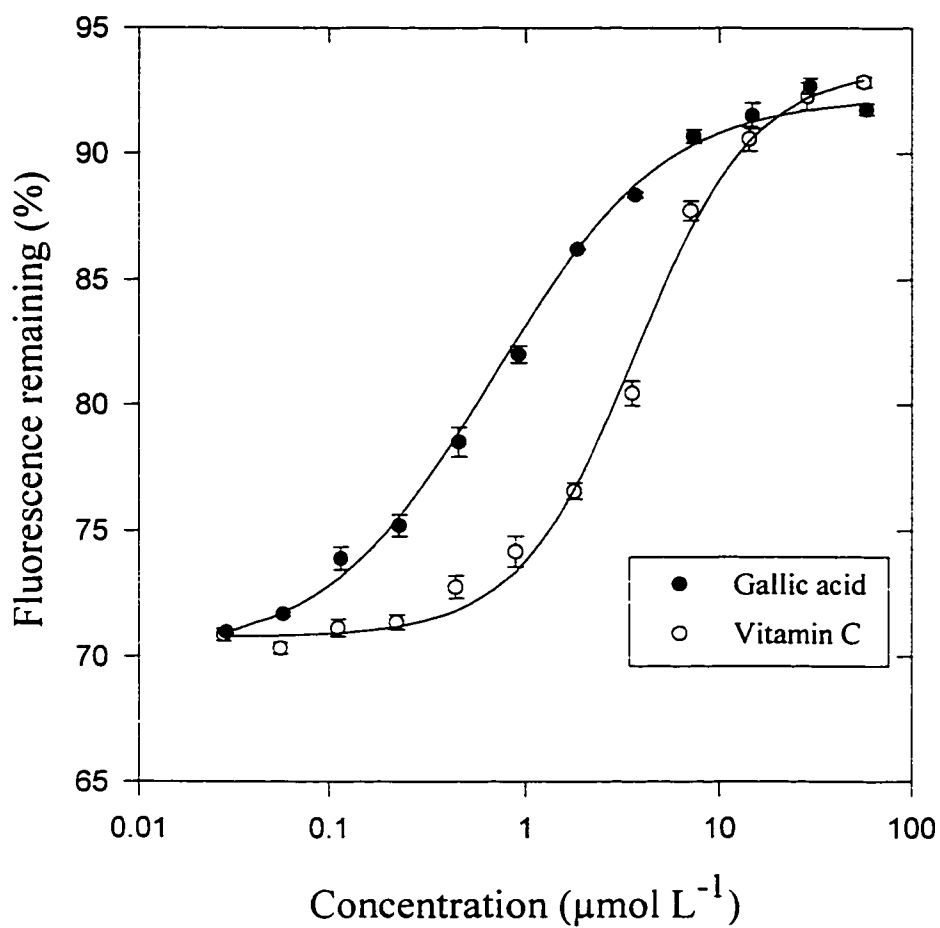
Figure 33: The reduction in fluorescence after irradiation of a BPE solution as a function

of test antioxidant (gallic acid) and reference (vitamin C) concentrations.
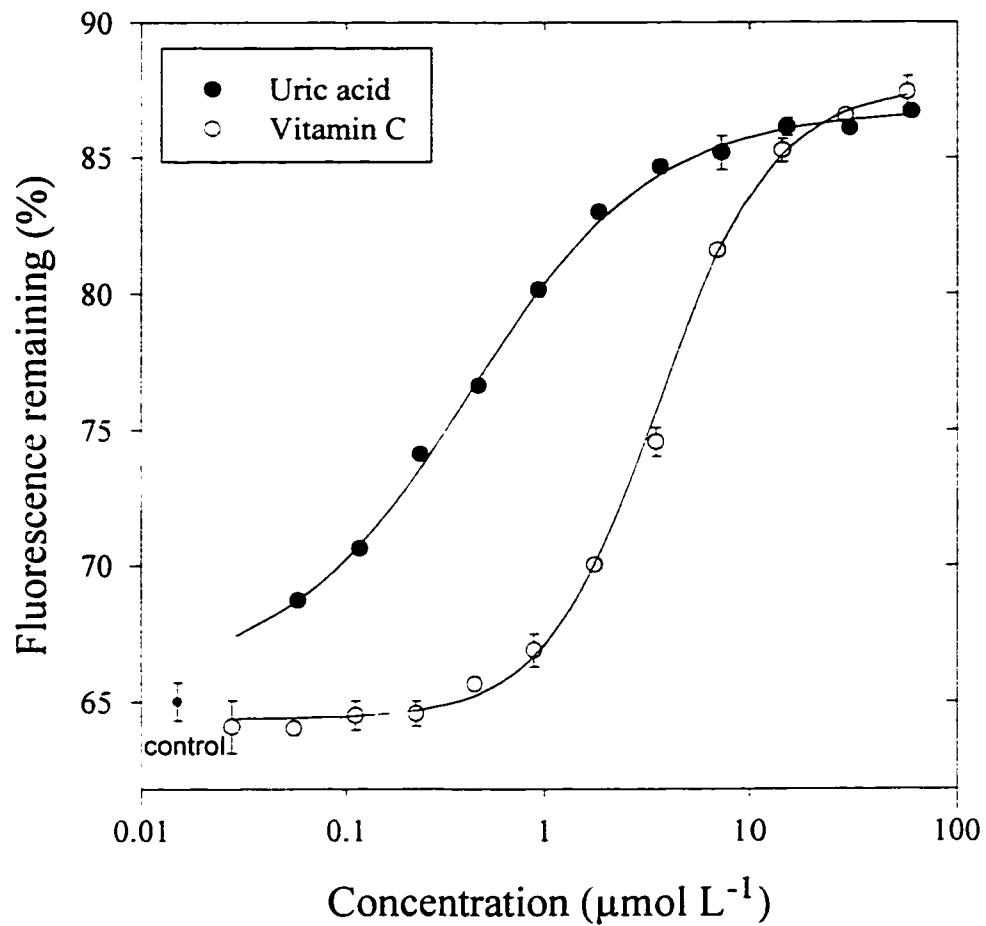
Figure 34: Changes in fluorescence of a BPE solution after irradiation as a function of uric acid and vitamin C concentrations.
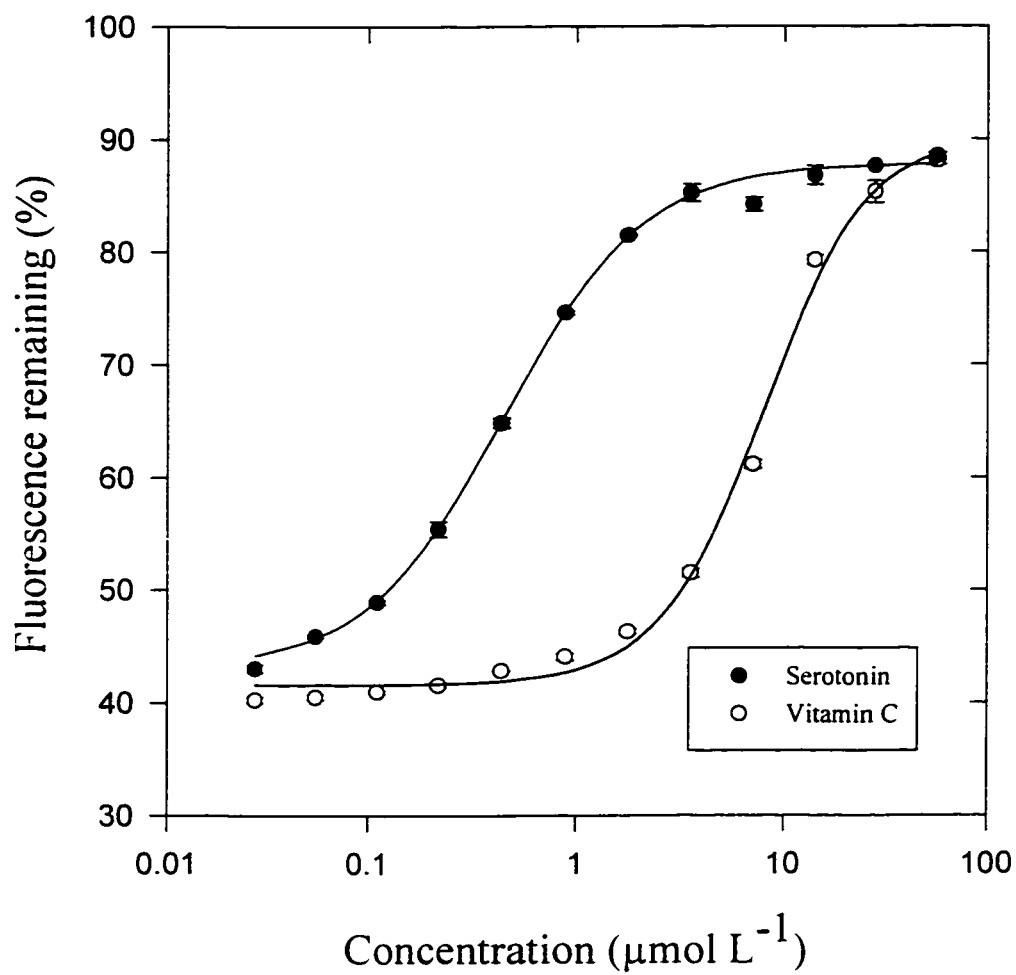
Figure 35: Changes in fluorescence of a BPE solution after irradiation as a function of serotonin and vitamin C concentrations.
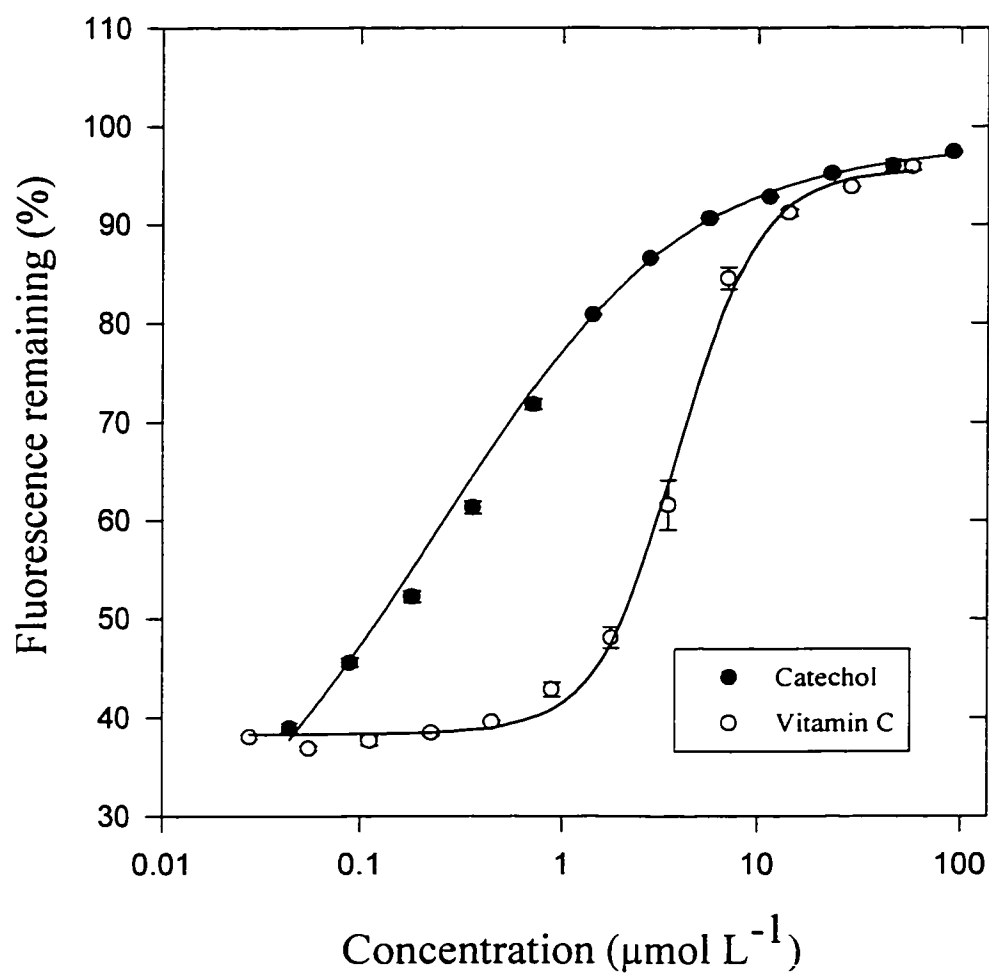
Figure 36: Changes in fluorescence of a BPE solution after irradiation as a function of

catechol and vitamin C concentrations.
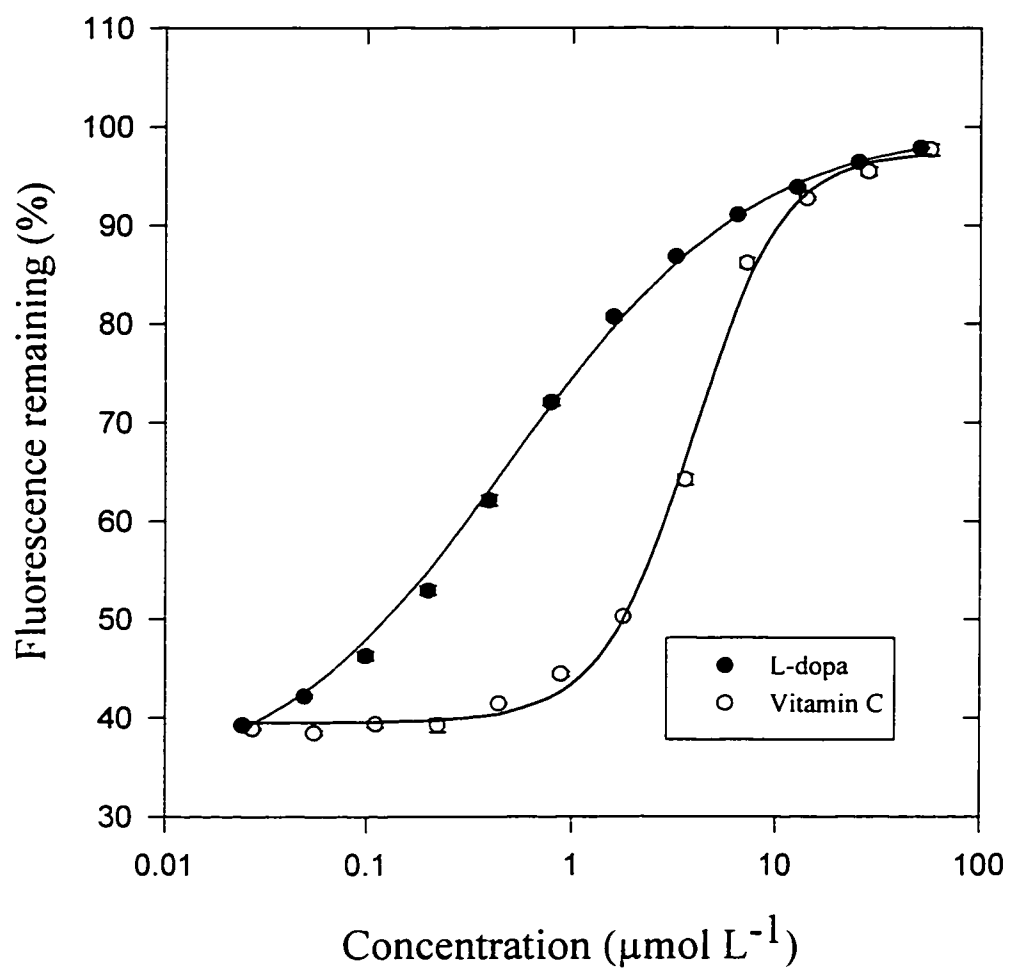
Figure 37: Changes in fluorescence of a BPE solution after irradiation as a function of L-dopa and vitamin C concentrations.

## Chapter 7: THE BPE ASSAY APPLIED TO SOME COMMON BIOFLAVONOID CONTAINING COMPOUNDS

Diets rich in fruit and vegetables are known to be protective against cardiovascular disease and cancer formation [ 80][ 81]. It has been shown that the flavanoid and phenolic fractions of these foods provide the protective effect [ 82]-[ 84]. These compounds act as hydrogen-donating antioxidants which can effectively scavenge free radicals. By protecting against oxidative stress, mediated by oxygen-derived free radicals, such antioxidants can protect against the free radical pathways that have been implicated in cancer initiation and promotion [ 85][ 86] .

The most widely cited study is the the Zutphen elderly study [ 80], which showed protection against heart disease was correlated with bioflavonoid intake. The majority of the total bioflavonoid intake was from tea (48%), onions (29%), apples (7%) and red wine (1%) totalling 20 mg to 1 g. Teas are known to have high concentrations of flavanols such as epigallocatchin gallate [ 84]. Grape products (wines) have high concentrations of flavonols and anthocyanidins and therefore high antioxidant potentials [ 87]. These plant-derived flavonoids and phenols should, therefore, be effective radioprotectors. Purified bioflavonoid compounds have already been shown to have radioprotective effects *in vivo* [ 88].

Measurements of total radioprotective capacity have been made on green and black teas and also on a semi-purified bioflavonoid extracts from grape seeds, using the BPE assay. The results indicate the relative radioprotective effectiveness of these dietary supplements.

## 7.1 Materials And Methods

Chinese green tea and a black tea, purchased from a local supermarket, were soaked in water of resistivity 18.2 MΩ cm (the most pure available) at room temperature for 1 hour. After this time the supernatant was collected and centrifuged at 600$g$ for 15 minutes. Both samples were then lyophilised overnight, and the resulting powder stored desiccated. Grape seed extract powder was kindly supplied by Melaleuca Inc., Idaho Falls ID.

## 7.2 Results And Discussion

Figure 38 shows a typical competition curve. Ascorbic acid was used as the reference compound and its radioprotective action is shown on this graph. Data are also shown for the grape seed extract. Unfortunately, due to the anthocyanidin absorption band at 450-560 nm [ 89], there is an interference with the fluorescence measurements at the higher extract concentrations. However, at the 50% restitution concentration no differences were observed between the fluorescence of the unirradiated sample and the unirradiated control, indicating that this interference was not a factor at the lower concentrations, and that calculated 50% restitution concentrations are a true indicator of the radioprotective effect.

Table 5 shows the results of three independent experiments for the grape seed extract, green and black teas. The relative protective effect is given by the ratio $[ref.]_{50\%}/[test]_{50\%}$. A molecular weight of 300, which is an average molecular weight for bioflavonoids, has been assumed for calculating molar ratios. All the test samples were more effective than ascorbic acid in terms of their radioprotective effect. The values for

green and black teas are quite similar which concurs with the data of Saleh *et al.* [ 90]. They also report that green tea is more effective than black tea in terms of total antioxidant activity. The grape seed extract was shown to be highly effective in this assay, with a total radioprotective capacity six times more effective than that of ascorbic acid. This confirms that the bioflavonoids found in grape seeds are highly effective antioxidants. This level of protection is similar to that of phenols measured in Chapter 6. The teas were not purified and because they contained carbohydrates and other compounds that dilute the effect of the hydrogen donors, this might explain their reduced effectiveness in this assay. It should be noted that only the aqueous soluble fraction of the teas was examined, and that the assay was carried out completely in the aqueous phase.

These data confirm that solutions containing bioflavonoid compounds represent a potent reductive environment which can protect against oxidative stresses, especially ionising radiation. This supports data showing that diets high in these nutrients are more effective in protecting against free-radical mediated carcinogenesis [27]. These nutritionally derived reductive compounds may be important in the overall protective strategy. These nutrients can also protect against low density lipid oxidation, which is implicated in heart disease formation [ 80].

| | Sample | 50% restitution concentrations ($\mu$mol L$^{-1}$) | | | [ref.]$_{50\%}$/[test]$_{50\%}$* |
|---|---|---|---|---|---|
| 1.TEST | Black tea | 2.89 | 2.97 | 3.17 | 1.42±0.11 |
| *REF.* | *ascorbic acid* | *4.58* | *4.05* | *4.21* | |
| 2. TEST | Green tea | 2.58 | 2.19 | 2.48 | 1.78±0.15 |
| *REF.* | *ascorbic acid* | *4.13* | *4.31* | *4.43* | |
| 3. TEST | Grape seed | 0.84 | 0.68 | 0.76 | 5.82±0.49 |
| *REF.* | *ascorbic acid* | *4.32* | *4.26* | *4.62* | |

Table 5: The results of the 50% restitution concentrations for bioflavonoid-containing nutrients in the BPE assay. A molecular weight of 300 has been assumed for conversion to $\mu$mol L$^{-1}$.

*The overall radioprotective effect of test samples relative to ascorbic acid is given as the ratio [ref.]$_{50\%}$/[test]$_{50\%}$, together with the standard deviation.
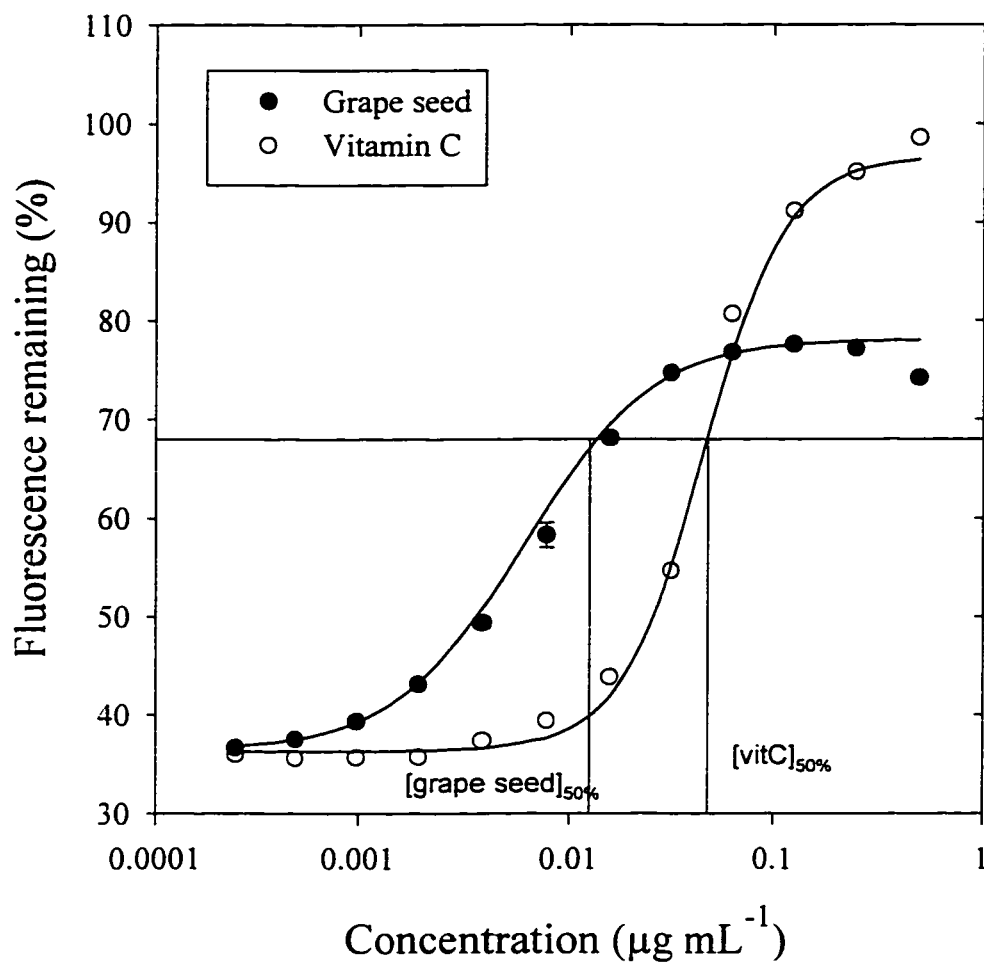
Figure 38: The change in fluorescence after irradiation of a BPE solution as a function

of increasing concentrations of added grape seed extract and also of ascorbic acid. The

50% restitution concentrations are also indicated.

# Chapter 8: BIOLOGICAL RADIOPROTECTION

It has been conclusively shown in Chapters 4 and 5 that free radical scavengers and antioxidants protect the target molecule BPE from ionising radiation-induced oxidative damage. The mechanisms of protection are free radical scavenging and hydrogen donation. There was also a link between the degree of radioprotection of cellular DNA as a function of added radioprotectant concentration. The natural antioxidants within cells should also afford a high level of radioprotection. It is undetermined to what extent variations in these antioxidant levels are responsible for differences in individual radiosensitivity. This leads to a testable hypothesis: **Natural antioxidants within cells can protect against radiation damage.**

This hypothesis can be tested by measuring the total radioprotective effect of biological extracts and comparing these measurements with radiosensitivity indices.

The total radioprotective effect includes all the antioxidant and scavenging components, as well as any combined effects due to interactions between the antioxidants.

## 8.1 Radioprotective Capacity and Antioxidant Enzyme Activity for some Lymphoblastoid Cell Lysates (LCLs)

If antioxidants and antioxidant enzymes protect against radiation damage then variations in the levels of these compounds might be responsible for some of the differences in individual radiosensitivity. To test this, a range of lymphoblastoid cell lysates (LCLs; see Appendix II) were measured in the BPE assay. LCLs were also tested for total superoxide dismutase and catalase activity. These values should correlate with radiosensitivity indices if total radioprotective capacity or enzyme antioxidant activity are a factor in determining radiation resistance.

The choice of LCLs is important. They are all lymphocyte derived cell lines and therefore have similar growing properties. They can also be grown to high density so that a large number of cells can be harvested in a short period of time.

Because of their fast growing nature in suspension cultures, the 'Grow Back Ratio' (GBR) is used as the measure of radiosensitivity. The GBR is defined as the rate of growth of a cell culture irradiated to a dose of 4 Gy over the rate of growth of an unirradiated culture [ 91]. Radioresistant cells grow at a rate closer to that of the control culture and therefore have a GBR closer to 1.0 . Radiosensitive cell lines have a GBR closer to 0. In reality the GBR ranges from 0.2-0.8. Values of GBR have been published for the cell lines in this study [ 92]. The GBR for the normal cell line GM2184 was checked and found to be consistent with the published value.

## 8.2 Materials And Methods:

### *8.2.1 Total Protein Assay*

A novel microwell-plate method was used for determining total protein

concentrations. It was based on the fluorescamine protein assay [ 93] . In this assay

proteins are denatured, allowing fluorescamine to react with the exposed amino acids.

This derivative is highly fluorescent and is linearly dependent on protein concentration.

In a typical protein measurement, six standard bovine serum albumin (BSA)

solutions were prepared in PBS with concentrations ranging from 0-100 $\mu$g mL$^{-1}$. In a

black 96-well fluor-NUNC plate, three 50 $\mu$L volumes from each standard solution were

placed in separate wells to generate a calibration curve. Triplicate 50 $\mu$L volumes from

the protein solutions to be measured were also placed in separate wells. To each well a

100 $\mu$L volume of an aqueous solution containing 300 mmol L$^{-1}$ sodium tetraborate (an

oxidising and denaturation agent), 5 mmol L$^{-1}$ calcium disodium tetraacetate (a metal

chelator) and 5.4 mmol L$^{-1}$ sodium dodecyl sulfate (a surfactant) was added. A 50 $\mu$L

volume of a 0.5 mmol L$^{-1}$ fluorescamine in acetone solution was quickly added to each

well and slightly agitated using a Gilman pipette. The plate was allowed to sit in the dark

for 10 minutes for the fluorescence to build and then the fluorescence of each well was

measured using the IDEXX Fluorescence Concentration Analyser (FCA) set on a gain of

5 and with excitation and emission filters of wavelengths 360 nm and 425 nm

respectively. As shown in Figure 39 the calibration curves were linear allowing the total
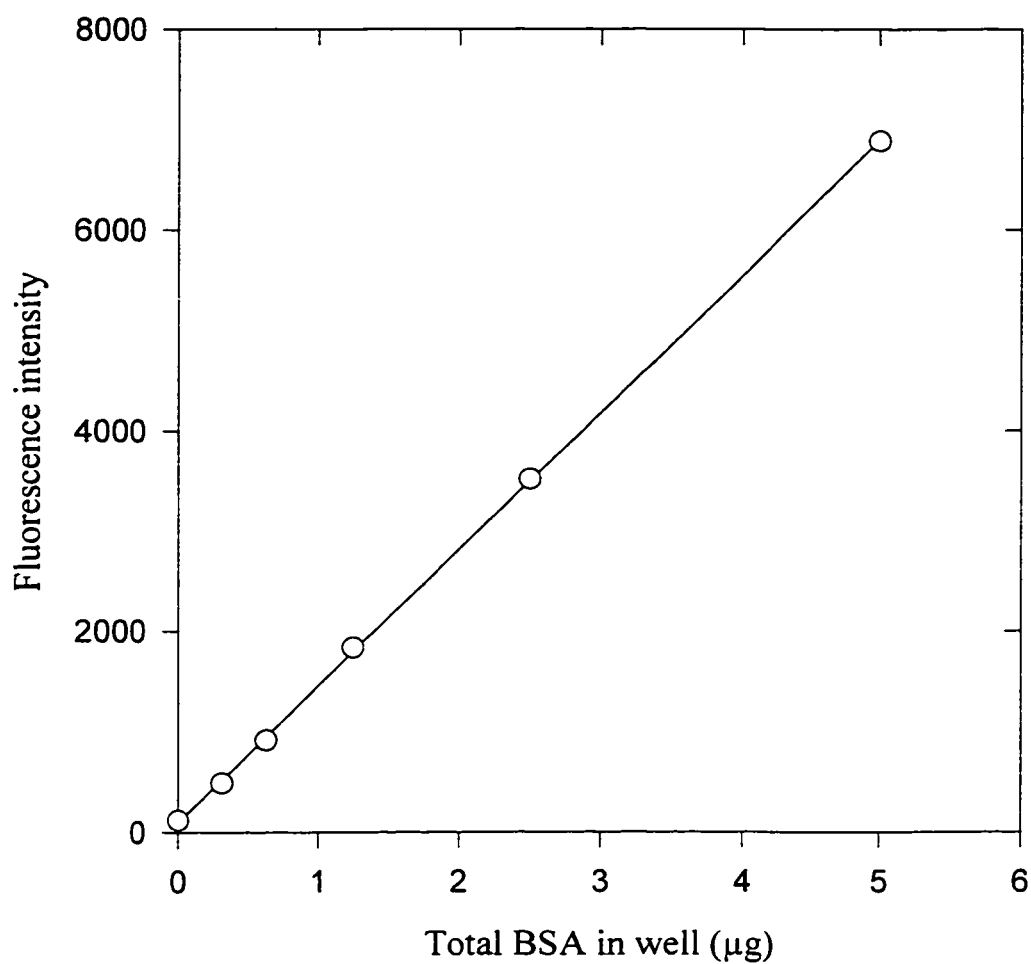
Figure 39: The fluorescence (excitation wavelength 360 nm; emission wavelength 425 nm) of a standard fluorescamine solution as a function of the mass of bovine serum albumin (BSA) added to each well.

protein content of unknown solutions to be determined from the regression fit parameters.

## 8.2.2 Antioxidant Enzyme Assays

The NBT Superoxide Dismutase Assay

The NBT (Nitro Blue Tetrazolium) (2-2'di-p-nitrophenyl 5-5' diphenyl 3-3'[3,3'dimethoxy-4,4'diphenylene]ditetrozolium chloride) superoxide dismutase assay used here was a microwell modification of the assay described by Fridovich [ 94]. This competition assay is based on the ability of superoxide dismutase to compete with NBT for superoxide anions via its catalytic dismutation reaction (see Reaction R3.1 in Chapter 3). The rate of production of the blue insoluble precipitate arising from the reaction of NBT with superoxide anions can be measured by kinetic changes in absorbance of the solution. This rate of production is linear up to about 5 minutes. As in the BPE assay, the concentration of substance required to inhibit the reaction by 50% is defined as one unit. Superoxide dismutase present in solution with these reactants catalyses the dismutation of the superoxide radical, reducing the extent of the reaction. The superoxide flux is generated by a xanthine-xanthine oxidase system.

The stock solutions were as follows:

Nitro blue tetrazolium: a 2.4 mmol $L^{-1}$ solution was prepared in PBS. The salt required initial solubilisation in ethanol but the final concentration of ethanol in this stock did not exceed 5% v/v.

Xanthine: This is the substrate for xanthine oxidase. An initial stock solution of

1.8 mol L$^{-1}$ was dissolved in a 0.5 N sodium hydroxide solution because the alkali solution was needed for complete solubilisation. The concentration of the working solution was 18 mmol L$^{-1}$, in PBS.

Catalase: This enzyme is required in small concentrations to limit the build up of hydrogen peroxide which can inhibit the superoxide reaction. The stock solution was 40 unit mL$^{-1}$. A catalase 'unit' is defined as the amount of catalase able to convert 1 μmol L$^{-1}$ of hydrogen peroxide to water and oxygen in 1 minute.

Detapac (diethylene triamine pentaacetic acid): This metal complexing agent was prepared to a concentration of 1.33 mmol L$^{-1}$ in PBS and was used as the main diluent in the final preparation.

Xanthine oxidase: This enzyme drives the superoxide production reaction and was prepared in the detapac solution to a concentration of ~60 μunit mL$^{-1}$. A xanthine oxidase unit is defined as the amount of xanthine oxidase required to reduce 1 μmol of cytochrome C.

The main solution (solution A) was prepared with final concentrations of 1.10 mmol L$^{-1}$ detapac, 1.27 unit mL$^{-1}$ catalase, 76 μmol L$^{-1}$ NBT and 1.95 mmol L$^{-1}$ xanthine. Due to inter-batch variation, and in particular storage degradation, the concentration of xanthine oxidase had to be adjusted to get a consistent superoxide flux that gave a change in optical density between 0.02-0.03 min$^{-1}$ for an initial control solution.

For batch measurement in a microwell plate 20 μL of PBS was placed in each of the wells. In each well in the first row (row A) a 20 μL sample was added. A serial dilution was made down the plate seven times, for each of the columns, with the
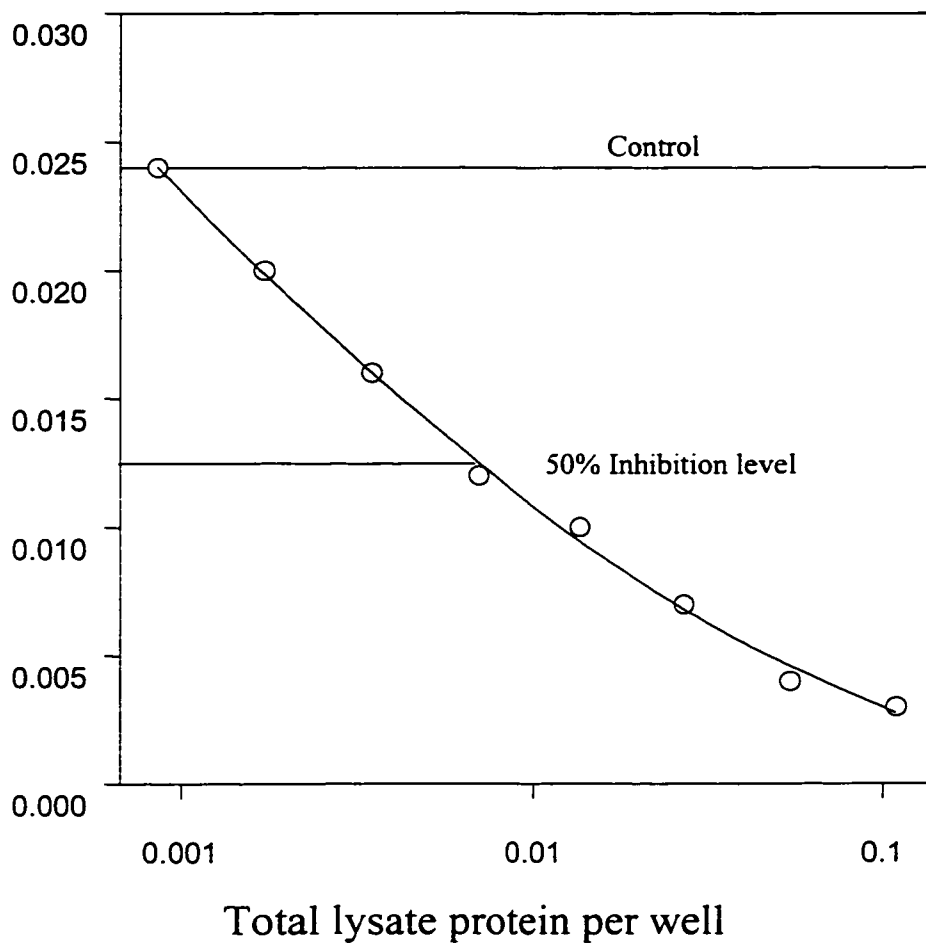
Figure 40: The rate of change in NBT absorbance at 540 nm in the presence of a superoxide generator (xanthine-xanthine oxidase) as a function of total cell lysate concentration.

concentration of sample being half that of the row above it. The last row was left as a control with just PBS. Next, 160 μL of solution A was added with 20 μL of the xanthine oxidase solution. Care was taken to reduce foaming which could interfere with absorbance measurements. The optical density for each well was measured over a period of a few minutes using a Dynatech MR650 microwell absorbance reader set on repetition mode to measure the absorbance at 540 nm every 20 s. The change in optical density is linear over this time period allowing the rate of change of optical density to be calculated for each well. This rate of change of optical density is indicative of the enzyme activity. By plotting the rate of change of optical density for each well as a function of sample concentration (see Figure 40), the concentration to give a 50% inhibition effect could be determined and thus the number of units per mL calculated.

## The $H_2O_2$ Catalase Assay

One unit of catalase activity is defined as the amount of substance to convert 1 μmole of hydrogen peroxide ($H_2O_2$) to water and oxygen in one minute (see Reaction R3.2 in Chapter 3). The spectrophotometric method [ 95] measures the rate of change of $H_2O_2$ concentration by monitoring the hydrogen peroxide absorption peak at 240 nm. The optical density is proportional to the concentration of $H_2O_2$. The second order reaction can be described as an exponential process $[H_2O_2]_t = [H_2O_2]_0 e^{-kt}$ where k is a constant and t is time. The measurement is made by recording the time for the optical density to decrease by a set amount. The exact protocol is as follows: 3 mL of a 12.5 mmol $L^{-1}$ $H_2O_2$ solution in PBS is placed in a quartz cuvette. The spectrophotometer is set to the correct wavelength and suitable zeroing adjustments made. A 10-50 μL

sample is placed in the cuvette and agitated for complete mixing. A stop watch was used to measure the elapsed time t(s) for the optical density to drop from 0.45 to 0.40. The number of μmoles of hydrogen peroxide (ΔS) catalysed in 60 s is then given by:

$$\Delta S = vol \cdot [H_2O_2]_0 \cdot (1 - e^{\frac{-60 \cdot \ln(\frac{0.45}{0.40})}{\Delta t}}) \qquad (E8.1)$$

This technique proved to be difficult to quantitate because it was unreliable and somewhat irreproducible, so just three cell lysates were measured.

### 8.2.3 LCL Culture and Harvest

LCLs were grown to a density of $10^6$ cell mL$^{-1}$ in spinner flasks as described in Appendix II. The media containing the cells ($10^8$ cells in total) were poured into 50 mL centrifuge tubes and spun at 600$g$ for 5 min. The media were decanted, the cells resuspended in Hank's buffered saline solution and then respun for 5 min. This was repeated twice, except that the final rinse was done with PBS. The resulting cell pellet was suspended in 1 mL PBS and vortexed with washed 100 μm diameter glass beads, to lyse the cells. The resulting cell lysate was frozen using dry ice and stored at -70 °C. For the measurements, the samples were warmed to 4°C and then spun at 20,000$g$ for 30 min at 4°C, to remove any debris, and the supernatant collected.

The total radioprotective capacities of the supernatants were measured by the BPE assay (see Chapter 4), superoxide dismutase measured by the NBT assay (see page 88) and catalase measured by the hydrogen peroxide assay. The data were normalised for total protein content using the total protein assay (see section 8.2.1).

## 8.3 Results and Discussion

Figure 41 shows the results of one sample lysate using the BPE assay. High levels of added sample concentration protect the BPE protein and low levels do not protect as well. The 50% restitution level is also shown. Because the average molecular weight cannot be calculated for these samples the analysis was done slightly differently. Just as an activity unit can be defined for catalase and superoxide dismutase activity, where an activity unit is defined by the amount of substance to provide a certain endpoint, a radioprotective unit can be defined using the BPE endpoint of 50% restitution. The final total protein mass per mL to give a 50% restitution concentration was defined as 1 radioprotective unit. For the sample shown in Figure 41 this was found to be 1.96 μg. This allows the total number of units in 1 mg to be calculated. For this sample, a radioprotective capacity of $509 \pm 17\%$ unit $mg^{-1}$ was calculated ($1/1.96\mu g \times 1000\mu g/mg$). All the measurements were made with a particular BPE batch under standard conditions in order to provide a direct comparison between lysates. The value of $509 \pm 17\%$ unit $mg^{-1}$ is comparable with ascorbic acid, which when analysed on a 'radioprotective unit per mg' basis, has a value equal to $312$ unit $mg^{-1}$. Although a comparison based on total protein is not complete, this shows that cell lysate is an excellent radioprotector and should provide a reductive environment for the target molecule, DNA.

Measurements of total radioprotective capacity for eight different LCL lysates were determined and the results are displayed in Figure 42 as a function of lysate radiosensitivity (GBR). The errors (~10%) were determined from the fit parameters rather than repeat measurements. The results clearly show that there is no correlation between total radioprotective effect and radiation sensitivity. These results are surprising and show

that, for these cells, radiosensitivity is entirely governed by parameters other than antioxidant status. They also show that this type of cell has a relatively consistent antioxidant status. A recent paper by Leist *et al.* [ 96] describes measurements to determine antioxidant levels in cells growing in tissue culture. They report that human tissue culture cells are deprived of the essential antioxidants vitamins C and E i.e. the total radioprotective capacity is due solely to antioxidant compounds produced internally, such as glutathione and protein thiol groups. The LCLs are of human origin. The *in vitro* lack of inter-individual variation in lysate radioprotective effect suggests that variations *in vivo* may be due to external (i.e. dietary or environmental as opposed to genetic) radioprotectants.

Figure 43 shows data for lysate superoxide dismutase activities of twelve cell lines and catalase activities in three cell lysates, as a function of GBR. These results show that radiosensitivity is also not correlated with these enzyme activities. There is a wide range of superoxide dismutase activities, from 10-50 unit (mg total protein)$^{-1}$ with an average of 26±12 unit (mg total protein)$^{-1}$.

A large number of cell lysates were measured in a standardised system using cell lines with a range of radiation sensitivities.

The results show that variations in internally produced antioxidants are not responsible for differences in radiosensitivity. However, the cell lysate itself is highly radioprotecting. This supports the Hypothesis that natural internal antioxidants do protect cells against oxidative stress. They do not however, seem to fully protect the most important target molecule DNA to the required level, as they are relatively ineffective in

protecting against important biological end-points including cell inactivation mutation

and chromosome aberrations.
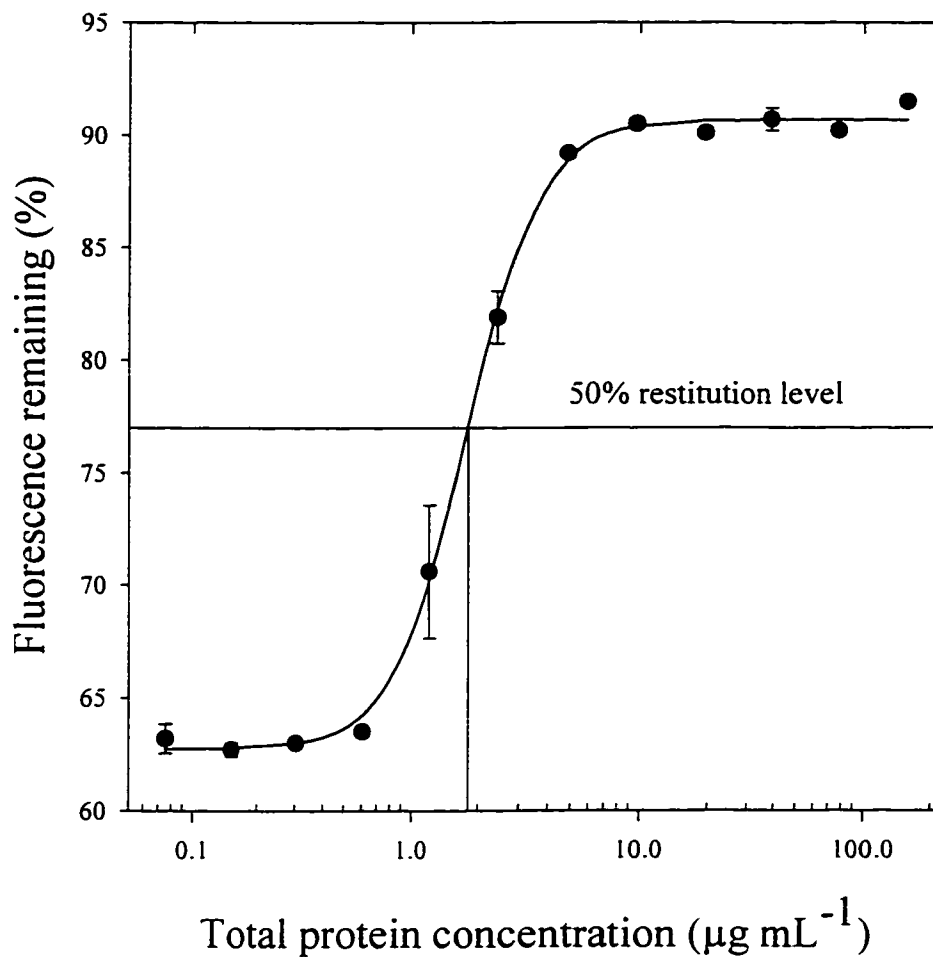
Figure 41: A semi-log plot showing the change in fluorescence of a 330 ng mL$^{-1}$ BPE

solution (excitation wavelength 545 nm; emission wavelength 575 nm) as a function of

dilutions of CP287 lymphoblastoid cell lysate after a 26 Gy gamma irradiation.
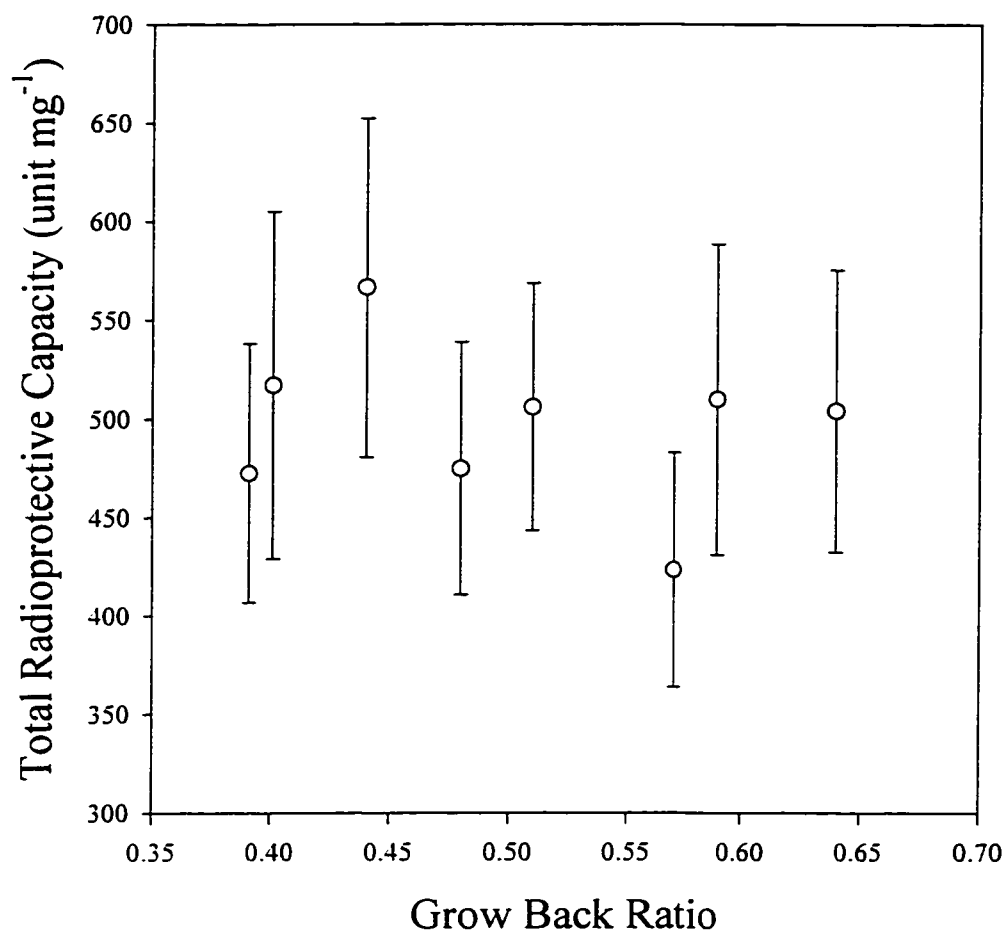
Figure 42: The total radioprotective capacity of eight lymphoblastoid cell lysates versus their 'Grow Back Ratio'.
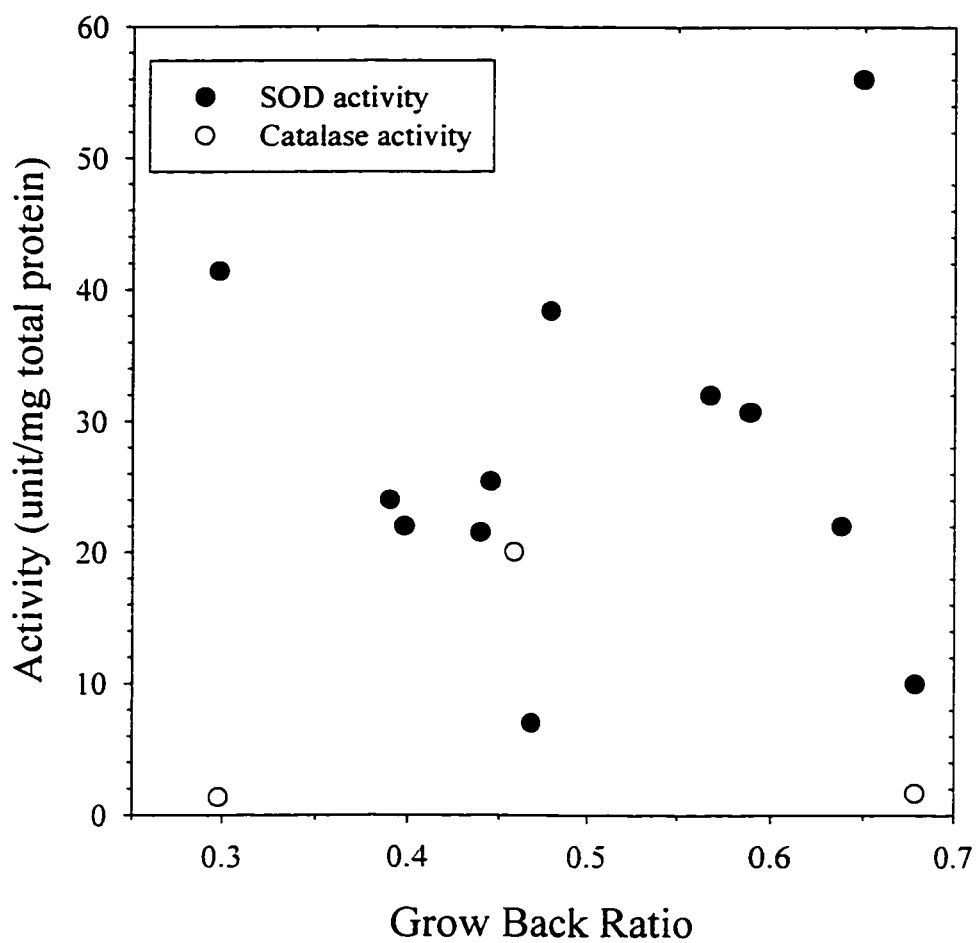
Figure 43 : The superoxide dismutase and catalase activities of cell lysates normalised for total protein content against the radiosensitivity indice, the 'Grow Back Ratio'.

# Chapter 9: BPE MEASUREMENTS ON HUMAN BLOOD PLASMA

Since cells *in vitro* did not show much variation in inherent radiosensitivity an *in vivo* model was investigated. This is impractical for most human cells so blood samples were used for convenience. The blood plasma fraction can be easily stored without further processing. Human blood serum contains large quantities of proteins, which contain hydrogen donating sulfhydryl moieties, as well as dietary antioxidants such as ascorbic acid and bioflavonoids. Uric acid and blood-specific superoxide dismutases are also found. Blood serum, therefore, represents a reductive environment that should be radioprotective. Pulse radiolysis measurements have been made on blood plasma by Cercek et al.[ 97][ 98]. They concluded that hydrated electrons were not an important damaging mechanism in a blood plasma system.

Thirty blood plasma samples from cancer patients across southern Ontario had been frozen down and stored at -30 °C in the freezers at AECL, Chalk River Laboratories. Twenty of these samples were supplied with information about donor age, sex and type of cancer. The samples had been taken before treatment was started on the patients. Measurement of the total radioprotective effect for these samples would confirm whether blood plasma has a significant radioprotective ability, and determine the degree of variability in the population. In addition, twenty relatively-fresh blood plasma samples from healthy donors were also analysed as a control group.

## 9.1 Materials And Methods

*Blood Collection*

Volumes of 25-30 mL of whole blood were taken from donors by venipuncture.

The blood was kept at 37 °C until processed. Heparin was added to a concentration of

10 unit mL$^{-1}$ and the blood agitated. Volumes of 4 mL whole blood were carefully layered

onto 5 mL ficoll solution in a 15 mL centrifuge tube. The tubes were spun at 600$g$ for

30 minutes. The blood plasma remains as a straw coloured solution above the ficoll. The

plasma samples were passed through a 0.8 μm filter and stored in a -30°C freezer. For

each experiment, the plasma samples were diluted by a factor of 100 in phosphate

buffered saline pH 7.4 (PBS). The radioprotective capacity of diluted samples was then

determined using the BPE assay.

Because the variation in the data set was expected to be large, the linear

correlation coefficient, r, was used a statistical marker. This is given by:

$$r = \pm\sqrt{\frac{\text{explained variation}}{\text{total variation}}} = \pm\sqrt{\frac{\Sigma(Y_{est} - \overline{Y})^2}{\Sigma(Y - \overline{Y})^2}} \qquad (E9.1)$$

r varies between -1 and +1. It is possible to calculate the significance level to which the

correlation coefficient differs from zero. The $t$ statistic for the two hypotheses giving a

zero and non-zero correlation coefficient is given by:

$$t = \frac{r\sqrt{N - 2}}{\sqrt{1 - r^2}} \qquad (E9.2)$$

where N - 2 = ν = number of degrees of freedom, with N being the number of data points.

The significance level, p, can be calculated from statistics tables.

## 9.2 Results and Discussion

Figure 44 shows the competition curve between a diluted plasma sample and the BPE solution. The error bars are the standard deviations of duplicate experiments. At high concentrations of added protectant a large proportion of the fluorescence remains (96%), although there is always some reduction due to the direct radiation action on the BPE itself. At low concentrations the damage is maximal, resulting in a large loss of fluorescence. The 50% restitution concentration is indicated and was used to calculate the number of radioprotective units normalised for total protein. For this sample the radioprotective ability was found to be $560\pm70$ unit (mg total protein)$^{-1}$, which represents a highly reductive environment.

It was a concern that the BPE might exhibit interferences with plasma proteins, however the BPE protein has been utilised in other assays for measurement of plasma antioxidants without interference. Also, experiments were performed with mixtures of proteins (e.g. BSA and catalase) which indicated that protein-BPE binding was not a problem (data not shown).

Figure 45 shows the results obtained with the blood plasma of the twenty cancer patients for whom age data were available. The total radioprotective units normalised for total protein are plotted against donor age. The results for the twenty samples varied by a factor of two over a forty year age range. The errors are typically 10-15% and were calculated from the fit parameters for the 50% restitution level. On analysis there was no

connection with sex or cancer type, but this was complicated by the reduced statistical power of having to subgroup the data.

There is an inverse trend between total radioprotective effect and age. The spread of data is quite large about the first order regression line which is described by: Radioprotective unit =980±130 unit -6.30±2.12 unit yr$^{-1}$ (r=0.56; P<0.01).

Twenty further blood plasma samples were collected from control donors working at Chalk River Laboratories. These samples were collected as part of another project and the plasma samples were surplus to requirements. This meant that the parameters of age and sex were not completely controlled. Unfortunately this resulted in a skewed group, with most donors falling in the 60-70 year age group and most being male. However the samples were tested as before. These samples were measured within two months of donation. The results for this batch are shown in Figure 46. The regression line was found to be given by : Radioprotective unit =1240±290 unit-9.99±4.56 unit yr$^{-1}$ (r=0.55; P<0.01). There is still quite a large spread but with a negative slope. The slope is dependent on just a few points at the lower age range which explains the larger uncertainties.

These data indicate that there is an inverse trend between radioprotective ability and donor age. This trend was observed in both cancer patient blood plasma and that of the control group, indicating that this could be a general response.

However blood plasma contains only $\mu$g mL$^{-1}$ concentrations of aqueous soluble antioxidants e.g. ascorbic acid, glutathione corresponding to a maximum of ~50 unit mg$^{-1}$ on the average which indicates that about 10% of the radioprotective effect of the cell lysate can be attributed to water soluble antioxidant action. The remaining 90% of the

action must come from protein molecules. Therefore proteins represent the most important radioprotective component.

It is interesting that samples from donors in the 65-80 year old range in Figures 39-40 have similar radioprotective units as the cell lysates (Chapter 8). It is reported that elders' diets are deficient in antioxidants, similar perhaps to the cells *in vitro*. Younger people who eat healthier diets would have higher protective levels. Only a very extensive breakdown of the samples, testing for all known antioxidants (not available in our laboratory) would test this. It would appear, however, that in these samples it is the protein protective effect that is providing the majority of the protective action. The large spread of data could probably be reduced by controlling factors such as the time of day at which blood was collected and other life style parameters such as smoking.

The slope of the control regression is steeper than that for the cancer patients, but is statistically indistinguishable given the lack of data at the lower age range of the control group. There also appears to be no gross alteration in protective effect due to the conditions or duration of storage, for the cancer patient group.

It has also been established that older animals are more radiosensitive[ 99] [ 100]. This is due to two factors: DNA repair capacity decreases with age [ 101][ 102], and levels of antioxidants are reduced [ 103]. This latter phenomenon is a combination of antioxidant enzyme reduction [ 104] as well as nutrition changes. This reduction in protection against oxidant assault results in increases in lipid peroxidation [ 105] and chromosomal damage markers, which can be negated by treatments with antioxidants [ 106].

The results support these data showing reductions in blood plasma antioxidant capacities with age. They indicate that older persons are less well protected against oxidative insult including that due to ionizing radiation, which may account for their increased residual levels of chromosomal and membrane damage.
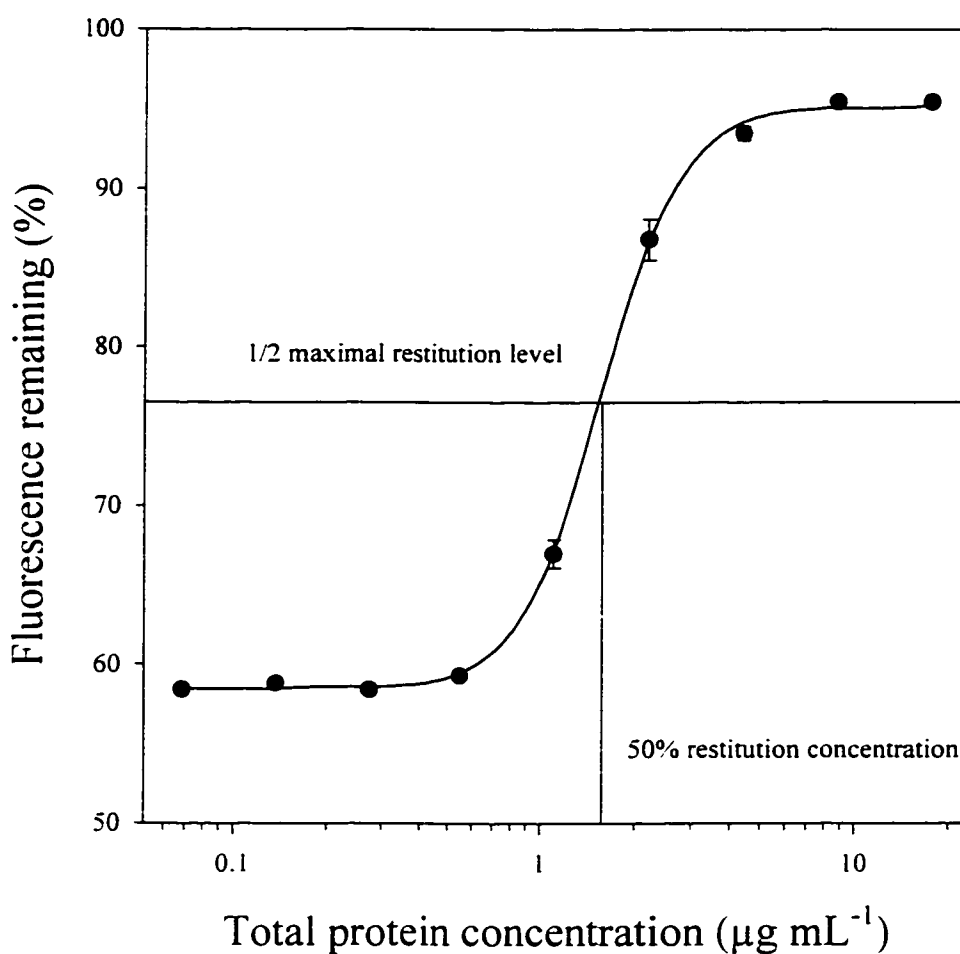
Figure 44: A semi-log plot showing the change in fluorescence of a 330 ng mL$^{-1}$ BPE solution (excitation wavelength 545 nm; emission wavelength 575 nm) as a function of dilutions of human blood plasma sample RD123 after 26 Gy gamma irradiation.
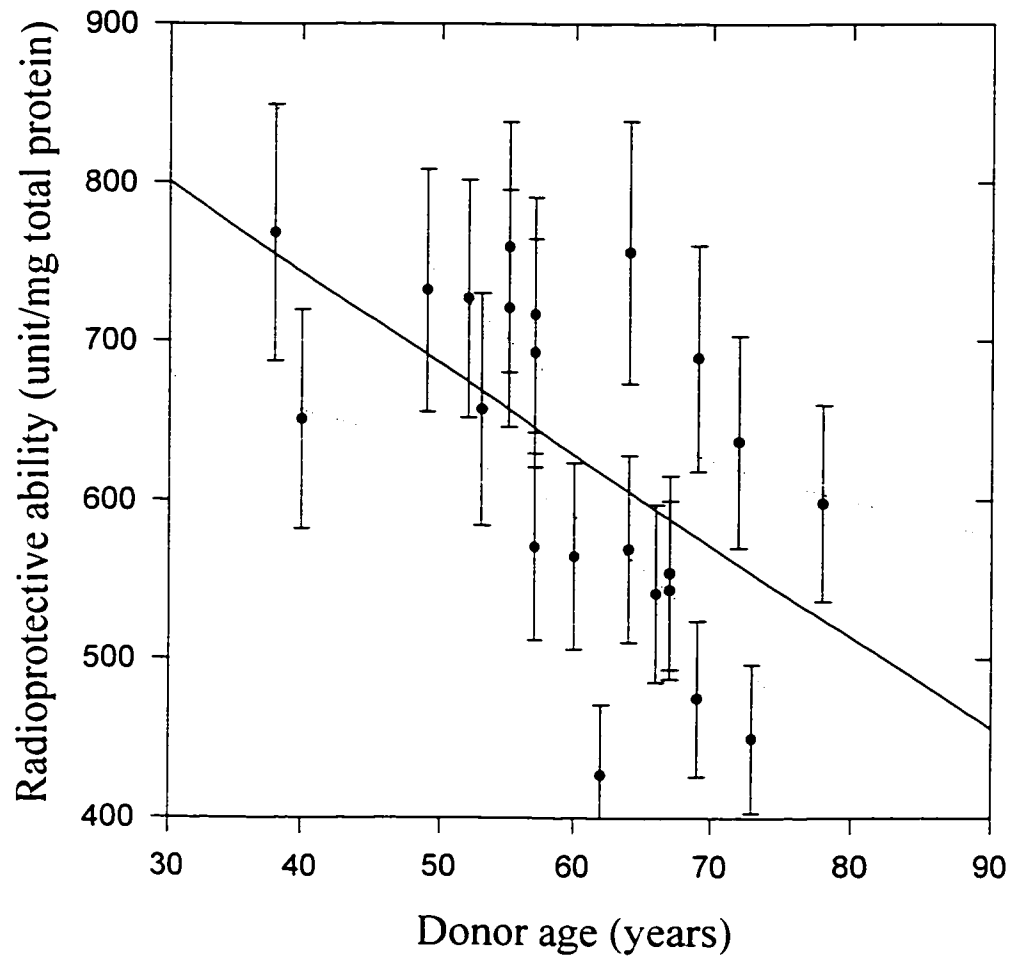
Figure 45: The radioprotective ability of cancer patient blood plasma and its relationship with donor age. The dotted lines show 95% confidence limits.
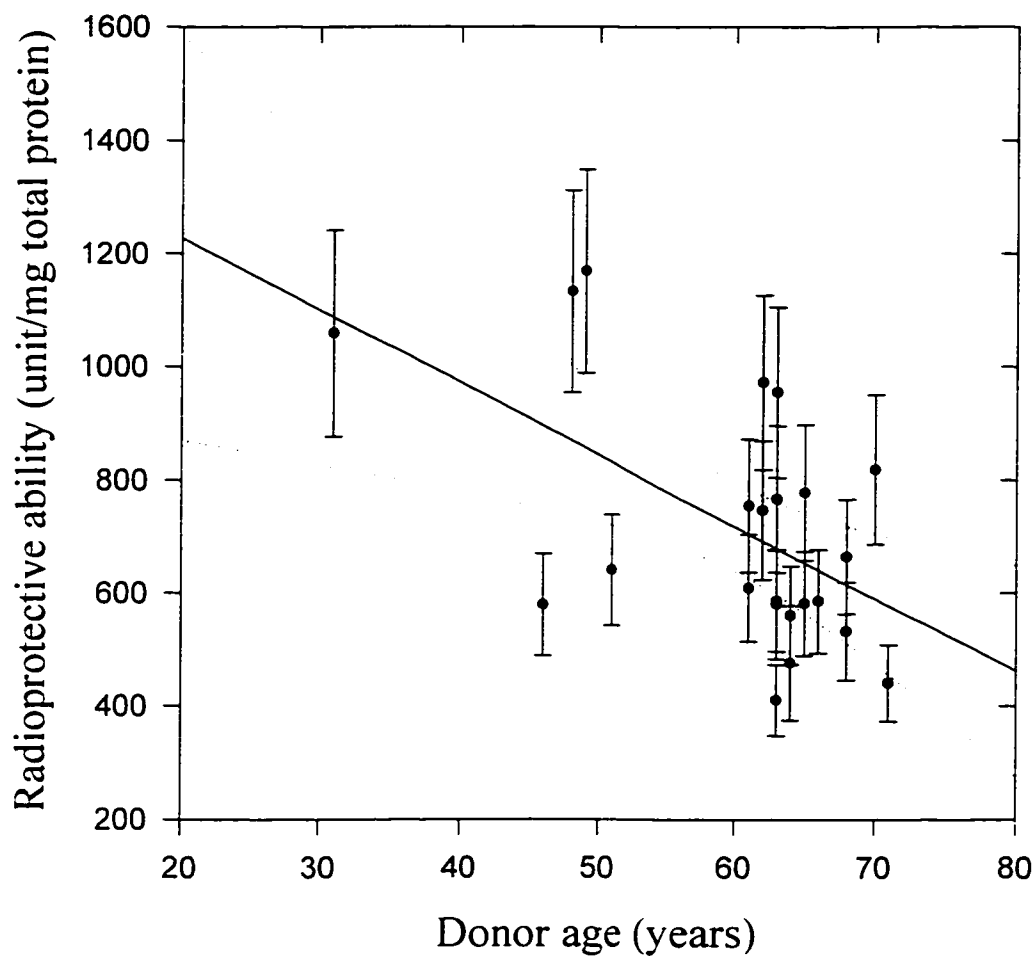
Figure 46:The radioprotective ability of normal healthy blood plasma and its relationship with donor age. The dotted lines show 95% confidence limits.

# Chapter 10: SURVIVAL AS A FUNCTION OF ADDED MELATONIN CONCENTRATION

Biological samples have been shown to have good radioprotecting properties. Additions of low molecular weight antioxidants are able to provide additional protection. Melatonin, the most protective water soluble compound measured in Chapter 6 was tested as a possible radioprotector using survival as the biological endpoint measured by a novel Alamar Blue assay (described in Appendix III).

## 10.1 Materials And Methods

HN-5a cells (passages 34-40) were trypsinised and the cell suspension passed through a syringe to make it a single cell suspension in DF media with 10% FBS. The concentration of cells was measured using a cytometer. Solutions of melatonin were made up at twice the final concentration (0-8.62 mmol $L^{-1}$ final concentration). The initial solvent was *tert*-butanol. The final concentration of solvent was less than 0.3% v/v and did not interfere with the assay. A 200 µL volume of a melatonin solution was added to 200 µL of the cell suspension. The mixture was incubated on ice for 30 minutes. The cells were then irradiated to 4 Gy in an AECL Gammacell 200 irradiator ($^{60}$Co source) at a dose rate of 0.01 Gy $s^{-1}$. The irradiated cells were then plated into microwell plates as described in Appendix III and incubated for a week at 37°C and in a 2% carbon dioxide atmosphere. The protocol for the Alamar Blue survival assay was then followed.

## 10.2 Results And Discussion

Figure 47 shows the results of a series of experiments for survival at 4 Gy as a function of seven added melatonin concentrations. The results show that high concentrations of melatonin can increase the survival of these cells by a factor of two at 4 Gy. Lower concentrations do not protect as well. An estimated $[P]_{50}$, the concentration of radioprotectant to provide a half maximum level of protection, can be calculated from these data. This value was found to be ~4.5±0.4 mmol $L^{-1}$, assuming a linear relationship over the changing region. This value differs from that of Vijayalaxmi *et al.* [79], whose data indicate a 50% restitution level of 1 mmol $L^{-1}$ for chromosome damage to human lymphocytes. This disagreement of 3.5 mmol $L^{-1}$ is most likely due to differences between the cells lines (a squamous cell carcinoma cell line as opposed to human lymphocytes) and the different end-points used (survival as opposed to chromosome breakage).

Superimposing the melatonin data onto the control survival curve (see Figure 48) a value for the 'Dose Reduction Factor' (DRF) can be estimated. The DRF is the fraction by which the control dose needs to be reduced for an effect equal to that in the radioprotected cells. An estimated value for the DRF at 4 Gy for an 8.6 mmol $L^{-1}$ addition was 1.8 . These results show that additions of antioxidants can have a dramatic impact on cellular survival.
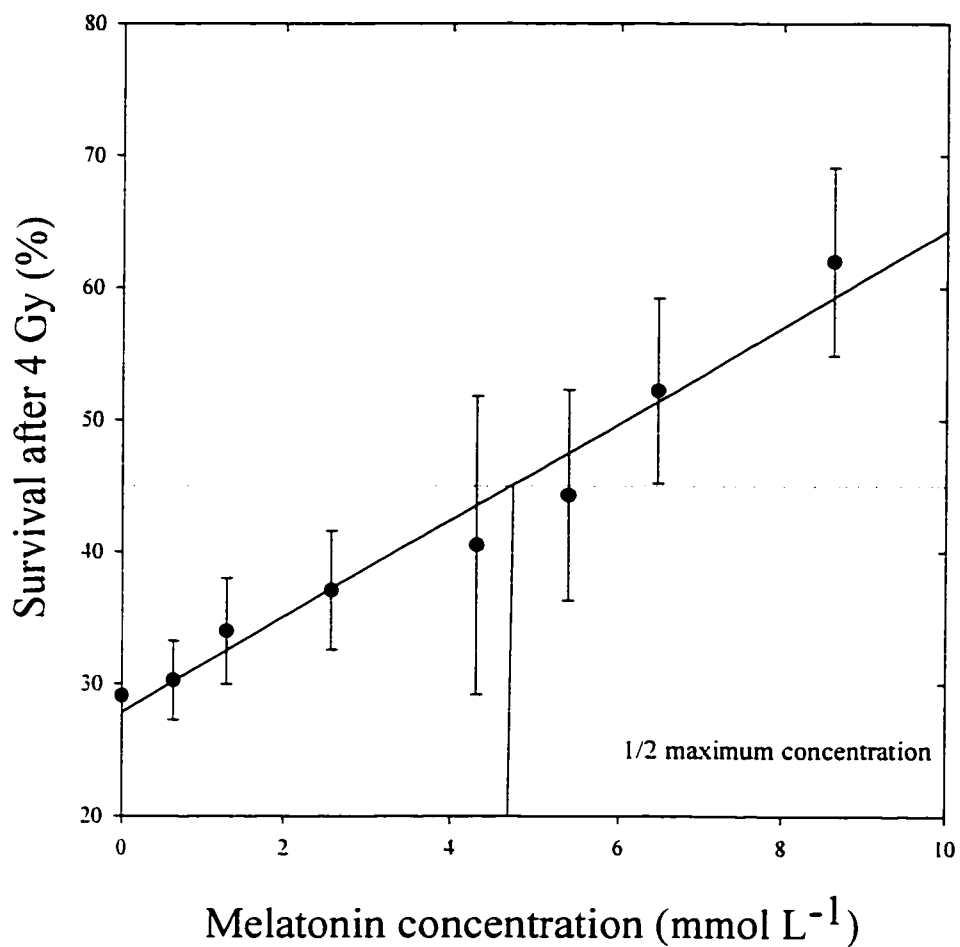
Figure 47: The survival of HN-5a cells after a 4 Gy irradiation as a function of eight

added melatonin concentrations. A further experiment was performed at 20 mmol L⁻¹,

which confirmed that the plateau is at 60% survival.
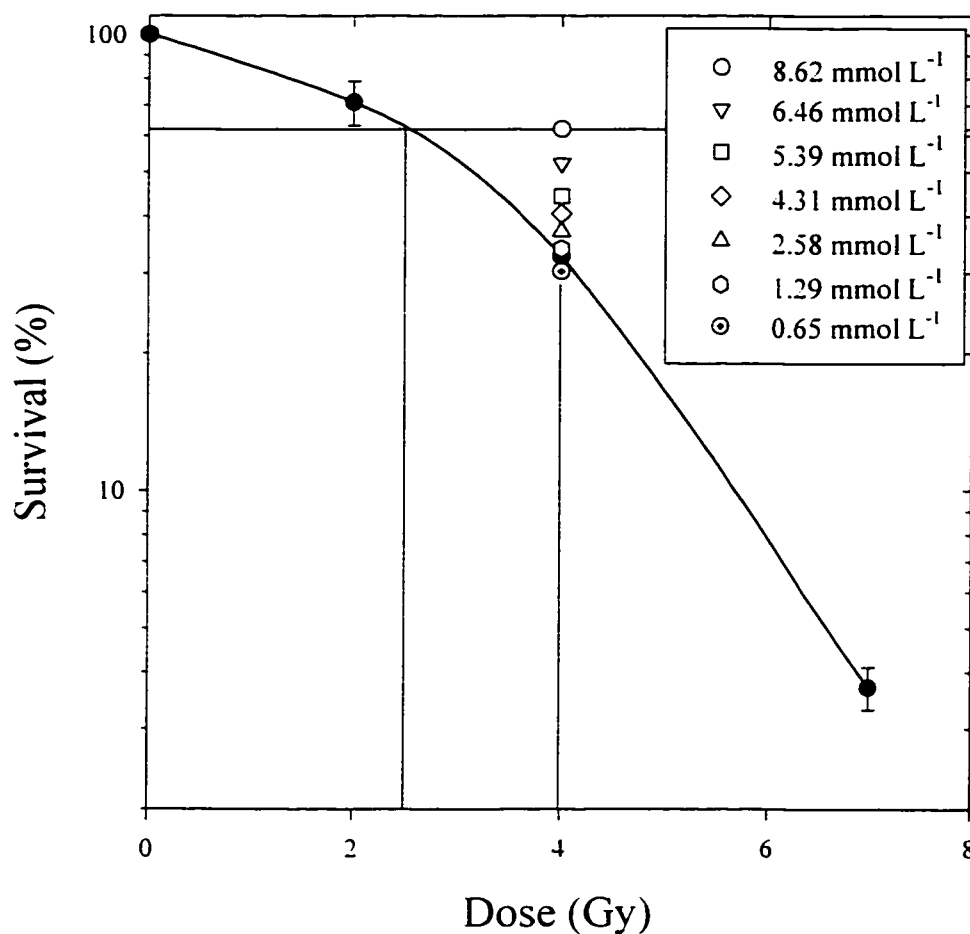
Figure 48: The control survival curve as a function of radiation dose of the HN-5a line
(solid symbols), with survival at 4 Gy for different added melatonin concentrations (open
symbols). The vertical lines indicate how the Dose Reduction factor (DRF) was
calculated.

# Chapter 11: CONCLUSIONS

There are two main mechanisms by which compounds can radioprotect target molecules in an aqueous system (Chapter 1). The first is by scavenging hydroxyl radicals, which are the most reactive, and therefore damaging, radicals produced during water radiolysis. All compounds are free radical scavengers to some extent; however, simple organic molecules such as sugars and solvents act solely by this mechanism. Using first-order reaction kinetics, relative rate constants for reactions between these compounds and hydroxyl radicals, which are a measure of the effectiveness of these compounds, can be calculated.

Antioxidants can also radioprotect by hydrogen donation and competition with oxygen in secondary reactions. Because oxygen fixation is much slower than primary hydroxyl radical attack, antioxidants can chemically 'repair' potential target radical damage and thus reconstitute irradiated target molecules at concentrations much lower than would be required purely on the basis of free radical scavenging.

A fluorescent protein, $\beta$-phycoerythrin, has been used as a model target molecule for studying induced ionising radiation damage mediated by generated free radicals (Chapter 4). The bleaching in fluorescence during irradiation serves as a measure of the oxidative stress induced by the radiation. Additions of compounds to solutions of this protein are able to reduce the bleaching effect thereby reducing the induced oxidative stress in the solution. This principle has been developed into a convenient microwell assay to test and characterize mechanisms of radiation protection. The use of a semi-automated microwell plate system, as opposed to manual measurements in cuvettes, improves both the quality and quantity of the data. Solvents and sugars show effective

protection and the BPE assay is able to predict rate constants for the reactions of these compounds with hydroxyl free radicals (Chapter 5). Although the experiments are carried out under steady state conditions, tertiary reactions are not an important source of interference, as indicated by the 'good' agreement between the majority of the results and those obtained from the literature.

The qualitative difference between pure hydroxyl radical scavengers and hydrogen donors is demonstrated by comparing the radioprotective effectiveness of ascorbic acid with DMSO. The two compounds have very similar rate constants for their reactions with hydroxyl radicals, as measured by pulse radiolysis [6]. However, ascorbic acid protects BPE solutions 37 times better than DMSO, consistent with the hydrogen donating properties of this compound (Chapter 5). Several different antioxidant compounds (thiols, phenols and indoles) were measured in the BPE assay to determine the radioprotective effect of each relative to ascorbic acid (Chapter 6). For some of these compounds, the data correlate with oxidation potentials from the literature, confirming that it is the reductive or hydrogen donating ability of the compounds that is the key to their radioprotective action.

The most protective set of compounds studied was the indole class, represented by melatonin and serotonin (~8-9 times more protective that ascorbate; see Table 4) . Derivatives of these compounds should be examined more for practical use. They are neuro-active, and therefore have implications for human use, but they are inherently non-toxic. A chemical modification to the epitope of these compounds might eliminate their neuro-activity without necessarily reducing their antioxidant capacity. Surprisingly, the

thiols, which have been the most widely used radioprotective compounds were the least protecting class of antioxidants studied.

An attempt was made to correlate the results from the BPE assay with data in the literature for protective effects *in vitro*. The limiting factor was the lack of available data, given that only similar protocols and cell lines could be reasonably inter-compared. However this very limited data set was compatible with an inverse correlation between the BPE data and effects *in vitro*, suggesting that these compounds also radioprotect by hydrogen donation within cells. It would be a valuable piece of research to perform a systematic evaluation of a range of these compounds in a standardised cell tissue culture system. Melatonin was tested as a radioprotector *in vitro* using a survival endpoint and shown to be highly radioprotective.

Uric acid was a better than expected radioprotector in the BPE system. This may be an artifact of its low solubility, but it should be tested *in vivo*, to ascertain its realistic potential. The problem of low solubility could be overcome by using transformation type experiments to monitor preventative aspects of these compounds in carcinogenesis. These experiments, which serve as an *in vitro* model for cancer induction, are more sensitive and therefore more responsive to the limiting low concentrations of poorly soluble additives.

The BPE assay reflects both mechanisms of radioprotection, hydroxyl radical scavenging and hydrogen donation, so it can be used as a measure of total radioprotective effectiveness. Measurements were made on biological samples, human blood plasma and cell lysates (Chapters 8, 9). The blood plasma data demonstrated a decreasing effectiveness with age, with an 80 year old having, on average, about half the protective

capability of an 18 year old. Although this is a widely observed phenomenon for oxidative stresses, it has not been specifically reported for studies involving radiation generated radicals. Only whole blood plasma was examined for total radioprotective capacity in this study. Although outside the scope of this study, future experiments could include measurements on the different blood sample components, e.g. protein fraction, lipid soluble fraction, aqueous fraction and antioxidant content etc., to determine the relative contributions of each to the total protective capacity.

Cell lysate measurements using the BPE assay did not show a correlation between lysate total radioprotective capacity and cellular radiosensitivity.

Both these plasma and lysate measurements demonstrate that biological systems have highly reductive environments. This conflicts with evidence which shows that cells and organisms containing these reductive mixtures are, in fact, quite sensitive to radiation. Plasma represents an environment external to cells, and the lysate is an averaged cellular environment. These biological samples are not, therefore, truly representative of the microenvironment of the most important radiation target: genomic DNA.

The results suggest that it is not the total protective capacity of the cell which is the important parameter, but rather that capacity in the immediate DNA-environment. Only compounds that are in close proximity to the DNA target are able to provide effective protection. This would explain why additions of highly mobile, rapidly diffusing, low molecular weight antioxidants (<500 Da) are able to radioprotect cells at high concentrations (Chapter 10), yet the highly reductive yet more static cellular milieu (which has a higher average molecular weight) cannot.

To test this conclusion, fluorescent molecules could be targeted to specific sites within cells using antibody technology. The fluorescent targets could then be used as an indicator of oxidative stress during irradiation in the targeted microenvironment. This approach has begun to be used by Makrigiorgos *et al.* [ 107], who are using fluorescein-tagged proteins to investigate lipid oxidative stress. A recent technical development is the ability to splice genes, which code for fluorescent proteins, directly into a cell's genome. This will make it possible to engineer a cell to create fluorescent tags for its own proteins. Proteins associated with DNA, e.g. histones, could be made fluorescent by this method. This would be a powerful method for examining microenvironments inside living cells, and their ability to modify their response to radiation and other forms of oxidative stress.

## 11.1 A Possible Application: Emergency Nuclear Response

The firemen fighting the graphite fire in the immediate aftermath of the Chernobyl accident received large radiation doses (up to 16 Gy whole body irradiation). Above a 4 Gy whole body dose, irreversible bone marrow damage was common and bone-marrow transplantation was attempted in 13 patients. Only two patients survived this treatment. In this highest dose group (6-16 Gy) there was a 95% mortality [ 108]. Although these patients also received very high skin doses from surface $\beta$-irradiation, it was the compromised immune system, due to reductions in blood cell production in the bone marrow, that was the limiting factor. Bone marrow stem cells are, therefore, the most radiosensitive target cells in the body. It is theoretically possible to radioprotect these cells.

A few assumptions need to be made. The first is that melatonin, found to be the most effective fully water-soluble radioprotector in the BPE system, can be made into a neuro-inactive, and non-toxic derivative of equal radioprotective effectiveness. The second is that this derivative protects the cells to the 50% level at a concentration of 1 mmol $L^{-1}$ as reported by Vijayalaxmi et al. [79] for human lymphocytes, rather than the 4 mmol $L^{-1}$ measured in this study for the HN-5a cell line. Using the data presented in Chapter 7, a concentration twice this 50% level allows approximately twice as many cells to survive at 4 Gy, corresponding to a DRF of 1.8. This is assumed to be a relative correction that can be applied at higher doses (i.e. the DRF at 6 Gy is assumed to be the

same as at 4 Gy). The final assumption is that only the blood fraction needs to be protected.

The average blood volume is 6 L. This volume would be protected with a DRF of 1.8 by an intake of 12 mmol (2.8 g melatonin). People often consume gram quantities of other antioxidants so 12 mmol would be reasonable. This blood concentration could be achieved by a one time injection followed by slow release tablets taken orally, to account for losses due to renal clearance and diffusion to non-blood compartments. This could provide the required protection for up to 1 hour.

Highly exposed workers in the 6-16 Gy range, a range in which there was a 95% mortality at Chernobyl, would have damage equivalent to 3-6 Gy if so protected, a dose range in which there was a 30% mortality. In addition, other body fractions would receive protection, although not to the same level, reducing secondary complications such as gastro-intestinal syndrome. This could reduce mortality further. It is probable that the risk of developing radiation induced neoplasms would also be significantly reduced.

Some more research is necessary to test these assumptions and if successful, antioxidants could become an important aspect of nuclear emergency response.

# References

[ 1] Glazer AN; Hixson CS. Subunit structure and chromophore composition of rhodaphytan phycoerythrins. Porphyridium cruentum B-phycoerythrin and β-phycoerythrin. J. Biol. Chem. 252:32-42; 1977.

[ 2] Johns HE; Cunningham JR. The Physics of Radiology. 4$^{th}$ ed. Charles C. Thomas: Springfield Ill.; 1983.

[ 3] Matheson MS. The formation and detection of intermediates in water radiolysis. Radiat. Res. suppl. 4:1-23; 1964.

[ 4] Braams R. Rate constants of hydrated electron reaction with amino acids. Radiat. Res. 27:319-329; 1966.

[ 5] Huels MA; Parenteau L; Sanche L. Substrate dependence of electron-stimulated O-yields from dissociative electron attachment to physisorbed $O_2$. J. Chem. Phys. 100:3940-3956; 1994.

[ 6] Buxton GV; Greenstock CL; Helman WP; Ross AB. Critical review of rate constants for reactions of hydrated electrons, hydrogen atoms and hydroxyl radicals (·OH/·O⁻) in aqueous solution. J. Phys. Chem. Ref. Data 17:513-886; 1988.

[ 7] Chuaqui CA; Petkau A. Chemical reactivity and biological effects of superoxide radicals. Radiat. Phys. Chem. 30:365-373; 1987.

[ 8] Bielski BH; Cabelli DE; Arudi RL; Ross AB. Reactivity of $HO_2$/$O_2^-$ radicals in aqueous solution. J. Phys. Chem. Ref. Data 14:1041; 1985.

[ 9] Tubiana M; Dutreix J; Wambersei A. Introduction to Radiobiology. Taylor and Francis, London; 1990.

[ 10] Michaels HB; Hunt JW. A model for radiation damage in cells by direct effect and by indirect effect: A radiation chemistry approach. Radiat. Res. 74:23-34; 1978.

[ 11] Milligan JR; Ward JF. Yield of single-strand breaks due to attack on DNA by scavenger derived radicals. Radiat. Res. 1377:295-299; 1994.

[ 12] Reuvers AP; Greenstock CL; Borsa J; Chapman JD. Studies on the mechanism of chemical radioprotection by dimethyl sulphoxide. Int. J. Radiat. Biol. 244:533-536; 1973.

[ 13] Lloyd SS; Chang AK; Taylor FB; Janzen EG; McCay PB. Free radicals and septic shock in primates: The role of tumor necrosis factor. Free Rad. Biol. Med. 14:233-242; 1993.

[ 14] McCord JM; Gao B; Leff J; Flores SC. Neutrophil-generated free radicals: possible mechanisms of injury in adult respiratory distress syndrome. Environ. Health Perspect.102:57-60; 1994.

[ 15] Duthie G; Arthur JR. Free radicals and calcium homeostasis: relevance to malignant hyperthermia. Free Rad. Biol. Med. 14:435-442; 1993.

[ 16] Palozza P; Gabrialla C; Gianna MB. Prooxidant activity of $\beta$-carotene under 100% oxygen pressure in rat liver microsomes. Free Rad. Biol. Med. 19:887-892; 1995.

[ 17] von Sonntag C. Topics in free radical-mediated DNA damage: purines and damage amplification-superoxic reactions- bleomycin, the incomplete radiomimetic. Int. J. Radiat. Biol. 66:485-490; 1994.

[ 18] Scaduto RC. Oxidation of DMSO and methanesulfinic acid by the hydroxyl radical. Free Rad. Biol. Med. 18:271-277; 1995.

[ 19] Petkau A. Free radicals, aging and degenerative diseases. Modern Aging Research 8:481-508; 1986.

[ 20] Breccia A; Greenstock CL; Tamba M. eds. Advances on Oxygen Radicals and Radioprotectors, Lo Scarabeo: Bologna, Italy; 1984.

[ 21] Spinks JWT; Woods RJ. An Introduction to Radiation Chemistry, J. Wiley and Sons, N.Y., U.S.A.; 1964.

[ 22] Blok J; Verhey WSD. The attack of free radicals on biologically active DNA in irradiated aqueous solutions. Radiat. Res.34:689-703; 1968.

[ 23] Dubner D; Gisone P; Jaitovich I; Perez M. Free radical production and estimation of oxidative stress related to $\gamma$-irradiation. Biol. Trace Elem. Res. 47:265-270; 1995.

[ 24] Olive P; Frazer G; Banath JP. Radiation-Induced apoptosis measured in TK6 human B lymphoblast cells using the comet assay. Radiat. Res. 136:130-136;1993.

[ 25] Akagi N; Ito K; Sawada S. Radiation-induced apoptosis and necrosis in Molt-4 cells: a study of dose-effect relationships and their modification. Int. J. Radiat. Biol. 64:47-56; 1993.

[ 26] Forman HJ; Fisher AB. Antioxidant defenses. In "Oxygen and Living Processes"; Gilbert DL ed. Springer-Verlag, New York; 1981.

[ 27] Greenstock CL. Redox processes in radiation biology and cancer. Radiat. Res. 86:196-211; 1981.

[ 28] Lane DP. p53, guardian of the genome. Nature 358:15-16; 1992.

[ 29] Burton GW; Ingold KU. Mechanisms of antioxidant action, studies on vitamin E and related antioxidants in biological systems. In "Protective Agents in Cancer"; McBrien DCH; Slater TF. eds. Academic Press, New York; 1983.

[ 30] Burton GW; Ingold KU. Autoxidation of biological molecules. 1.The antioxidant activity of vitamin E and related chain-breaking phenolic antioxidants in vitro. J. Amer. Chem. Soc. 103:6672-6477; 1981.

[ 31] Kayushin LP. ed. Water in biological systems. Consultants Bureau, New York; 1969.

[ 32] North AM. The collision theory of chemical reactions in liquids. Methuen, London; 1964.

[ 33] Fisher GJ; Johns HE. Photohydration of pyrimidines. In "Photochemistry and Photobiology of Nucleic Acids"; Wang,S.Y. ed., Gordon and Breach, New York; 1974.

[ 34] Ebert M; Keene JP; Swallow AJ; Baxendale JH. eds. Pulse Radiolysis Academic Press, London; 1965.

[ 35] Adams GE; Fielden EM; Michael BD eds. Fast Processes in Radiation Chemistry and Biology. John Wiley and Sons; London; 1975.

[ 36] Hunt JW; Greenstock CL; Bronskill MJ. Design considerations for nanosecond pulse radiolysis studies using kinetic spectrophotometry. Int. J. Radiat. Phys. Chem. 4:87-105; 1972.

[ 37] Vermeil C. Effets de concentration en chimie des radiations des solutions aqueuses. Int.J.Radiat.Biol. 3:307-326; 1961.

[ 38] Moroson HL; Quintiliani M. eds. Radiation Protection and Sensitization. Taylor and Francis, London; 1970.

[ 39] Arley N. Theory of the kinetics of enzyme inactivation in solution by ionizing radiation. Radiat. Res. 29:1-17; 1966.

[ 40] Bartosz G; Leyko W. Radioprotection of bovine erythrocytes to haemolysis. Int. J. Radiat. Biol. 39:39-46; 1981.

[ 41] Shubin VN; Dolin PI. The method of a competitive scavenger in radiation chemistry. Radiat. Res. 19:345-358;1963.

[ 42] Cao G; Alessio HM; Cutler RG. Oxygen radical absorbance capacity assay for antioxidants. Free Rad. Biol. Med. 14:303-311; 1993.

[ 43] Ghiselli A; Serafini M; Maiani G; Azzini E; Ferro-Luzzi A. A fluorescence based method for measuring total plasma antioxidant capability, Free Rad. Biol. Med. 18:29-36; 1995.

[ 44]McKenna R; Kezdy FJ; Epps DE. Kinetic analysis of the free-radical-induced lipid peroxidation in human erythrocyte membranes: Evaluation of potential antioxidants using cis-parinaric acid to monitor peroxidation. Anal. Biochem. 196:443-450; 1991.

[ 45] Jay-Gerin J-P; Ferradini C eds. Cahiers de radiobiologie, aspects physiques, chimiques et biologiques. Numero 2; 1995.

[ 46] Bacq ZM. Ed. Chemical Protection against Ionizing Radiation. Charles Thomas, Springfield, Ill.; 1965.

[ 47] Latarjet R; Ephrati E. Influence protectrice de certaines substances contre l'inactivation d'un bactériophage par les rayons X. C.R soc.Biol. 142:497; 1948.

[ 48] Bacq ZM; Herve A. Protective action of methylamine against X irradiation. Nature 168:1126; 1951.

[ 49] Herve A; Bacq ZM. Cyanure et dose léthale de rayons X. C.R. soc. Biol. 143:881; 1949.

[ 50] Michaels HB; Peterson EC; Epp ER. Effects of modifiers of the yield of hydroxyl radicals on the radiosensitivity of mammalian cells at ultrahigh dose rates. Radiat. Res. 95:620-636; 1983.

[ 51] Roots R; Okada S. Protection of DNA molecules of cultured mammalian cells from radiation-induced single-strand scissions by various alcohols and SH compounds. Int. J. Radiat. Biol. 21:329-342; 1972.

[ 52] Sasaki MS; Matsubara S. Free radical scavenging in protection of human lymphocytes against chromosome aberration formation by gamma-ray irradiation. Int. J. Radiat. Biol. 32:439-445; 1977.

[ 53] Davies KJA. Oxidative stress: the paradox of aerobic life. Biochem. soc. symp. 61:1-31; 1994.

[ 54]Packer L. ed. Oxygen Radicals in Biological Systems. Academic Press, Orlando; 1984.

[ 55] Buettner GR. The pecking order of free radicals and antioxidants: Lipid peroxidation, $\alpha$-tocopherol and ascorbate. Arch. Biochem. Biophys. 300:535-543; 1993.

[ 56] Sharma M; Buettner G. Interaction of vitamin C and vitamin E during free radical stress in plasma: An ESR study. Free Rad. Biol. Med. 14:649-653; 1993.

[ 57] Bump EA; Brown JM. Role of glutathione in the radiation response of mammalian cells in vitro and in vivo. Pharmac. Ther. 47:117-136; 1990.

[ 58] Dubinina EE; Shygaley IV; Melenevsky AT; Tslinskii IV. Characteristics of low molecular weight substances regulating plasma superoxide dismutase activity. Free Rad. Biol. Med. 17:351-353; 1994.

[ 59] Kedziora J; Sibinska E; Rozga B; Bartosz G. Gamma-radiation sensitivity of fibroblast DNA in trisomy 21. Hereditas 105:161-162; 1986

[ 60] Schwaiger H; Weirich HG; Brunner P; Rass C; Hirsch-Kauffmann M; Groner Y; Schweiger M. Radiation sensitivity of Down's syndrome fibroblasts might be due to overexpressed Cu/Zn-superoxide dismutase. Europ. J. Cell Biol. 48:79-87; 1989.

[ 61] Rushmore TH; Morton MR; Pickett CB. The antioxidant responsive element. J. Biol. Chem. 266:11632-11639; 1991.

[ 62] Jaworska A; Rosiek O. Paraquat increases superoxide dismutase activity and radiation resistance in two mouse lymphoma L51178Y cell strains of different radiosensitivities. Int. J. Radiat. Biol. 60:899-906; 1991.

[ 63] Green MHL; Lowe JE;Waugh APW; Aldridge KE; Cole J; Arlett CF. Effect of diet and vitamin C on DNA strand breakage in freshly-isolated human white blood-cells. Mutat. Res. 316:911-102; 1994.

[ 64] Gerster H. Anticarcinogenic effect of common carotenoids. Int. J. Vit. Nutr. Res. 63:93-121; 1993.

[ 65] Jaworska A; Rosiek O;Witkowska K. Activities of superoxide dismutase and catralase in two L5178Y murine lymphoma cell strains with different radiosensitivities. Nukleonika 32:193-200; 1987..

[ 66] Marklund SL; Westman G; Roos G; Carlsson J. Radiation resistance and the Cu, Zn superoxide dismutase, Mn superoxide dismutase, catalase and glutathione peroxidase activities of seven human cell lines. Radiat. Res. 100:115-123; 1984.

[ 67] Adams GE; Michael BD; Willson RL. Radiation Chemistry vol.1 Advances in Chemistry Series, Gould RF ed., Amer. Chem. Soc.; 1968 p289.

[ 68] Littlefield LC;  Joiner E;  Colyer S; Sayer A; Frome E. Modulation of radiation -

induced chromosome aberrations by DMSO and OH radical scavenger. 1: Dose-response

studies in human lymphocytes exposed to 22 kV X-rays. Int. J. Radiat. Biol..53: 875-890;

1988.

[ 69] Redpath JL; Willson RL. Reducing compounds in radioprotection and

radiosensitization: Model experiments using ascorbic acid. Int. J. Radiat. Biol. 23: 51-65;

1973.

[ 70] Chapman  JD; Reuvers  AP; Borsa  J; Greenstock  CL. Chemical radioprotection

and radiosensitization of mammalian cells growing *in vitro*. Radiat. Res. 56:291-306;

1973.

[ 71] Shimoi K; Masuda S; Furugori M; Esaki S; Kinae N. Radioprotective effect of

antioxidative flavonoids in γ-ray irradiated mice. Carcinogenesis 15:2669-2672; 1994.

[ 72] Sarma L; Kesavan PC. Protective effects of vitamins C and E against γ-ray-induced

chromosomal damage in mouse. Int. J. Radiat. Biol. 63:759-764; 1993.

[ 73] Reiter RJ; Melchiorri D; Sewerynek E; Poeggeler B; Barlow-Walden L; Chuang J;

Ortiz GG; Acuna-Castroviejo D. A review of the evidence supporting melatonin's role as

an antioxidant, J. Pineal Res. 18:1-11; 1995.

[ 74] van Acker SABE; van den Berg D; Tromp MNJL; Griffioen DH; van Bennekom

WP; van der Vijgh WJF; Bast A. Structural aspects of antioxidant activity of flavonoids.

Free Rad. Biol. Med. 20:331-342; 1996.

[ 75] Ghiselli  A; Serafini  M; Maiani  G; Azzini  E; Ferro-Luzzi A. A fluorescence based

method for measuring total plasma antioxidant capability, Free Rad. Biol. Med. 18:29-36;

1995.

[ 76] Marshall KA; Reiter RJ; Poeggeler B; Aruoma OI;Halliwell B. Evaluation of the antioxidant activity of melatonin *in vitro*. Free Rad. Biol. Med. 21:307-315; 1996.

[ 77] Meites L; Zuman P; Scott WJ; Campbell BH; Kardos AM. eds. Electrochemical Data. J.Wiley & Sons: New York; 1974.

[ 78] Sasaki MS; Matsubara S. Free radical scavenging in protection of human lymphocytes against chromosome aberration formation by gamma-ray irradiation. Int. J. Radiat. Biol. 32:439-445; 1977.

[ 79] Vijayalaxmi; Russel JR; Meltz ML. Melatonin protects human blood lymphocytes from radiation-induced chromosome damage. Mutat. Res. 346:23-31; 1995.

[ 80] Hertog MGL; Feskens EJM; Hollman PCH; Katan MB; Kromhout D. Dietary antioxidant flavonoids and risk of coronary heart disease: The Zutphen elderly study. Lancet 342:1007-1011; 1993.

[ 81] Kono S; Ikeda M; Tokudome S; Kuratsune M. A case control study of gastric cancer and diet in northern Kyushu, Japan. Jpn. J. Cancer Res.79:1067-1074; 1988.

[ 82] Cook NC; Samman S. Flavonoids-chemistry, metabolism, cardioprotective effects, and dietary sources. Nutrit. Biochem. 7:66-76; 1996.

[ 83] Wang ZY; Huang MT; Ho CT;Chang R; Ma W;Ferraro T; Reuhl KR; Yang CS; Conney AH. Inhibitory effect of green tea on the growth of established skin papillomas in mice. Cancer Res. 52:6657-6665; 1992.

[ 84] Rice-Evans CA; Miller NJ; Paganga G. Structure-antioxidant activity relationships of flavonoids and phenolic acids. Free Rad. Biol. Med. 20:933-956; 1996.

[ 85]Kennedy AR; Troll W; Little JB. Role of free radicals in the initiation and promotion of radiation transformation. Carcinogenesis 5:1213-1218; 1984.

[ 86]Kong Z; Liu Z; Ding B. Study on the antimutagenic effect of pine needle extract. Mutat. Res. 347:101-104; 1995.

[ 87] Campos AM; Lissi EA. Total antioxidant potential of Chilean wines. Nutr. Res. 16:385-389; 1996.

[ 88] Shimoi K; Masuda S; Furugori M; Esaki S; Kinae N. Radioprotective effect of antioxidative flavonoids in gamma-ray irradiated mice. Carcinogenesis 15:2669-2672; 1994.

[ 89] Mabry TJ; Markham KR; Thomas MB.eds. The Systematic Identification of Flavonoids. Springer: New York; 1970.

[ 90] Saleh N; Miller NJ; Paganga G; Tijburg L; Bolwell GP; Rice-Evans C. Polyphenolic flavonols as scavengers of aqueous phase radicals and as chain-breaking antioxidants. Arch.Biochem.Biophys. 322:339-346; 1995.

[ 91] Gentner NE; Morrison DP; Myers DK. Impact on radiogenic cancer risk of persons exhibiting abnormal sensitivity to ionizing radiation. Health Phys. 55:415-425; 1988.

[ 92] Gentner NE; Morrison DP; Cecil D; Courchesne L; Gale K; Johnson LD; Joyce T; Norton G; Ostrom J; Paterson L; Plattner M; Smith BP; Walker J-A; Werner MM; Wills A; Danjoux CE. Screening human populations for abnormal radiosensitivity. AECB Report Ref.No. 85.8.20; 1985.

[ 93] Lai CY. The measurement of terminal amines.Methods Enzymol. 47:236-243; 1977.

[ 94] McCord JM; Fridovich I. Superoxide dismutase: an enzymic function for erythrocuprein (hemocuprein). J.Biol.Chem. 244:6049-6055; 1969.

[ 95] Lück H. Catalase. In "Methods of Enzymatic Analysis". Bergmeyer H-U ed. Academic Press, New York; 1965.

[ 96] Leist M; Raab B;Maurer S; Rosick U; Brigelius-Flohe R. Conventional cell culture media do not adequately supply cells with antioxidants and thus facilitate peroxide-induced genotoxicity. Free Rad. Biol. Med. 21:297-306; 1996.

[ 97] Cercek L; Cercek B; Keene JP. Pulse-radiolysis study of human blood plasma. Int. J. Radiat. Biol. 20:1-6; 1971.

[ 98] Cercek B; Cercek L. Radiolytic processes in human blood plasma. In "Proceedings of the first european congress" Verlay, Vienna; 1971.

[ 99] Harris G; Holmes A; Sabovljev SA; Cramp WA; Hedges M; Hornsey S; Hornsey JM; Bennett GC. Sensitivity to X-irradiation of peripheral blood lymphocytes from aging donors. Int. J. Radiat. Biol. 5:685-694; 1986.

[ 100] Fowler JF. The effect of age on radiosensitivity, in "Radiation Effects" Ebert M and Howard A eds., North Holland Publishing, Amsterdam; 1963 pp 310-332.

[ 101] Higami Y; Shimokawa I; Okimoto T; Ikeda T. Vulnerability to oxygen radicals is more important than impaired repair in DNA damage in aging. Labor. Invest. 71:650-656; 1994.

[ 102] Singh N; Danner D; Tice R; Brant L ; Schneider EL. DNA damage and repair with age in individual lymphocytes. Mutat. Res. 237:123-130; 1990.

[ 103] Becker K; Boetticher D ; Leichseuring W. Ubiquinone-10 plasma concentrations in healthy European children. Redox Report 1:97-98; 1995.

[ 104] Warner HR.Superoxide dismutase, aging and degenerative disease. Free Rad. Biol. Med. 17:249-258; 1994.

[ 105] Yamaoka K; Edamantsu R; Itoh T;Mori A. Effects of low dose X-ray irradiation on biomembrane in brain cortex of aged rats. Free Rad. Biol. Med. 16:529-534; 1994.

[ 106] Gaziev A; Sologub G; Fomenko L; Azichkina S; Kosyakova N;Bradbury R. Effect of vitamin antioxidant micronutients on the frequency of spontaneous and *in vitro* γ-ray induced micronuclei in lymphocytes of donors: The age factor. Carcinogenesis 17:493-499; 1996.

[ 107] Makrigiorgos MG; Kassis AI; Mahmood A; Bump EA; Savvides P. Novel fluorescein-based flow-cytometric method for detection of lipid peroxidation. Free Rad. Biol. Med. 22:93-100; 1997.

[ 108] Chernobyl ten years on; Radiological and health impact. OECD, Paris; 1996.

[ 109] Spinks JWT; Woods RJ. An Introduction to Radiation Chemistry, J. Wiley and Sons, N.Y., U.S.A.; 1964.

[ 110] Puck TT; Markus PI. Action of X-rays on mammalian cells. J. Exp. Med. 103:653-666; 1956.

[ 111] Cole SPC. Rapid chemosensitivity testing of human lung cancer cell lines using the MTT assay. Cancer Chemother. and Pharmacol. 17: 259-263; 1986.

[ 112] Carmichael J; DeGragg WG;Gazdar AF. Evaluation of a tetrazolium-based semiautomated colorimetric assay: assessment of radiosensitivity. Cancer Res. 47:943-946; 1987.

[ 113] Twentyman PR; Luscombe M. A study of some variables on a tetrazolium dye (MTT) based assay for cell growth and chemosensitivity. Brit. J. Cancer 56 :279-285; 1987.

[ 114] Eble MJ; Hensley FW; Flentje M. A modified computer-assisted colorimetric microtitre assay (MTT) to assess *in vitro* radiosensitivity of V79, CaSki, HeLa and WiDr cells. Int. J. Radiat. Biol. 65:193-201; 1994.

[ 115] McDonnell TJ; Marin MC; Hsu B; Brisbay SM; McConnell K; Tu S-M; Campbell ML; Rodriguez-Villanueva J. The bcl-2 oncogene: Apoptosis and neoplasia. Radiat. Res. 136:307-312; 1993.

# APPENDIX I : DOSIMETRY

The radiation facility used to irradiate samples was an AECL Gammacell 220. The basic arrangement is shown in Figure 49. The cell consists of a chamber into which a sample can be placed. The chamber is then lowered into a cage surrounded by pencils of $^{60}Co$, to receive a dose determined by the length of time in the fully down position, plus a 'dead time dose', as the cage is raised and lowered. Because there is a dose variation throughout the chamber volume it was important to determine the dose distribution to a 96-well plate in the Gammacell 220. This is not straight forward. It is easy to determine the dose to a point in the chamber using an ionisation chamber, but not the dose to a small liquid volume in 96 microwells. The strategy was to first calibrate a Fricke solution and use this to calculate the dose to 1 mL volumes of water in polystyrene cuvettes. Next BPE solutions themselves were used as a crude dosimeter to link the dose to a cuvette to the dose to the microwell volumes. Fricke is also necessary because there are significant buildup and backscatter complications arising from the use of such small sample volumes. Other measurement techniques would not be also to account for these.

Fricke dosimetry [21] relies on the conversion of $Fe^{-}$ to $Fe^{--}$ during the irradiation of aqueous solutions. The $Fe^{---}$ ion can be detected by measuring changes in optical density. The Beer-Lambert Law describes the extent to which radiation is absorbed by a substance at a particular wavelength. The measured parameter is absorbance or optical density (OD) and is given by :

$$OD = \log_{10} \frac{I_0}{I} = \varepsilon l c \qquad (A1.1)$$

where $I_o$=intensity of incident radiation

$I$ = intensity of transmitted radiation

$l$ = path length (m)

$c$ = concentration (mol m$^{-3}$)

$\varepsilon$ = molar absorption coefficient (m$^2$ mol$^{-1}$)

First a polystyrene jig, designed to position four standard cuvettes (Figure 50) was made to fit exactly into the 15 cm diameter chamber of the Gammacell 220. To measure the dose-rate at position 1, a 0.6 cc Farmer type Keithley ion chamber was used. This device was a tertiary standard. The probe was placed in position 1 in a consistent way (see Figure 51) and irradiated for different lengths of time to determine total exposure (X). The results are shown in Figure 52. The regression fit

is: $X(kR) = (0.324 \pm 2.2\%)kR + (0.0685 \pm 0.1\%)kRs^{-1} \times t$ \hfill (A1.2)

giving a dose rate to water of 0.649 Gy s$^{-1}$ for this meter[1]. Using this probe it was possible to show that the dose rate between the four cuvette positions varied by 0.3%.

A Fricke solution was made with 0.5 mol L$^{-1}$ ferrous sulphate (FeSO$_4$H$_2$O), 0.5 mol L$^{-1}$ sodium chloride and 2% concentrated sulphuric acid. The solution was made using water of resistivity 18.2 M$\Omega$ cm .

The maximum absorbance wavelength of the Fe$^{3+}$ ion was determined by scanning 2 mL irradiated (~100 Gy) solutions in quartz cuvettes over the 290-310 nm range with a

---

[1] $Dose = X(0.00873 \dfrac{J}{kgR})(\dfrac{\overline{\mu_{ab}}}{\rho})_{air}^{water} k$ where $(\dfrac{\overline{\mu_{ab}}}{\rho})_{air}^{water} = 1.111$ and k=0.98

Beckman UV 5240 Spectrophotometer. For these experiments the maximum absorbance

occurred at 301 nm. All absorbance measurements were then made at this wavelength.

To calibrate the Fricke solution, an arrangement was required to reduce the solution

volume, and geometry to approximate that of the probe. The exact arrangement is shown in

Figure 51. The 0.6 mL Fricke solution is housed in the inner tube, with a build up 'cap' of

water and polystyrene. These Fricke tubes were irradiated in exactly the same position as

the probe for different times. The results are shown in Figure 53. The regression fit

parameters are: $\Delta OD = (0.01819 \pm 14.2\%) + (0.00229 \pm 0.76\%)s^{-1} \times t$          (A1.3)

Comparing this rate of change in absorbance with the dose-rate for the same position gives

a calibration factor for the solution in the fully down position of 283.4 ±0.8% Gy per unit

change in optical density .

This calibration factor was used to calculate the dose to the 1 mL volumes in the

polystyrene cuvettes.

Four 1 mL volumes of the Fricke solution in cuvettes were irradiated for different

times in the jig. The samples for each time were pooled and the absorbance measured as

described above. The results are shown in Figure 54. The response is linear with regression

parameters given by : $\Delta OD = (0.025 \pm 0.01) + (0.00245 \pm 1.7\%)s^{-1} \times t$          (A1.4)

Using the calibration value for this solution the dose rate for this new geometry in the fully

down position was found to be 0.695 ±1.9% Gy s$^{-1}$ .

Using established constants for Fricke [21] the absolute dose rate was found to be

0.702±1.7% Gy s$^{-1}$. This absolute dose rate compares very well with the value calculated

from the calibration factor, adding credibility to the results.

The dose for solutions in cuvettes has been established, but the microwell plates are in a different geometry. Fricke, or other methods of dose measurement would not be able to adequately measure the small volumes. The fact that BPE, together with high levels of radioprotectant, gives a linear decrease in fluorescence as a function of dose, means that it can be used as a crude dosimeter. A BPE solution with 800 μg mL$^{-1}$ trolox was irradiated for 30 s in 1 mL cuvettes. Solutions were also irradiated in the centre of a microwell plate for the same time. The cuvettes had an average fluorescence of (90.6±2.45) % (n=8) and the microwells (87.38±0.34) % (n=3). These data indicated that a correction factor of 0.964±2.5% has to be applied to the cuvette measurements to generate the central microwell dose. Using this information the dose rate to a microwell plate on 25 November 1994 was 0.670±3.1% Gy s$^{-1}$. More detailed analysis is limited by the large errors associated with the BPE measurements. Using the ratio

$$\frac{\text{Dead time exposure}}{\text{Exposure rate}} = \frac{\text{Dead time dose}}{\text{Dose rate}} = \frac{0.324}{0.0685}s = 4.73s \quad \text{to find the dead time, a value}$$

for the dose to a microwell plate for a down time of 30 s was found to be 23.3 Gy (=0.67 Gy s$^{-1}$ × (30+4.73)s).

Central post lowers
sample into fields

Door to sample
chamber

Concrete
shielding

Cobalt pencils
surround
irradiating
chamber

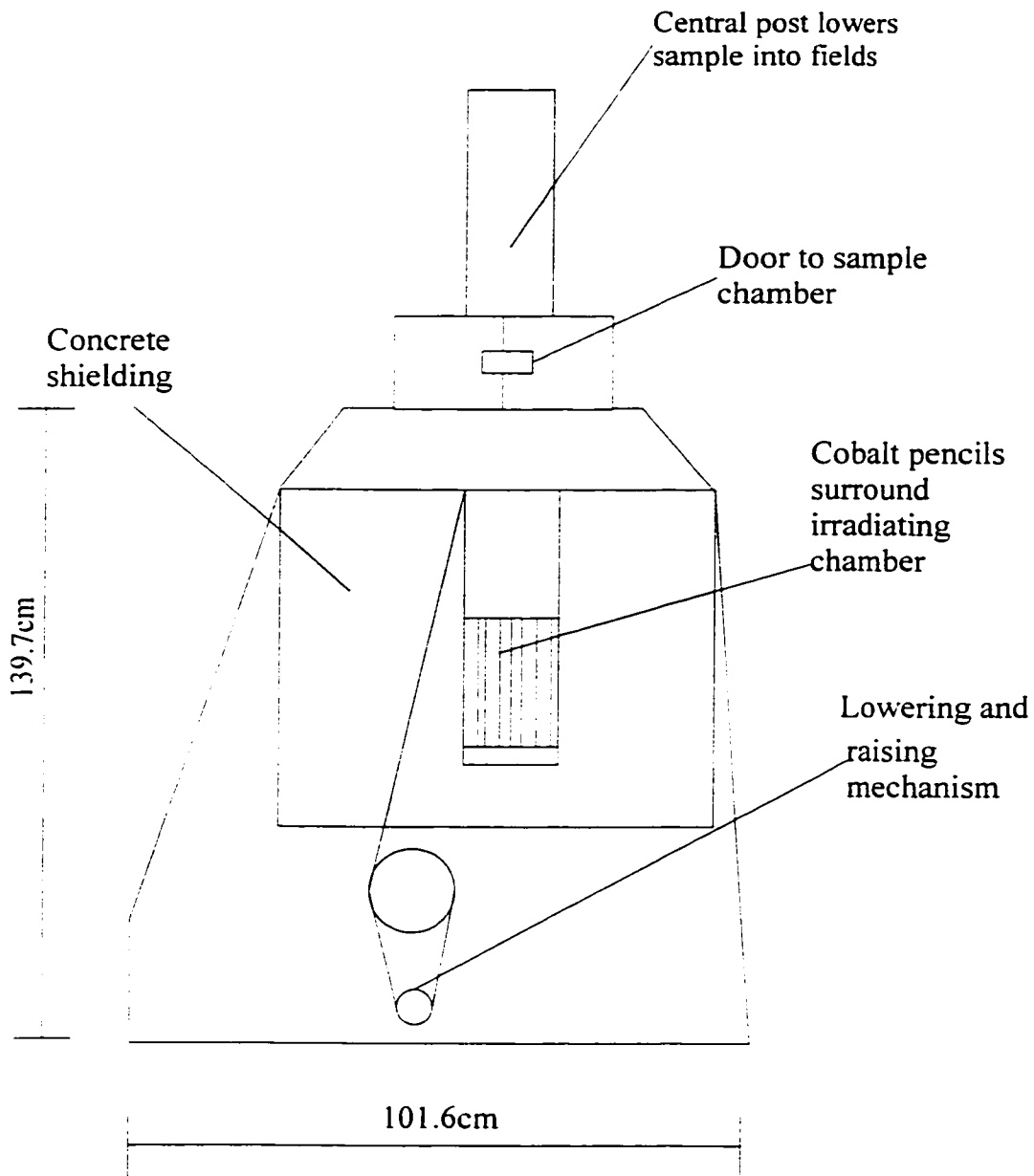139.7cm

Lowering and
raising
mechanism

101.6cm

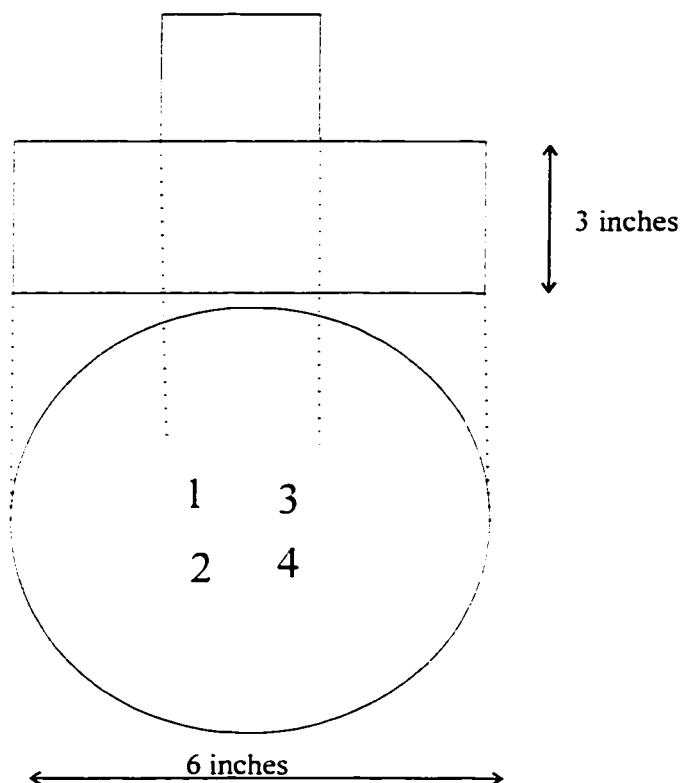Figure 49: A simplified cross-sectional view of a Gammacell 220.

Figure 50: The general arrangement of a positioning jig used in the Gammacell 220. The four cuvette positions in the central attachment are shown.
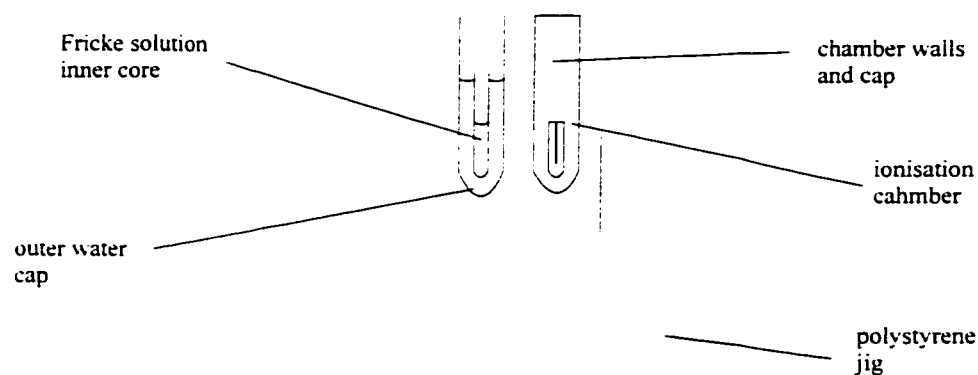
Figure 51: A diagram showing the position of the reference ionisation chamber. The Fricke solution is shown in a similar geometry for calibration purposes. Here the two arrangements are shown in different cuvette positions. For actual calibration the same position was used.
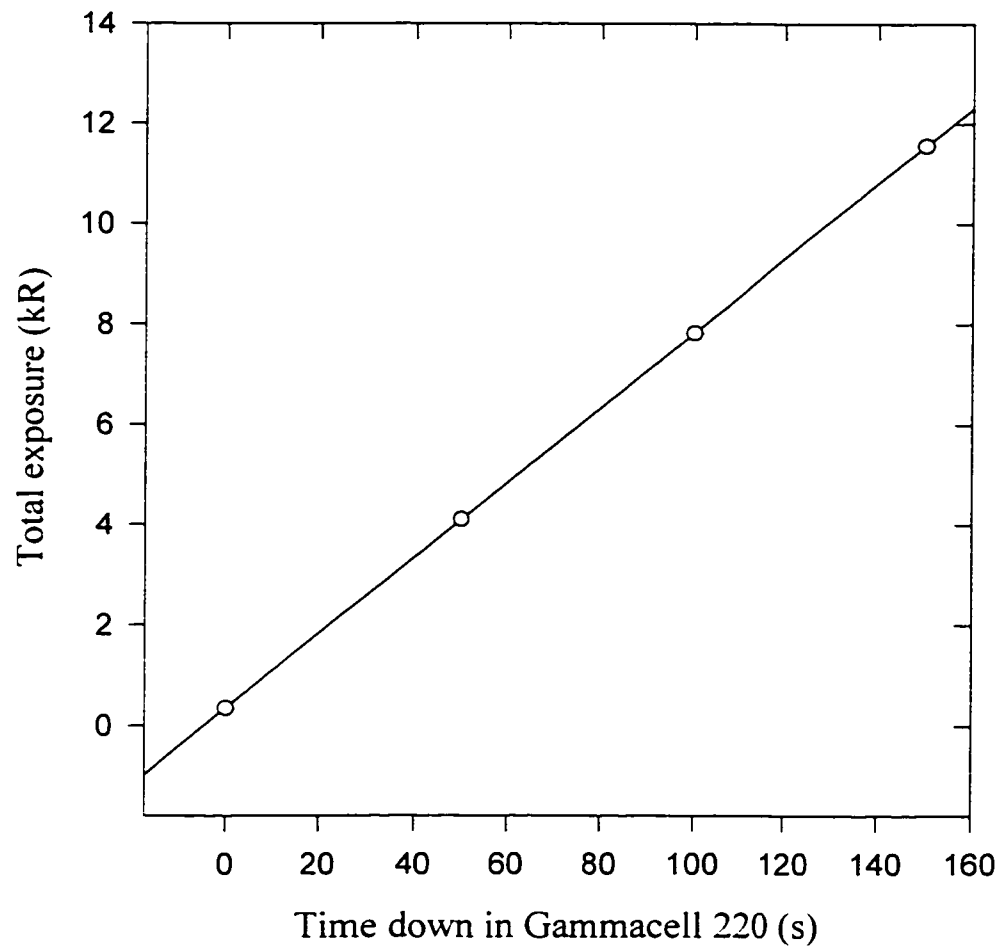
Figure 52: The increase in total exposure as measured by an ion chamber as a function of

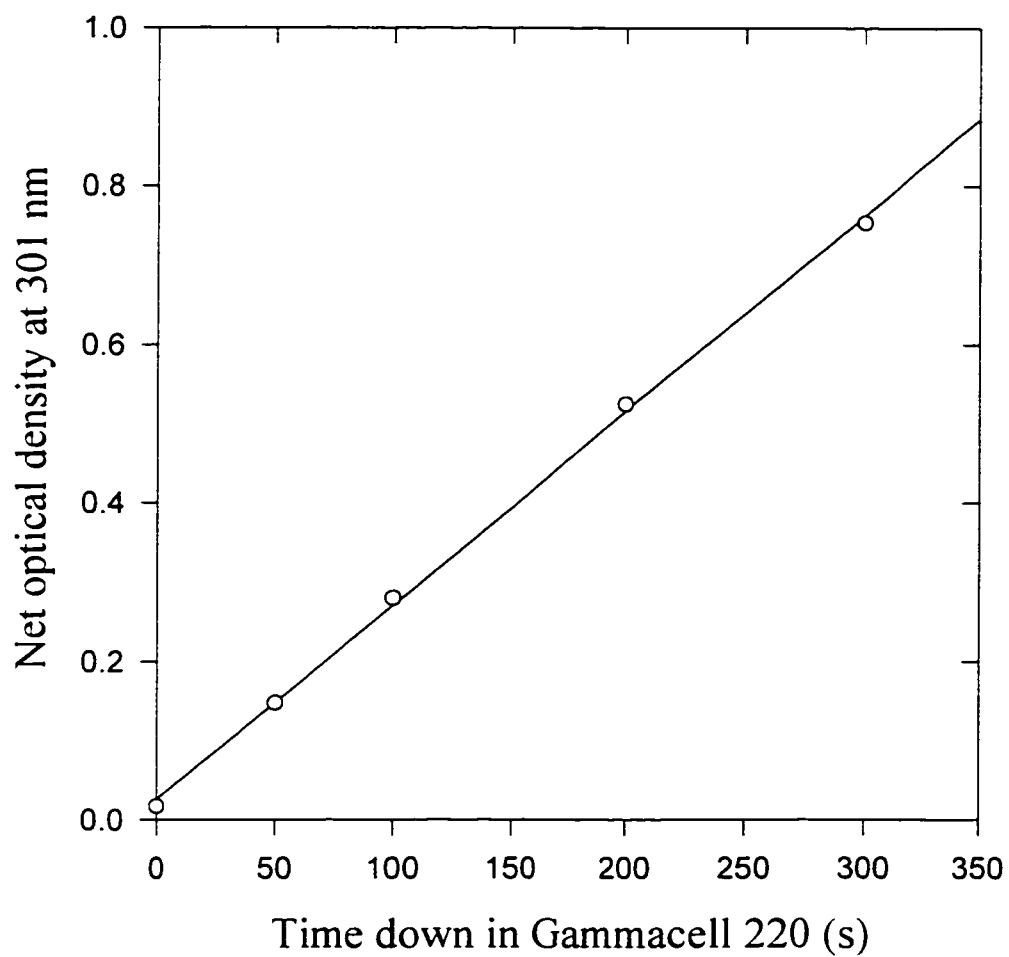time in the fully down position in a Gammacell 220.

Figure 53: The change in optical density at 301 nm of a Fricke solution in cuvettes as a function of time in the fully down position in a Gammacell 220.
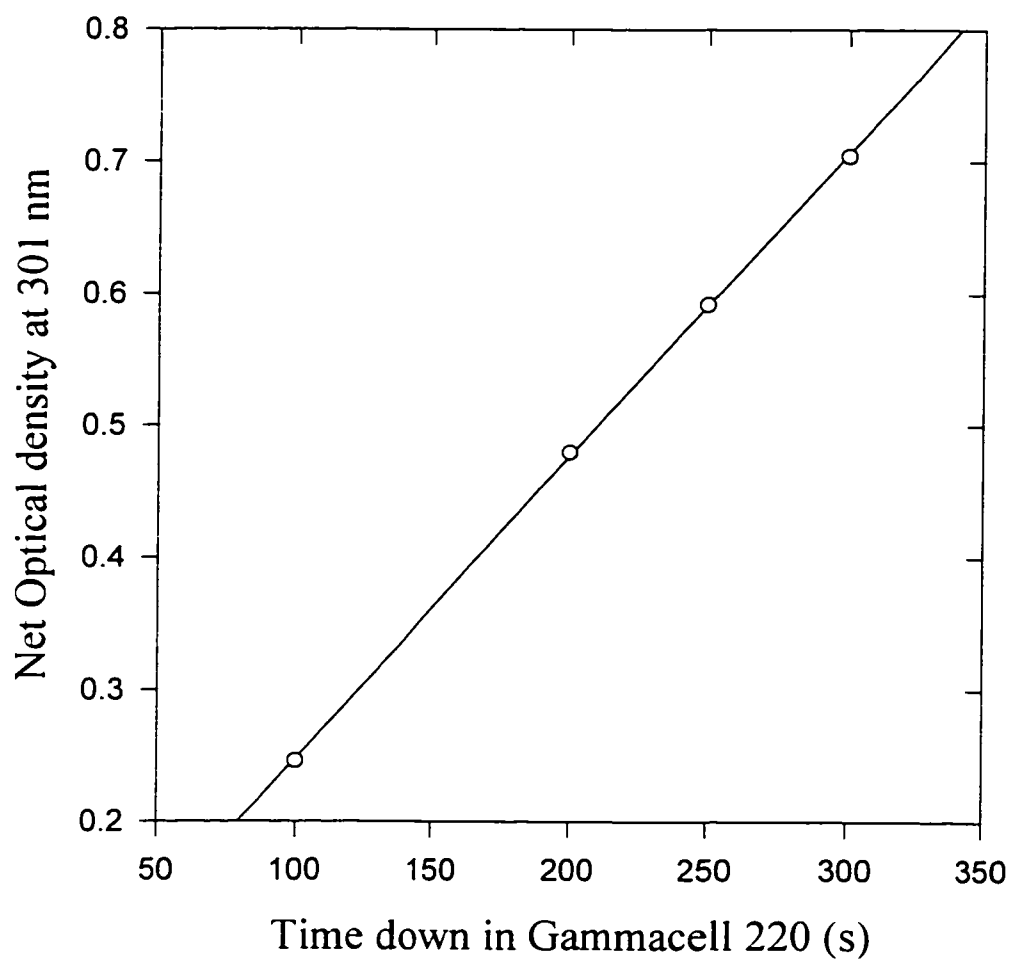
Figure 54: The increase in optical density at 301 nm of a Fricke solution as a function of time in the fully down position in a Gammacell 220.

# APPENDIX II : TISSUE CULTURE

## II.1 Fibroblast and Attached Cell Culture as used for experiments in Chapter 8

Fibroblasts and other attached cell lines will grow in mono-layer sheets on surfaces that provide adequate support and adhesion. This involves polystyrene flasks specially treated to allow for cell growth. These cell lines also require foetal bovine serum (FBS) to be present in the media to provide essential growth factors. The medium used here was Dulbecco's/F12 (DF), which allows optimum growth of fibroblasts, as it contains amino acids, sugars, vitamins and other essential nutrients. The medium was obtained from Gibco in powdered form and was made up according to the manufacturer's instructions to a pH 7.45-7.55 before filtration. Media were filter-sterilised by passage through a 0.2 μm Nunc filter. Phials of Cells in a 10% DMSO medium were removed from liquid nitrogen cryostorage locators. They were placed on dry ice for 1-2 hours and then in a -20 °C freezer for an additional hour. This allowed a gradual increase in temperature. The phial then quickly thaws at room temperature. The contents of the phial were suspended in 10 mL of DF media and spun out for 10 minutes at 600$g$. The cell pellet was resuspended and the cells placed in a T75 flask with fresh media. The cells resumed exponential growth after 18 hours at 37 °C and a 2 % carbon dioxide atmosphere.

Attached cell cultures need to be periodically detached from the flask surface and allowed to resettle for healthy exponential growth. This is achieved by cleaving the cell adhesion proteins that attach the cells to the plate surface with the protease trypsin.

*TRYPSINISATION OF ATTACHED CELLS*

The confluent cell cultures were washed with media containing no FBS three times to remove all proteins present in the media. A wash was then made with 1 mL trypsin solution. This was removed and 1 mL fresh trypsin solution added, ensuring that the entire culture area was covered. The flask was incubated for 5 minutes at 37 °C. A quick knock of the plate detached the cells into a cell suspension. The cells could then be diluted to the appropriate concentration for replating or experimental use.

## II.2 Lymphoblastoid Cell Line Culture

Lymphoblast cells derive from human B-lymphocytes infected with Epstein Barr virus. This onco-virus incorporates into the lymphocyte genome overriding the cell's normal cell cycle controls and immortalising the cell. Lymphoblast cell culture is different from that required for fibroblasts, mainly because these cell lines do not attach but grow in suspension. They also require different nutrient ratios which are met by RPMI1640, another medium supplied by Gibco. FBS was added to a concentration of 20%. Cells were retrieved from the freezer and warmed to 37 °C in a water bath. They were then spun out and resuspended in RPMI1640 with FBS. The cells were incubated at 37 °C with a 5% carbon dioxide atmosphere and quickly resume exponential growth as a thick layer on the bottom of the flask. The cultures needed to be kept at a cell concentration of between $0.2\text{-}1.3 \times 10^6$ cell mL$^{-1}$ for optimum growth. The cells tended to clump into balls of 10-100 cells so the culture requires passage through a syringe to produce a single cell suspension for experimental purposes. Large volume cultures were also grown in a spinner flask, where the culture was constantly agitated to redistribute the nutrients equally, and to reduce the size of the cell clumps.

## II.3 Blood Separation and Lymphocyte Culture

Volumes of 25-30 mL of whole blood were taken from a donor by phlebotomy (venous puncture). The blood was kept at 37 °C until processed. Heparin, as an anti-coagulation factor, was added to a concentration of 10 unit mL$^{-1}$ and the blood agitated. Volumes of 4 mL whole blood were carefully layered onto 5 mL ficoll solution (an osmotically balanced, sugar density gradient) in a 15 mL centrifuge tube. The tubes were

spun at 600*g* for 30 minutes to separate the blood into three fractions. The blood serum remained as a straw coloured solution above the ficoll. Lymphocytes collected in a ring at the serum/ ficoll interface and erythrocytes collected at the bottom of the tube. The serum supernatant can be removed for storage or discarded. The lymphocyte ring was removed carefully with a pipette and the red blood cells disposed of. The lymphocytes were transferred to a fresh 15 mL centrifuge tube with 14 mL Hank's solution. This tube was spun for 10 minutes at 600*g*. The supernatant was discarded and the cell pellet gently resuspended. The cell suspension could be counted, diluted and used for experimental purposes.

All surfaces were washed with a 10% bleach solution before and after use. Discarded products were bleached and autoclaved after the experiment was finished.

# APPENDIX III: THE ALAMAR BLUE ASSAY

## III.1 Survival as an Endpoint

The clonogenic survival assay was first described by Puck and Marcus [ 109] and

has become the predominant assay used in radiobiology. Basically the end-point is the

surviving fraction ($S_F$) of cells capable of forming a colony of at least 50 cells following a

radiation treatment compared with unirradiated controls:

$$S_F = \frac{\# \ of \ colonies \ formed \ in \ treatment \ group}{\# \ of \ colonies \ formed \ in \ control \ group} \qquad (A3.1)$$

.     Semi-log plots of survival as a function of radiation dose show a characteristic

shoulder repair curve and a 'linear' exponential portion. The curves usually fit a linear-

quadratic model ( $S_F = e^{-\alpha D - \beta D^2}$  $\alpha,\beta$: constants ; D: Dose).

## III.2 Development of the Alamar Blue Cell Survival Assay as used in Chapter 10

The clonogenic survival assay is time-consuming, labour intensive and requires

considerable skill and experience to obtain reproducible results. In an attempt to produce

a more quantitative instrument-based, semi-automated technique a novel viability assay

was developed. This assay utilises Alamar Blue, a commercially available indicator. This

non-toxic, non-carcinogenic product is modified by enzymes within cells to produce a

fluorescent intermediate. The rate of fluorescence production is a measure of the

metabolic activity of a cell. Assuming that cells of a particular cell line, under the same

conditions, are equal in metabolic activity, the total fluorescence produced becomes an indicator of viable cell number. This approach is similar to that for the MTT (3-4,5-dimethylthiazol diphenyl tetrazolium bromide) assay [ 110] ,which produces a measurable precipitate after incubation with viable cells. The MTT assay has been widely studied [110]-[ 112]. The Alamar Blue metabolite is more easily measured and the product is simply added to the culture medium with no preparatory steps. The formulation described here has similarities to that described by Eble *et al.* for the MTT assay [ 113].

An observation is that the fluorescence generated by light exposure at 545 nm (excitation) and measured at 575 nm (emission) after Alamar Blue incubation with cells, is proportional to the logarithm of the number of cells present [i.e. fluorescence (F) $\propto \log_{10}$(number of cells plated (k))]. This is probably due to the logarithmic nature of fluorescence intensity measurement.

This can be described by $F = m_D \, \log_{10}(k) + b$ where $m_D$ is the proportionality constant and b is the y-intercept. By measuring the fluorescence for different cell numbers plated (k) the parameters $m_D$ and b can easily be determined.

For two sets of cells- one irradiated with a dose D Gy, one with a control dose (0 Gy)- the equation becomes:

$$F_D = m_D \cdot \log_{10}(k_D) + b_D$$
$$F_0 = m_0 \cdot \log_{10}(k_0) + b_0$$

(A3.2)

The surviving fraction $S_F$ is defined as the fraction of cells surviving or, for equal effect, the number plated in the control over the number plated in the irradiated group $\dfrac{k_0}{k_D}$.

For an equal effect: $F_D = F_0$

$$\therefore \ m_D \cdot \log(k_D) + b_D = m_0 \cdot \log(k_0) + b_0$$

$$\frac{m_D}{m_0} \log_{10}(k_D) = \log(k_0) + \frac{b_0 - b_D}{m_0}$$

$$\frac{k_D^{\frac{m_D}{m_0}}}{k_0} = 10^{\frac{b_0 - b_D}{m_0}} \qquad\qquad\qquad (A3.3)$$

Knowing from a Taylor expansion in the limit $m_D/m_0 \sim 1$ that:

$$\frac{k_D^{\frac{m_D}{m_0}}}{k_0} \approx \frac{m_D}{m_0} \cdot \frac{k_D}{k_0}$$

A3.3 then becomes:

$$\frac{m_D}{m_0} \cdot \frac{k_D}{k_0} = 10^{\frac{b_0 - b_D}{m_0}}$$

$$\Rightarrow S_F = \frac{k_0}{k_D} = \frac{m_D}{m_0} \cdot 10^{\frac{b_D - b_0}{m_0}} \qquad\qquad (A3.4)$$

The surviving fraction is calculated from the slopes and constants of 'fluorescence versus cell number plated' curves. The benefit of this assay is its applicability to both fixed and suspension cells and the automation, which improves measurement. Variations in plating efficiency do not have to be taken into account since these are internally controlled. The drawback is that viability rather than clonogenicity is the final endpoint. This means that cells that are sterilised but continue to metabolize may interfere with the result.

## III.3 Experimental Protocol

A single cell suspension of the cell line was prepared in appropriate media with 10% foetal bovine serum (FBS). The cell concentration was measured using a Coulter cytometer. A 0.6 mL volume of the cell suspension was placed in 1.5 mL microcuvettes, one sample for each irradiation dose. The cells were placed on ice for 20 minutes. They were then taken to the irradiation facility and irradiated for the appropriate length of time (0-4 minutes). Although the samples were not on ice in the irradiation chamber, they were on ice both immediately before and after the irradiation. The sample temperature did not rise above a temperature at which repair processes become important (~15 °C). This is consistent with a dose of 4 Gy ($=4$ J kg$^{-1}$) raising the sample temperature by $10^{-3}$ °C ($=4$ J kg$^{-1}$/4.2×$10^{3}$ J kg$^{-1}$°C$^{-1}$).

After irradiation, the samples were diluted to about 600 cells/200 μL (3000 cells mL$^{-1}$), in media with FBS. A 200 μL volume of the complete media is placed in each well of a 96-well Coulter Tissue plate. Then, 200 μL of the diluted cell suspensions was placed in the first row (row A) of the plate. Each sample was measured in triplicate, so that four samples could be measured per plate. Using a multi-channel pipetter, a serial dilution was made down the plate with each subsequent row having half the cell concentration of the row above it. The plate was incubated at 37 °C and in either a 2% (fibroblasts) or a 5% (lymphocyte derived cells) carbon dioxide atmosphere for seven days. After this period, 20 μL of an Alamar Blue solution was added to each well and the plate incubated for four hours, or until a sufficient fluorescence had developed. The plate was then placed in the IDEXX FCA and the fluorescence of each well measured at

excitation and emission wavelengths of 545 nm and 575 nm respectively. The data were analysed to determine the $m_D$ and b values, and the survival calculated.

Because all cells have a tendency to settle on the bottom and clump under these conditions, care was taken to agitate the cells on a regular basis and to break up clumps by passage through a pipette tip. Each sample was treated the same in this respect.

## III.4 Results and Analysis

Figure 55 shows a set of Alamar Blue curves for the C3H 10T1/2 fibroblast cell line (a kind gift from J.B. Little of the Harvard School of Medicine), following the protocol in the Methods section. The responses are linear in the range 100-600 cells plated per well. The exact response depends on the cell line, irradiation conditions and incubation time. The slopes and intercepts of these lines were used to calculate survival using Equation (A3.4).

The survival curve plotted in Figure 56 is the average of three independent experiments measured by the Alamar Blue method. The values show good agreement with clonogenic assays for this cell line. The close agreement between them also indicates that the metabolic enzymes themselves are not radiation responsive.

Figure 57 shows data for the squamous cell carcinoma cell line HN-5a (a kind gift from Dr. P.J. Ferguson of the University of Western Ontario). This cell line has a similar radiation response to the 10T1/2 cell line. A clonogenic survival curve made under identical conditions confirmed that the Alamar Blue data are comparable to clonogenic survival for this cell line.

shows survival data for a normal LCL. This cell line shows a distortion at high doses. It is unclear if this is due to a highly resistant subpopulation (due to population kinetics) or, more likely, the remaining metabolism of 'dead' cells.

The Epstein Barr viral incorporation induces LCLs to overexpress the bcl-2 protein which suppressed apoptosis [ 114]. Killed cells therefore do not disintegrate but remain in the culture. To test these two factors Alamar Blue measurements were also made on serum starved cells. These cells were grown without serum for two weeks which slows their growth rate. It can be seen from

that they are more radiosensitive than cells fed normally. The similar slopes of the curves at 7 Gy however indicate that it is not cell population kinetics that is responsible for this effect, but remaining inactivated cell metabolism.

The Alamar Blue assay works well for attached cell lines and correlates well with clonogenic assays. Each cell line tested must also be tested against clongenic survival if comparisons are going to be made.
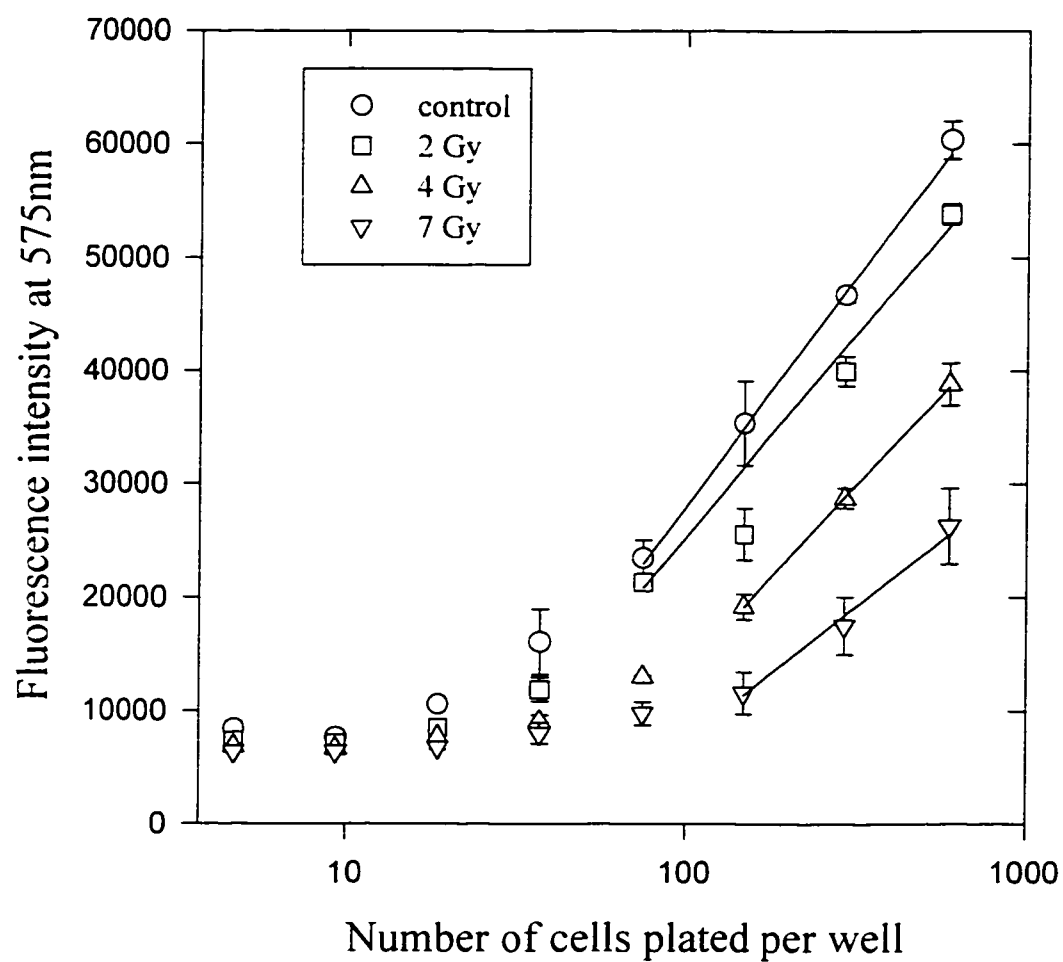
Figure 55: Typical results for the Alamar Blue fluorescence after incubation with C3H

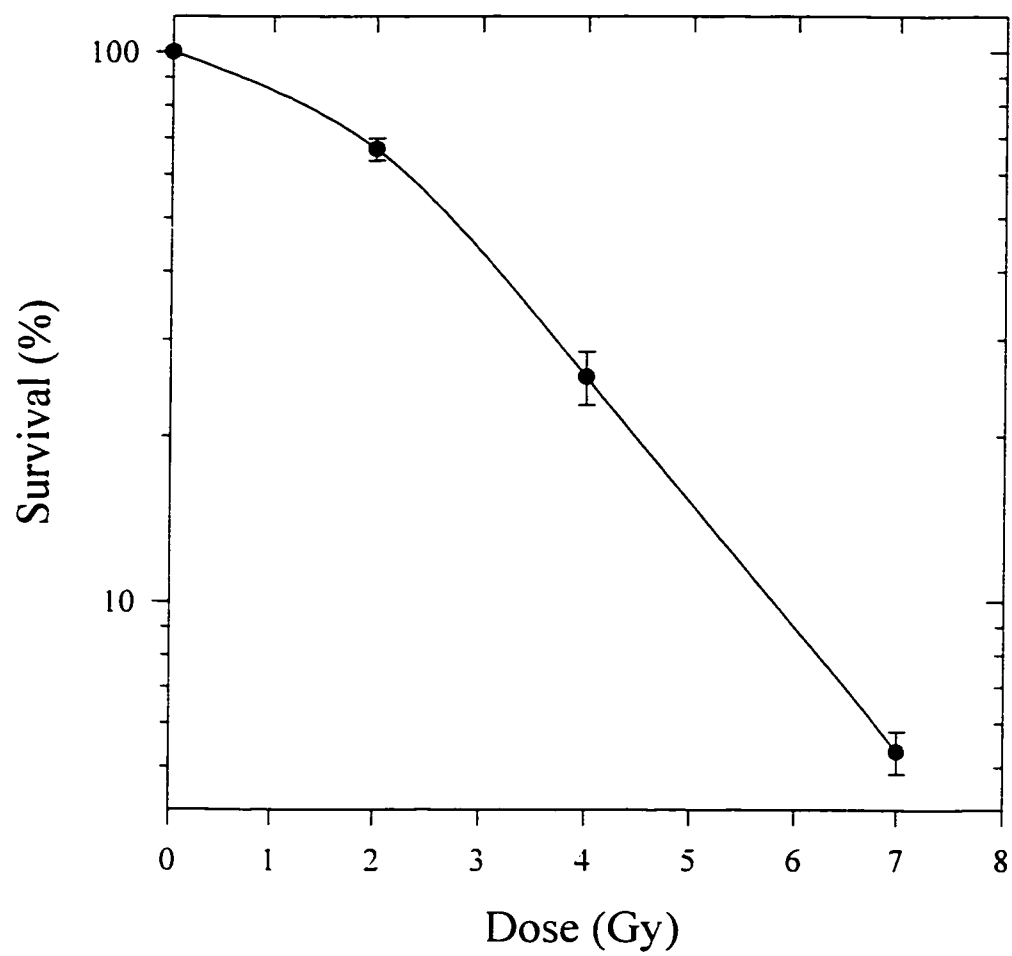10T1/2 cells as a function of cell number plated, for a series of radiation doses.

Figure 56: A survival curve for C3H 10T1/2 cells using the Alamar Blue assay. The error
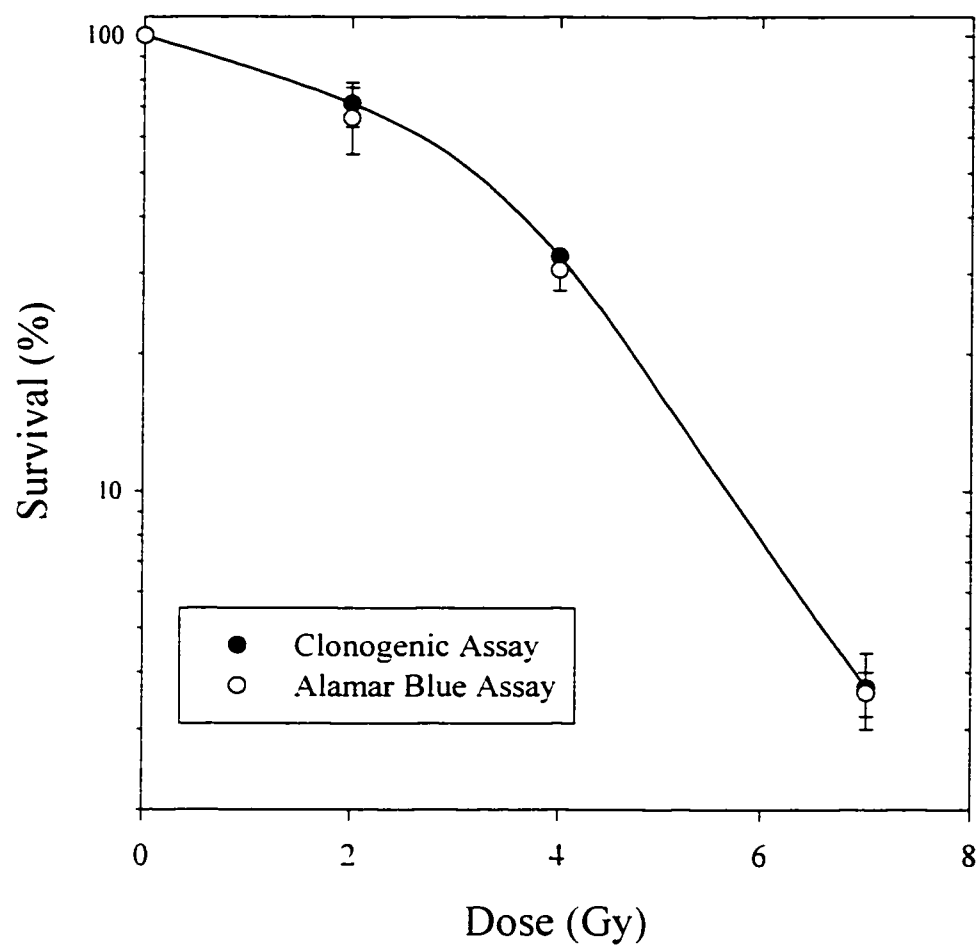
bars are standard deviations for three experiments.

Figure 57: A survival curve for HN-5a cells using the Alamar Blue (two experiments) and the clonogenic assay (two experiments).
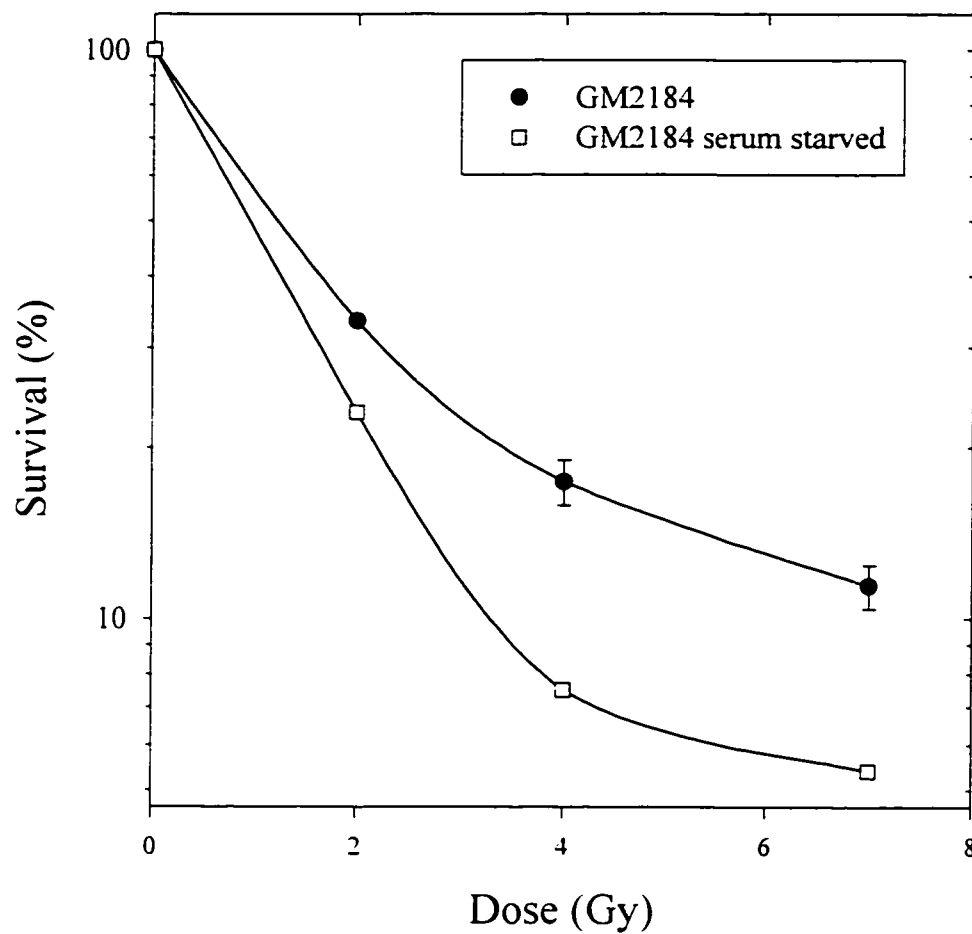
Figure 58: Survival curves for normally fed (average of two experiments) and serum starved (one experiment) GM2184 cells using the Alamar Blue assay.

# GLOSSARY

AECL: Atomic Energy of Canada Limited, CRL, Chalk River, Ontario, K0J 1J0.

BPE : β-phycoerythrin.

BSA : Bovine serum albumin.

Cat : Catalase.

Detapac: diethylene triamine pentaacetic acid.

DF : A medium consisting of a 1:1 mixture of Dulbecco's and F-12 media.

DMSO : dimethyl sulphoxide.

DNA: Deoxy ribonucleic acid.

DRF : Dose Reduction Factor. The DRF is the fraction by which the dose given to a control cell population is decreased to give the same level of survival as a radioprotected cell population.

$E_{1/2}(V)$: half-wave oxidation potential.

e⁻(aq): Hydrated electron.

e.g. : for example (*exempli gratia*)

FBS : Foetal bovine serum.

FCA : Fluorescence Concentration Analyzer.

G value: a measure of the quantity of chemical species produced per unit absorbed dose. It is defined as the number of resultant molecules formed per 100 eV deposited.

GBR: Grow Back Ratio is a measure of radiosensitivity. The GBR is defined as the rate of growth of a cell culture irradiated to a dose of 4 Gy over the rate of growth of a control culture.

GSH : glutathione.

H· : Hydrogen radical.

$H_2O_2$ : Hydrogen peroxide.

i.e. : that is to say (*id est*)

*in vitro* : 'on glass'; in tissue culture.

*in vivo* : in the live animal.

$k_{OH}$: rate constant (L mol⁻¹s⁻¹) for reaction with hydroxyl radicals.

LCLs : Lymphoblastoid cell lysates or lymphoblastoid cell lines.

M : mol L⁻¹

MTT : 3-4,5-dimethylthiazol diphenyl tetrazolium bromide.

NBT: Nitro Blue Tetrazolium 2-2'di-p-nitrophenyl 5-5' diphenyl 3-3'[3,3'dimethoxy-4,4'diphenylene]ditetrozolium chloride.

·OH : Hydroxyl radical.

OD: optical density or absorbance.

$O_2^{·-}$: superoxide radical anion.

$P_{1/2}$ or $P_{50\%}$: the 50 % inhibition concentration or concentration for half maximal inhibition of BPE fluorsence.

PBS : Phosphate buffered saline consisting of 0.137 mol L⁻¹ NaCl, 0.00268 mol L⁻¹ KCl, 0.0064 mol L⁻¹ $Na_2HPO_4.7H_2O$, 0.00147 mol L⁻¹ $KH_2PO_4$; filter sterilised and buffered to pH 7.4 .

$Scav_{·H}$ : Hydroxyl radical scavenger.

$S_F$ : Surviving fraction. The fraction of cells capable of forming a colony of at least 50 cells following a radiation treatment as compared with unirradiated controls.
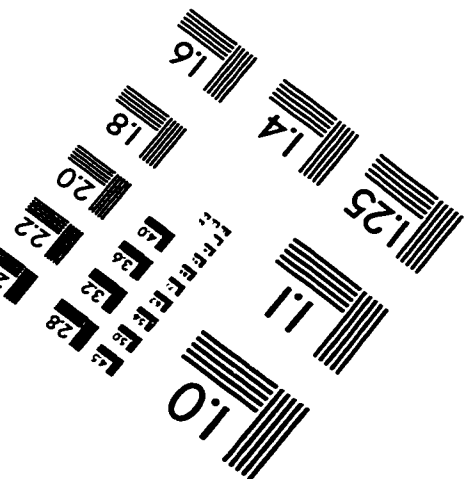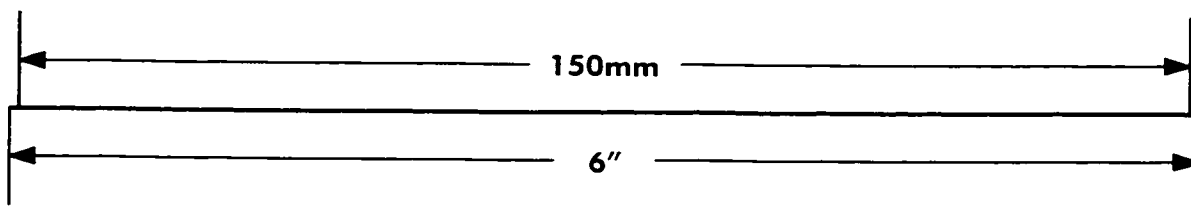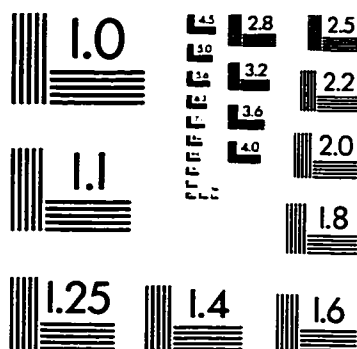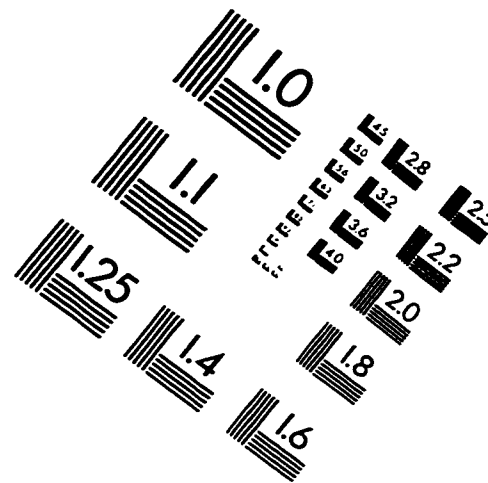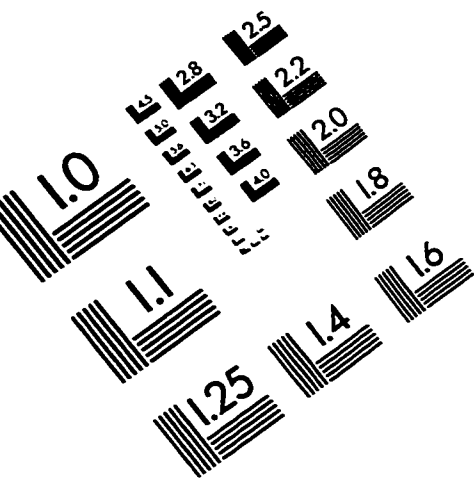SOD: Superoxide dismutase.
SSB : single strand break.
vitamin C : vitC; ascorbic acid.
vitamin E : vitE; α-tocopherol.
WR: Walter Reed; a class of potent thiol compounds.

# IMAGE EVALUATION
# TEST TARGET (QA-3)

150mm

6"